AD-A059 847 NORTHERN RESEARCH AND ENGINEERING CORP CAMBRIDGE MASS F/G 21/2
FLAMEHOLDER COMBUSTION INSTABILITY STUDY. VOLUME II. EXPERIMENT--ETC(U)
MAY 78 E R NORSTER F33615-76-C-2112
UNCLASSIFIED NREC-1294-2 AFAPL-TR-78-27-VOL-2 NL

1 OF 2
AD
A059847

LEVEL

AFAPL-TR-78-27, VOL II

FLAMEHOLDER COMBUSTION INSTABILITY STUDY

VOLUME II - EXPERIMENTAL PROGRAM

E. R. Norster

Northern Research and Engineering Corporation
219 Vassar Street
Cambridge, Massachusetts 02139

MAY 1978

Final Report May 1976 - January 1978

AIR FORCE AERO PROPULSION LABORATORY
AIR FORCE SYSTEMS COMMAND
WRIGHT-PATTERSON AIR FORCE BASE, OHIO 45433

NOTICE

This technical report has been reviewed and is approved for publication.

F. N. UNDERWOOD, Captain, USAF
Project Engineer

JOSEPH C. HURST, Major, USAF
Chief, Components Branch

FOR THE COMMANDER

ERNEST C. SIMPSON
Director, Turbine Engine Division

UNCLASSIFIED

SECURITY CLASSIFICATION OF THIS PAGE (When Data Entered)

REPORT DOCUMENTATION PAGE

READ INSTRUCTIONS BEFORE COMPLETING FORM

1. REPORT NUMBER: AFAPL-TR-78-27- VOL II	2. GOVT ACCESSION NO.
3. RECIPIENT'S CATALOG NUMBER	
4. TITLE (and Subtitle): FLAMEHOLDER COMBUSTION INSTABILITY STUDY. VOLUME II. - EXPERIMENTAL PROGRAM	5. TYPE OF REPORT & PERIOD COVERED: Technical - Final 1 May 1976 - 1 Jan 1978
	6. PERFORMING ORG. REPORT NUMBER: 1294-2
7. AUTHOR(s): E. R. Norster	8. CONTRACT OR GRANT NUMBER(s): F33615-76-C-2112
9. PERFORMING ORGANIZATION NAME AND ADDRESS: Northern Research and Engineering Corp. (NREC) 219 Vassar Street Cambridge MA 02139	10. PROGRAM ELEMENT, PROJECT, TASK AREA & WORK UNIT NUMBERS: 3066-05-38
11. CONTROLLING OFFICE NAME AND ADDRESS: Air Force Aero Propulsion Laboratory (TBC) Wright-Patterson AFB OH 45433	12. REPORT DATE: May 1978
	13. NUMBER OF PAGES: 96
14. MONITORING AGENCY NAME & ADDRESS (if different from Controlling Office)	15. SECURITY CLASS. (of this report): UNCLASSIFIED
	15a. DECLASSIFICATION DOWNGRADING SCHEDULE

16. DISTRIBUTION STATEMENT (of this Report)

Approved for public release; distribution unlimited.

17. DISTRIBUTION STATEMENT (of the abstract entered in Block 20, if different from Report)

18. SUPPLEMENTARY NOTES

19. KEY WORDS (Continue on reverse side if necessary and identify by block number)

Flameholder	Afterburner	Combustion
Combustion Stability	Turbofan	Combustion Response
Augmentor	Flame Stability	Rumble

20. ABSTRACT (Continue on reverse side if necessary and identify by block number)

This report details the experimental portion of the Flameholder Combustion Instability investigation of the low frequency combustion instability (rumble) problem found in turbofan augmentors. The study examines: (1) the spacial and temporal variations of pressure and heat-release in a flameholder rig designed to simulate augmentor operating conditions; (2) some possible mechanisms for rumble under widely varying flow conditions; (3) the characteristic response of different flameholder configurations to

DD FORM 1 JAN 73 1473 EDITION OF 1 NOV 65 IS OBSOLETE

UNCLASSIFIED

SECURITY CLASSIFICATION OF THIS PAGE (When Data Entered)

20. longitudinal pressure disturbances.

FOREWORD

This document presents the results of the experimental effort in the flameholder combustion instability study. The work was carried out in accordance with the plan outlined in an NREC Proposal No. 959-161, entitled "Flameholder Combustion Instability Study".

This report is the second of two volumes. It contains the experimental approach, a description of the test rig and its instrumentation, the test plan and procedures, as well as the test data and a discussion of the results. The first volume contains the results of the analytical effort.

The work was carried out at Northern Research and Engineering Corporation under the technical direction of Dr. W. Jansen, with Mr. E. R. Norster assuming project responsibility. Other major participants in the program include Messrs. G. E. Smith, A. E. Sotak, M. Platt, and J. A. Given.

TABLE OF CONTENTS

LIST OF TABLES

LIST OF ILLUSTRATIONS

LIST OF ILLUSTRATIONS (CONT'D)

LIST OF ILLUSTRATIONS (CONT'D)

INTRODUCTION

The observed phenomenon of rumble, low frequency longitudinal augmentor instability, is described in the introduction of Volume 1 of this report. However, it should be added that the physical aspects of the phenomenon, for example, the initiation process, mechanism and the effects of augmentor variables are far from established. The underlying problem here is a lack of understanding of the unsteady heat-release process and its interaction with physical processes and the acoustic characteristics of augmentors. The heat-release process is complex even in the case of steady-state combustion. During unsteady conditions physical processes such as turbulent mixing and droplet vaporization may become more significant than chemical kinetics. Those processes which are sensitive to pressure and velocity fluctuations will cause oscillations to the heat-release rate during unsteady combustion. The complexity of these factors necessitates some experimental as well as analytical investigation of the specific contributions they make to combustion instability. The objectives of the experimental study, described in this second volume, are therefore focussed on improving our understanding of these physical factors and providing qualitative and quantitative input to the analytical model under development.

Specifically the study examines:

1) The spacial and temporal variations of pressure and heat-release in a flameholder rig designed to simulate augmentor operating conditions.
2) Some possible mechanisms for rumble under widely varying flow conditions.
3) The characteristic response of different flameholder configurations to longitudinal pressure disturbances.

EXPERIMENTAL APPROACH

The experimental approach adopted in examining the physical parameters effecting longitudinal instability in augmentors was that of imposing a pressure pulse on a flameholder combustion rig designed to simulate augmentor operating conditions. The main features of the flameholder rig, which will be described in detail later, are shown in Figure 1 and consist of:

1) Fan and core stream section.
2) Pulse generator section.
3) Fuel injector and flameholder section.
4) Combustion observation duct.

High response pressure and radiation transducers were located at various axial locations throughout the rig in order to record the transient pressure and heat-release characteristics due to the imposed pulse on the system. In general each test consisted of establishing steady flow conditions while burning liquid or gaseous fuel, initiating a flow pulse and measuring the response (principally the longitudinal distribution of unsteady pressure) for a given geometry. Test series were devised to examine parameters related to the following possible coupling mechanisms for instability:

1) Turbulent mixing.
2) Atomization and vaporization.
3) Fuel-air distribution.
4) Unsteady shear flow.
5) Blowout and relight.

Although complete isolation of different mechanisms is not possible in practice, the approach in this study consisted of separate groups of tests which focussed on individual mechanisms to as great an extent as possible. The basis for examination of the possible mechanisms of instability is described in the following section.

TURBULENT MIXING

Turbulent mixing is known to be a dominant mechanism controlling the spread of the flame from the flameholder during steady combustion

(Ref 1). The influence of this mechanism on the unsteady heat release rate through its effect on the distribution of burning is also significant. The importance of mixing on the unsteady heat release depends on the sensitivity of the mixing rates (of burned and unburned mixtures) to the fluctuations in pressure and velocity. To eliminate droplet effects the turbulent mixing mechanism was examined predominantly with premixed natural gas. Parametric variations in flameholder geometry, upstream pressure, velocity, fuel/air ratio were investigated.

ATOMIZATION AND VAPORIZATION

In typical augmentor fuel injection systems, the principal source of atomizing energy is the approaching gas stream velocity. Consequently, the atomization quality (droplet size and distribution) is greatly influenced by flow conditions. The droplet vaporization rate is strongly dependent on the initial droplet size, flow conditions and particularly temperature. It is apparent that perturbations in the flow conditions can drastically affect the character of the mixture entering the flame region and consequently the heat release rate. This effect is particularly significant in the case of the comparatively low temperatures that exist in the fan stream. This possible mechanism was examined by introducing liquid fuel at different distances upstream of the flameholder through various injector arrangements. Parametric variations of initial spray quality, temperature, fuel-air ratio and flameholder geometry were investigated.

FUEL-AIR DISTRIBUTION

Combustion instability in augmentors is not only dependent on the mean value of fuel-air ratio in the flame region but also on the distribution about the mean value. The importance of this aspect in producing low frequency pressure oscillations is well illustrated by the work of Lewis (Ref 2) and also turbofan rumble is apparently responsive to fan-core stream fuel distribution changes. This mechanism was investigated through selective liquid fuel tests at different values of injector-to-flameholder spacing, and also through supplementary tests with combined local and premixed gas injection.

UNSTEADY SHEAR FLOW

The fan and core streams presented to the augmentor of a turbofan engine may differ greatly in temperature and velocity and therefore drastically alter the mixing rate in the vicinity of the interface. At the interface mixing and distribution of fuel upstream of the flameholder will be significantly different than at other locations as will be the burning rate downstream of the flameholder. The stability or sensitivity of this possible mechanism of flow perturbations is unknown and warrants investigation. Tests with controlled nonuniformities in temperature and velocity were conducted through different temperatures of the core stream and different mass flows in fan and core streams.

BLOWOUT AND RELIGHT

This mechanism corresponds to a case where adjacent flameholders are located in parallel streams during different flow conditions, for example the core and fan streams of a turbofan engine augmentor. A flow pulse of sufficient magnitude could blow out the flame on the fan stream flameholder without significantly affecting the core stream flame. The combustible mixture in the fan stream would not ignite until it had proceeded downstream sufficiently to contact the adjacent flame. The subsequent ignition of this mixture would cause a pressure pulse which would allow the flame to propagate back upstream to the flameholder. This could be observed as a transient "lifting-off" of the flame from the flameholder. This possible mechanism appears to be a likely candidate as a source of rumble. A series of tests was conducted with increasing fan stream pulse amplitude until fan stream blow-out occurred while attempting to maintain burning on the core stream flameholder. Parametric variations of flow conditions and fuel/air ratio were investigated with a specific flameholder geometry.

DESCRIPTION OF RIG AND INSTRUMENTATION

Rumble is a special type of combustion instability that occurs in certain turbofan engine augmentors when operating at high altitude and low flight Mach number conditions. Augmentor pressures over which rumble occurs range from 7.6 to 16 psia with fan and core stream temperatures close to 220 and 1,250 deg F, respectively. Generally at these conditions the onset of rumble coincides with augmentor fuel flows corresponding to approximately 0.04 over-all fuel-air ratio. Also rumble appears to be sensitive to geometric alterations of the fan stream flameholder and the fuel distribution between fan and core streams.

Two basic requirements of the experimental investigation are therefore a test rig which simulates adequately the relevant conditions existing in augmentors exhibiting rumble and instrumentation sufficient to measure the important performance variables. These requirements and the approaches used to satisfy them are discussed below.

FLAMEHOLDER TEST RIG

To satisfy all the above requirements ideally it would be necessary to confine testing to intermediate and actual size augmentors. Provided the operating conditions are representative, however, the requirement for a full-scale duct is not critical for the study of unsteady heat release in the low frequency range predominantly associated with longitudinal waves. The approach adopted therefore is the flameholder rig design illustrated in Figure 1.

The test rig consists of four main sections: fan and core stream section, pulse generator section, fuel injection and flameholder section, and combustion observation duct. During normal operation both fan and core stream inlets are supplied with separately measured air flows from a Solar gas turbine driven compressor. The upper core portion of the section contains one Pratt & Whitney J60-P3A combustor liner with suitably adapted fuel injector and igniter. Burning JP-5 fuel the combustor provides an efficient and uniform supply of core gas to the downstream pulse generator and subsequent working sections. Core stream temperature is indicated by an exhaust thermocouple in the upper 8-inch by 3-inch rectangular exit from the section. The lower portion of the section contains suitable transition ducting to convey the fan air from the 6-inch circular inlet to the lower 8-inch by 3-inch rectangular exit. The over-all arrangement is illustrated in Figure 2 and exit details are shown in Figure 3.

The pulse generator section shown in Figure 4 is a symmetrical rectangular flanged section 16 inches long which attaches to the exit flange on the fan and core stream section described above. The upper 8-inch by 3-inch core stream passage is separated from an identical lower fan stream passage by a splitter plate which extends the entire length of the section. The pulse generator mechanism is essentially a set of eight movable vanes mounted in carbon bushes. The size and location of the vanes are such that synchronous rotation of each vane presents uniform closure of the passage and virtually complete blockage after 90 degrees rotation. The vanes are positioned and synchronized with the aid of a rack and adjustable pinions attached to the stub shaft of each vane. Linear movement of the rack is accomplished through a high response servo-valve operated hydraulic actuator. Both fan and core stream passages have identical pulse generator mechanisms which may be operated simultaneously or independently through electronic control signals to the servo-valves. Additional details of the pulse generator assembly are shown in Figure 5.

The fuel injection and flameholder section shown in Figure 6 is essentially a slightly tapered rectangular section duct approximately 22 inches long. After the 8-inch by 6.6-inch inlet section the upper and lower walls gradually taper so as to produce an 8-inch by 5-inch section close to the exit. The upper, lower, and side walls are constructed in the main of dettachable panels to allow easy removal of gas and liquid fuel injectors and also the different flameholder assemblies required in the test program. Simple multinozzle spray bars, of the required fuel flow number, for fan and core streams, are mounted from side panels. The local gas injection tubes are mounted on upper and lower panels as illustrated. (Premixed gas injection tubes are located well upstream at the entrance to the fan and core stream section.) During liquid fuel injection tests the local gas injection assemblies are replaced with blank panels. A large observation window is located in one side wall between the fuel injection and flameholder sections to allow spray patterns to be observed under normal operating conditions. The flameholder assembly is normally secured to an upper mounting panel by rods attached to the flameholder. Additional support is provided through location holes for these rods in the lower panel of the duct. A gas supply for torch ignition of the flameholder passes through one support rod into the recirculation region of the flameholder. Ignition of this gas is accomplished with a high voltage electrode suitably positioned in the side panel of the section. Figure 7 shows the fuel injection and flameholder section in the assembled test rig during torch operation.

The combustion observation duct (Fig 8) is a rectangular duct 22.5 inches long, similar in cross-section to the fuel injection and flameholder section described above. During normal operation of the test rig assembly the observation duct is flange connected to the flameholder section and conveys the burning mixture to a water cooled exhaust section of the facility. The construction of the duct is such that four windows may be mounted in each side wall allowing combustion to be observed from the flameholder to a point 16 inches downstream. Five equispaced mounting bosses are located on both upper and lower walls of the duct to facilitate installation of pressure and radiation transducers. Figure 9 shows combustion throughout the observation duct during normal operation with local gas injection. The over-all arrangement of the component parts of the test rig is shown in Figure 10.

To allow maximum coverage of operating conditions the test facility (Fig 11) provides for subatmospheric and superatmospheric pressures in the flameholder rig. In the subatmospheric mode of operation the rig is evacuated through an air driven ejector. Within the limits of air flow available flameholder approach velocities between 250 and 300 feet per second are attainable at pressures down to 8 psia. With direct blowing of the rig velocities from 200 to 350 feet per second in both fan and core streams and flameholder pressures up to 1.5 atmospheres may be obtained. To avoid problems with the operation of the pulse generator, core combustor exhaust temperature is limited to 1,100 deg F for continuous operation and 1,250 deg F for short periods of time. The available test rig air flow rates over both subatmospheric and superatmospheric operation pressures are shown in Figure 12.

DESCRIPTION OF INSTRUMENTATION

The main objective of the test program was to investigate the unsteady pressure response characteristics of the flameholder test rig using conventional high response pressure instrumentation. The flameholder test rig was also instrumented with steady-state pressure, temperature, and flow instrumentation to permit continuous evaluation of the basic operating conditions throughout the test program. Much of this steady-state instrumentation is required to define the flow conditions (both fan and core streams) entering the flameholder rig.

Steady-State Instrumentation

Figure 11 illustrates schematically the major items of steady-state instrumentation in the flameholder rig and test facility. Air flow from the Solar gas turbine driven compressor is controlled and metered through two separate supply lines to the fan and core stream section inlet. The air flow is measured by individually sized orifice plates with appropriate temperature and pressure tappings. Pneumatically actuated flow control valves are operated through separate servo-control systems in the test cell control room. Core and fan stream temperature and pressures are measured with chromal-alumel thermocouples and manometers at the inlet to the pulse generator section. Additional pressures and temperatures are monitored in the downstream sections of the rig. Temperatures are recorded on a Doric Model 460A indicator incorporating manual switching.

The JP-5 liquid fuel flow to the core combustor is measured by a Fischer Porter flow meter and controlled via a needle valve and pressure gauge. Flow isolation is accomplished with a solenoid operated shut-off valve located close to the core combustor fuel injector. Individual fan and core stream liquid fuel flows are similarly controlled but measured with calibrated Cox type turbine flow meters with digital indicators. High perssure fuel is supplied to the system by a Denison vane type pump with a maximum flow capacity of 5 gpm at 1,000 psig.

The premixed and local injection of natural gas is measured with separate fan and core Fischer Porter flowmeters. The system is arranged to allow for separate or combined premixed/local gas injection. A separate tee line and metering valve provides a small gas supply to the flameholder for torch ignition.

Dynamic Instrumentation

The dynamic instrumentation consists essentially of seven high response PCB Piezotronic Model 112A21 pressure transducers which may be located at the various positions indicated in Figure 13. Each transducer is mounted in a special water cooled adapter to avoid exceeding the normal thermal limits of the transducer. The PCB Model 112A21 is an acceleration compensated transducer with built-in charge amplifier producing 50 mv/psi output. Power for the transducers is supplied by a standard 12 channel Series 483A rack power unit with appropriate microcabling. The pressure transducer output signals are transmitted via coax cable to preamplifiers for a Honeywell Model 5600C multichannel tape recorder. As can be seen in the dynamic recording instrumentation layout (Fig 14) signals from the transducers may also be transmitted to the Model 104 preamplifiers of the Honeywell Model 2106 multichannel optical galivanometer Visicorder. A Tektronics Model 504 dual beam oscilloscope is used to monitor the amplitude levels of signals and make appropriate gain adjustments prior to recording on the Honeywell 5600C recorder. Playback of the recorded pressure transducer signals may be monitored on the osclllosope and additionally analyzed by a Hewlett Packard 3580A spectrum analyzer. Hard copies of the analysis may be prepared on the attached Hewlett Packard Model 7046A plotter.

As indicated earlier, in addition to the above pressure instrumentation attempts were also made to record the unsteady heat release rate through flame radiation probes. Figure 15 shows the basic radiation probe built by NREC to perform these measurements. The basic sensing element of the probe is a high response photodiode which, when subjected to appropriately filtered radiation from the flame (0.43 microns) produces a signal proportional to the rate of heat released per unit volume. The validity of the technique has been demonstrated previously (Refs 3 and 4) and probes of this type have been used to investigate rocket motor instability. In this case, although the approach was not wholly satisfactory because of the low signal to noise ratio and signal interference, the results obtained proved to be particularly useful in showing the qualitative changes occurring locally in the flame.

The final item of dynamic instrumentation to be described is the pulse generator control unit. The electronic servo-controller system provides single shot actuation of the pulse generator with variable amplitude, zero to full closure, and also pulse durations from 20 to 300 milliseconds. Figure 16 illustrates the essential circuitry of one of the two units employed for each hydraulic servo-valve on the fan and core stream pulse generator actuating mechanisms.

TEST PLAN AND PROCEDURES

As indicated earlier in the Technical Approach section, five possible mechanisms for rumble were considered of interest in this test program. These mechanisms together with three configurations of flameholder constitute the basic matrix of testing. Incorporating the additional requirements for gas and liquid fuels, different injection schemes, various fuel-air ratios and velocities resulted in a schedule of eight different test series as indicated in Table 1. The simple Vee gutter flameholder assembly shown in Figure 17 was used for the preliminary rig shakedown tests and subsequently for test series 1 and 8. The preliminary configurations for the remaining flameholders are shown in Figure 18. Testing with flameholder "A" was confined to the liquid fuel test series 5 and 6 whereas configuration "C" (double gutter) was extended to both liquid and gaseous fuels in series 2, 3 and 7. Final details of configurations A and C are shown in Figures 19 and 20 respectively. All flameholders were of practical size and arranged to present approximately 25 percent blockage in the flameholder section.

Prior to conducting a test all steady-state and dynamic measuring instruments are checked for proper operation and adjustment. Pressure transducer and radiation probe recording channels are calibrated at the appropriate gain settings. After applying the required air flow to the rig the hydraulic supply and the electronic servo-controller unit for the pulse generator are switched on and checked out. During this pre-test check-out the pulse generator amplitude and duration are monitored and appropriate pressure transducer signals recorded to establish correct operation of the system. Typical recordings of the pressure pulses generated are shown in Figure 21.

All fuel pumps are switched on and cooling water flows and pressures adjusted before the core combustor air flow is set for light-off conditions. Immediately after light-off of the core combustor, air flow and fuel flow adjustments are made such that the flow condition and temperature in the rig correspond to the desired operating conditions.

Torch gas is applied, ignited and a pilot flame established on the flameholder. Operation of the dynamic recording instrumentation is again checked before applying the main fuel to the rig. When steady burning of the main fuel at the appropriate fuel-air ratio exists, the torch gas supply is turned off and readings of the pressure, temperature and flows recorded. The dynamic instrumentation recording equipment is switched on and a command signal applied to the pulse generator. The recording equipment is then switched off and the traces examined for appropriate response. If necessary, the effect of pulse amplitude and duration on pressure response may be examined through adjustment of the servo-controller unit and repeat application of pulses. The above procedure may be repeated at additional fuel-air ratios, various fan and core stream flows and different core stream temperatures depending on the requirements of the test series.

TEST-DATA AND DISCUSSION OF RESULTS

The test data for the eight series outlined in the schedule shown in Table 1 are tabulated in Tables 2 through 8. All tests were performed near atmospheric pressure conditions and confined to the three basic flameholder configurations--simple vee gutter, vee gutter with stubs and double vee gutter. Fuel injection covered premixed and local gas injection and JP5 liquid fuel injection at 16 and 20 inches upstream of the flameholders. Spray bars were arranged with different sets of nozzles such that type "A" had considerably finer droplets than that of type "B". The fan to core stream velocity ratio varied from 0.4 to 1.3 for liquid fuel tests and values from 1.0 to 2.5 when gaseous fuel was used. Whereas core stream heating provided core to fan inlet temperature ratios from 1.7 to 2.4 during the liquid fuel burning series no heating was used for the gaseous fuel test series. It should be noted that during the liquid fuel series of tests the core stream fuel-air ratios were generally held lower than those of the fan stream in order to limit high temperature differences between upper and lower walls of the combustion observation section. A total of eighty-three tests are reported.

TEST SERIES 1

These tests were confined to burning of natural gas with the simple vee gutter flameholder. Tests were performed at three fuel-air ratios 0.31, 0.34 and 0.36 and covered fan to core velocity ratios 1.0, 1.7 and 2.5. The initial tests were carried out with premixed natural gas to establish a datum for the effects of turbulent mixing on combustion stability. Subsequently, localized gas injection at 16 inches from the flameholder was also examined. The use of gaseous fuel eliminated any effects of droplet vaporization in this test series.

Because of the potential for "chugging" with a low pressure gaseous fuel injection system, it was expected that operation with premixed natural gas would make that rig more sensitive to instability. However, it was not anticipated that this would occur over most of the premixed operating conditions of interest. Figure 22 shows a typical trace of the unsteady pressure at pulse generator and rig exit together with pressure and radiation signals at the flameholder location during premixed fuel operation. The operating conditions correspond to approximately 0.03 fuel-air ratio and a fan to core velocity ratio of one. At these conditions the burning was relatively smooth compared with all those at higher fuel-air ratios. However, it can be seen that the introduction of a small pressure pulse (approximately 50 msec and low amplitude) induced a significant increase in the radiation and heat release rate and subsequent pressure disturbances at the rig exit.

The more general unsteady pressure characteristics for premixed fuel injection are shown in Figure 23. At fuel-air ratios close to 0.034 a 30 HZ synchronous pressure oscillation dominates throughout the rig. It can also be seen that a 400 HZ minor oscillation is present. Pressure amplitudes between 10 and 15 percent were typically measured during these conditions. At fuel-air ratios in the region of 0.036, severe pressure amplitudes (20-30 percent) limited operation of the rig to short periods of time. Figure 24 indicates a change in wave form of the 30 HZ pressure oscillation at the rig exit location during these more severe operating conditions. It would appear that the behavior of the premixed system stems from the low impedance of the fuel injection arrangements, which is designed to satisfy a maximum available pressure of 40 psig. The characteristics indicate "chugging" occurs at a frequency close to the first longitudinal mode of the system.

Tests with localized gas injection, Table 2, covered approximately the same fuel-air ratios and velocity ratios as those above for premixed injection. In general, steady burning with localized injection was much smoother than premixed burning. Figure 25 illustrates the typical levels of unsteady pressure and radiation on the rig. It is apparent in the traces shown that pressure and radiation at the flameholder location are in good qualitative agreement and appear to be more responsive than previously. Figures 26 and 27 show the effects of fixed amplitude short and long duration pulses while operating at fuel-air ratios close to 0.031 and with a fan to core stream velocity ratio of 1.0.

The effect of the pulse is similar in both cases bringing about an initial lowering of radiation or heat-release. Subsequently bursts of combustion, from almost extinction levels, induce pressure oscillations which appear to have a characteristic frequency around 50 HZ. In some instances substantial pressure amplitudes ($\pm$ 8 percent) are generated at the flameholder location and are seen to propagate upstream. In the cases shown whereas the short pulse does not blow-out the flame the long pulse does so. Similar unsteady pressure characteristics are found at higher fuel-air ratios with generally higher pressure amplitudes. Figures 28 and 29 show the effects of increased fan to core velocity ratio. Generally the unsteady pressure amplitude and radiation changes are higher than previous and more irregular at the highest velocity ratio. However, characteristic frequencies of 50 and 100 HZ are evident.

A detail prevailing in all the above tests is worthy of note. In comparing unsteady radiation and pressure signals at the flameholder position it is evident that a positive value of unsteady pressure $\partial P/\partial t$ induces an increase in radiation or heat release. The increased rate of heat release brings about a negative pressure pulse which then reduces the rate of heat release. This cyclic characteristic of radiation and pressure is seen to be particularly dominant during the application of the main pressure pulse.

TEST SERIES 2

The second test series examined the effects of fuel-air ratio distribution and mixing on the characteristics of the double vee gutter flameholder. Premixed and localized injection of natural gas were examined together with combinations of both injection arrangements. Variations in the amount of premixed and local fuel applied allowed significant changes in fuel-air ratio distribution at the flameholder to be studied. The general operating levels of fuel-air ratio and fan to core stream velocity ratio were consistent with test series 1 and are given in Table 3.

During premixed fuel injection, Figure 30, the unsteady pressures were similar to those found earlier with the simple vee gutter flameholder. However, the pressure amplitude of the 30 HZ oscillation was significantly reduced in comparison to the 400 HZ frequency oscillation. The change observed is possibly due to a more significant contribution of transverse instability with the double vee gutter flameholder, since the space immediately downstream of the flameholder is relatively fuller with flame. Local fuel injection of natural gas produced much steadier burning than seen previously. Figures 31, 32 and 33 show the effect of increasing a short pulse amplitude to the point of flame blow-out. The characteristic frequency of pressure oscillations during these pulses is close to 100 HZ. Again the cycling between pressure and heat release, referred to in the previous discussion, is evident.

The addition of approximately 50 percent premixed fuel to local fuel injection to give a mean fuel-air ratio close to 0.034 with equal fan and core stream velocities, produced the results shown in Figure 34. A steady 100 HZ pressure oscillation is evident at the flameholder and upstream positions. The radiation is also more consistent than with local fuel injection alone and in the main corresponds to the pressure oscillation occurring. The application of nominal pressure pulses while operating under these conditions invariably resulted in flame blow-out. During the application of higher proportions of premixed fuel, particularly with fan to core stream velocity ratios of 1.9, unusually rough combustion was encountered. Figure 35 illustrates the severity of those conditions. The radiation signals shown have been attenuated substantially but show unusually high bursts of 17 HZ burning. In constrast pressure oscillations at the flameholder and upstream are at twice the radiation oscillation frequency. The cyclic pressure-radiation characteristics referred to above are dominant in these results.

TEST SERIES 3 AND 4

Both test series 3 and 4 were confined to burning of JP5 liquid fuel with the double vee gutter flameholder. The tests in series 3 were performed with spray bar type "A" having low flow number nozzles to provide fine initial atomization of the fuel. Spray bar type "B" was set up with higher flow number nozzles for use in test series 4. The mean droplet size predicted for bars "A" and "B" was 60μ and 100μ respectively at a fuel flow rate of 4.3 lb/min. It was expected that these differences in spray quality would effect not only the characteristic evaporation time of each injector but also the proportion of evaporated to liquid fuel arriving at the flameholder. In both series tests were conducted with bars positioned at upstream and downstream locations corresponding to 20 and 16 inches respectively from the flameholder. Fuel-air ratios of approximately 0.035 and 0.04 were examined for fan to core stream velocity ratios of 0.4 and 0.7. Core stream operating temperatures were maintained close to the 1500 deg R level.

No significant difference was found in the unsteady pressure characteristics with spray bar "A" in the upstream or downstream position. The general characteristics were found to be similar to those of local gas injection as may be seen in Figure 36. The application of short and long pulses induced the same cyclic pressure-heat-release effects noted above, although generally of a lower intensity. Large amplitude short duration pulses normally induced flame blow-out as shown in Figure 37. However, in some instances re-ignition burst would occur. As shown in Figure 38 the re-ignition normally occurred with positive values of flameholder unsteady pressure $\partial p/\partial t$, indicating the conducive effect this has on the heat release rate.

Series 4 testing with spray bar type "B" downstream exhibited considerably different unsteady pressure characteristics which may be seen in Figure 39. During steady burning the radiation signal at the flameholder location indicated a regular 160 HZ oscillation with superimposed 40 HZ synchronous pulses. The unsteady pressure oscillations at the same flame position was dominantly 80 HZ with superimposed high frequency of approximately 420 HZ. Although data at higher fuel-air ratios was limited by pressure transducer failure in general the above unsteady pressure and radiation feature persisted. In Figure 40 it can be seen that the application of short duration pulses do not effect substantially the flame radiation in contrast to previous observations. Although in these particular tests the pressure transducer at the flameholder position failed signals from the upstream transducer (close to the pulse generator exit) indicated substantial 40 to 60 HZ pressure oscillations induced by the pulse.

TEST SERIES 5 AND 6

Test series 5 and 6 both examined the characteristics of flameholder type A, vee gutter with stubs, illustrated in Figures 18 and 19. Spray bar type "B" was used in test series 5 initially in the upstream position. Subsequent tests were performed under similar operating conditions with the spray bar at the downstream location. Operating conditions for these tests are tabulated in Table 6. During test series 6 spray bar "A" was also used at both locations and the operating conditions, shown also in Table 6, held closely to those of series 5. Since previous fuel-air ratio adjustments had shown only marginal changes in the unsteady pressure characteristics in series 5 and 6 a common mean fuel-air ratio of approximately 0.039 was maintained. Fan to core stream velocity ratios of 0.4, 0.7 and 0.9 were examined through adjustments of fan and core mass flows. Core gas temperature for the lower velocity ratios was maintained close to 1450 deg R and adjusted to approximately 1150 deg R for the highest ratio.

No significant differences were found in the unsteady pressure characteristics for the upstream and downstream location of the spray bars. Differences were found, however, on comparing the behavior of spray bar "A" with spray bar "B". Figure 41 shows the general behavior of unsteady pressures and radiation for spray bar "B" for a fan to core velocity ratio of approximately 0.72. The flameholder pressure oscillations appear more random than previous and the radiation signal has relatively few intense regions. The application of a long (400 msec) low amplitude pulse, Figure 42, indicates flameholder pressure oscillations more generally around 80 to 100 HZ. Amplification of these characteristics is evident in Figure 43 with the application of a higher amplitude 400 msec pulse. Flameholder radiation bursts appear to follow the more severe pressure excursions. Shorter duration pressure pulses, 100 and 200 msec, Figures 44 and 45 respectively, introduce no significant changes in these unsteady pressure characteristics.

In contrast the operation of the same flameholder with spray bar "A" (fine spray) at the same conditions has regions of higher radiation and appears to be more sensitive than the above case. The application of a short duration pulse, Figure 46, induces an immediate increase in heat release and subsequent pressure oscillations. With increasing pulse amplitudes, Figures 47 and 48, a substantial 50 to 60 HZ flameholder pressure oscillation is induced together with similar bursts of heat release. It would appear therefore that the vee gutter flameholder with stubs is somewhat sensitive to mixture preparation.

TEST SERIES 7

In test series 7 the double vee gutter flameholder was examined for the effects of unsteady shear and possible blow-out and re-light. In the case of unsteady shear a range of fan to core stream velocity ratios from 0.45 to 1.36 was examined through variations in fan and core mass flow and also core temperatures of approximately 1450 deg R and 1050 deg R. Fuel-air ratios were maintained close to 0.038 through and only spray bar type "A" was used at the downstream location.

The effects of a 75 msec fan stream pulse on the unsteady pressure and radiation characteristics are shown in Figures 49, 50 and 51 for velocity ratios of 0.45, 0.76 and 0.98 respectively. The core gas temperature was approximately 1450 deg R and the mean fuel-air ratio 0.038. It can be seen that the pulse in addition to producing a sudden change in radiation or heat release rate induces substantial pressure oscillations at the flameholder position. Significant amplitude low frequency oscillations 25-30 HZ persist sometime after the pulse while higher frequency 60-80 HZ pulsations are evident during the pulse transient. Significant bursts of radiation are also present during the initial transient, corresponding in most instances with the dominant pressure oscillations. At the lower core operating temperature of 1050 deg R and the extended fan to core velocity ratios listed in Table 7, the low frequency characteristics of the flameholder pressure oscillations are still evident, Figures 52, 53 and 54. Higher frequency oscillations are not immediately apparent and radiation bursts are limited. No sustained oscillation is evident in these tests.

Of the flow conditions listed in Table 7 only the highest velocity ratios 0.98 and 1.36 appeared to present suitable conditions for blow-out and re-light. At conditions corresponding to Test no. 67 a generous 100 msec pulse produced the result shown in Figure 55. Although re-light could not be sustained it is apparent that a significant flameholder pressure oscillation of approximately 45 HZ supports re-ignition of the flame as indicated by the corresponding radiation bursts shown. At conditions corresponding to Test no. 70 the result shown in Figure 56 was obtained. Here the flameholder pressure oscillation decays more quickly than that shown in Figure 55 and, although an erratic burst of radiation is apparent, no sustained re-ignition occurs. Under similar conditions a pulse of much larger amplitude was applied with the result shown in Figure 57. Whereas a pressure oscillation of approximately 55 HZ is sustained during the pulse transient no blow-out occurs at the effective time and it is evident from the rig exit pressure build-up that an unstable situation is approached very quickly.

TEST SERIES 8

The final test series was conducted with the simple vee gutter in order to complete the examination of atomization and vaporization on all three flameholder configurations. Type "A" spray bar was employed at both upstream and downstream locations and generally fuel-air ratios of 0.035 and 0.04 were examined. The velocity conditions were those previously used for atomization and vaporization tests and the test data acquired is given in Table 8.

No significant differences were evident due to changes in fuel injection distance and the normal steady burning characteristics were typically those shown in Figure 58. Flameholder pressure oscillations of approximately 200 HZ were generally evident and reflected the high frequency of radiation signals. During the application of short-low amplitude pulses substantial increases in radiation or heat release were apparent and resulted in significant pressure pulses at the rig exit, Figure 59. With increased pulse amplitudes in the fan stream, Figure 60, substantial low frequency transient pulses were apparent in the flameholder region. The frequency of these pulses ranged from 30-50 HZ generally. Application of various pulses simultaneously in both fan and core streams induced similar effects as shown in Figures 61 and 62. Subsequent to the passage of the pulse it can be seen that bursts of radiation correspond to the cyclic characteristics of the flameholder unsteady pressure. Again it is apparent that positive values of unsteady pressure pulse induce an increase of radiation or heat release.

SUMMARY OF OBSERVATIONS

The experimental part of the Flameholder Combustion Instability Studies has examined partially the effects of turbulent mixing, fuel-air ratio distribution, fuel atomization and unsteady shear flow on the unsteady pressure and flame radiation characteristics of three basic flameholder configurations. The observations summarized below are limited to those found at near atmospheric pressure conditions in a rectangular augmentor simulation rig.

1) Mixing and unsteady pressures affect significantly local combustion heat-release ratios. Regions which are locally fuel rich are seen to undergo particularly large heat-release changes when subjected to pressure oscillations and offer a possible mechanism for sustained pressure fluctuations.

2) Changes in mixture distribution which tend towards more uniform burning conditions, appear to make the system more susceptible to instabilities.

3) The introduction of pressure pulses are seen to cause ringing and pressure oscillations of various frequencies which tend to couple with combustion. However, no sustained oscillations were evident in the normal range of operating conditions.

4) Larger proportions of droplet burning, as evident in comparisons of spray bar A ano B, appear to attenuate the effects of unsteady pressure on heat-release. The vee gutter with stubs appears to be more susceptible to these effects than the other flameholders examined.

5) All flameholder configurations indicated the presence of low frequency unsteady pressures, 40 to 60 HZ when subjected to pressure pulses. This was particularly evident at high fan to core velocity ratios where unsteady pressure amplitudes were invariably larger than at lower velocity ratios.

6) Although some instances of blow-out and re-light were observed over the limited range of conditions examined, this phenomena could not be sustained.

TABLE I

TEST SERIES SEQUENCE

Test Series	Flameholder	Fuel	Injector Position/ Injector Type	Core/Fan	Remarks
1	VEE	PREMX GAS	US/TUBE	Cold/Cold	PREMIXED GAS
1	VEE	GAS	DS/I	Cold/Cold	LOCAL INJECTION
2	C	PREMX GAS	US/TUBE	Cold/Cold	PREMIXED GAS
2	C	GAS	DS/I	Cold/Cold	LOCAL INJECTION
2	C	GAS	US/TUBE,DS/I	Cold/Cold	COMBINATIONS
3	C	LIQUID	US/A	Hot/Cold	ATOMIZATION AND VAPORIZATION
3	C	LIQUID	DS/A	Hot/Cold	ATOMIZATION AND VAPORIZATION
4	C	LIQUID	US/B	Hot/Cold	ATOMIZATION AND VAPORIZATION
4	C	LIQUID	DS/D	Hot/Cold	ATOMIZATION AND VAPORIZATION
5	A	LIQUID	DS/B	Hot/Cold	ATOMIZATION AND VAPORIZATION
5	A	LIQUID	US/B	Hot/Cold	ATOMIZATION AND VAPORIZATION
6	A	LIQUID	US/A	Hot/Cold	ATOMIZATION AND VAPORIZATION
6	A	LIQUID	DS/A	Hot/Cold	ATOMIZATION AND VAPORIZATION
7	C	LIQUID	DS/A	Hot/Cold	VARIOUS VELOC-ITIES AND TEMPERATURES
7	C	LIQUID	DS/A	Hot/Cold	VARIATION OF PULSE
8	VEE	LIQUID	DS/A	Hot/Cold	SIMILAR TO 3
8	VEE	LIQUID	US/A	Hot/Cold	SIMILAR TO 3

Series 1 - Turbulent Mixing

Series 2 - Fuel/Air Distribution

Series 3 - Automization - Vaporization

Series 4 - Atomization - Vaporization and Fuel-Air Distribution

Series 5 - Atomization - Vaporization

Series 6 - Atomization - Vaporization and Fuel-Air Distribution

Series 7 - Unsteady Shear and Blow-Relight

Series 8 (6 & 3) - Atomization and Vaporization/Flameholder Configuration

TABLE 2

TEST DATA

TEST SERIES - 1 FUEL - NATURAL GAS FLAMEHOLDER - VEE

Test No.	FAN (1)					CORE (1)							
	$\dot{M}$ lb/s	T ^oR	V ft/s	$\dot{M}_F$ lb/m	F/A 10^{-1}	$\dot{M}$ lb/s	T ^oR	V ft/s	$\dot{M}_F$ lb/m	F/A 10^{-1}	P_{FH} PSIA	$\bar{F}/A$ 10^{-1}	$\frac{V_F}{V_c}$
1	1.50	602	156	2.84	.315	1.48	601	156	2.70	.304	15.23	.310	1.00
2	1.48	602	155	3.05	.343	1.50	602	155	3.03	.336	15.35	.340	0.98
3	1.48	603	152	3.18	.363	1.51	602	152	3.25	.358	15.55	.361	0.98
4	2.52	625	258	4.68	.309	1.51	602	149	2.77	.306	16.18	.308	1.73
5	2.50	626	256	5.05	.336	1.48	601	145	3.02	.340	16.25	.338	1.76
6	2.48	627	254	5.37	.361	1.48	601	145	3.18	.358	16.30	.360	1.75
7	2.50	627	264	4.65	.310	1.06	588	105	2.01	.316	15.65	.312	2.51
8	1.51	601	157	2.72	.300	1.50	600	155	2.84	.315	15.20	.308	1.01
9	1.53	603	159	3.20	.348	1.56	602	163	3.14	.335	15.32	.342	0.97
10	2.48	627	254	4.61	.309	1.52	603	150	2.94	.320	16.22	.315	1.69
11	2.42	628	248	5.08	.349	1.46	602	143	3.02	.344	16.25	.348	1.73
12	2.48	628	262	4.60	.309	1.04	592	104	1.86	.298	15.60	.306	2.52
13	2.46	628	260	5.10	.345	1.01	590	100	2.08	.343	15.72	.345	2.60

Tests 1 through 7 premixed fuel; Tests 8 through 13 local fuel injection.

TABLE 3

TEST DATA

TEST SERIES - 2 FUEL - NATURAL GAS FLAMEHOLDER - "C"

Test No.	FAN $\dot{M}$ lb/s	FAN T ^oR	FAN V ft/s	FAN (1) $\dot{M}_F$ lb/m	FAN (2) $\dot{M}_F$ lb/m	FAN F/A 10^{-1}	CORE $\dot{M}$ lb/s	CORE T ^oR	CORE V ft/s	CORE (1) $\dot{M}_F$ lb/m	CORE (2) $\dot{M}_F$ lb/m	CORE F/A 10^{-1}	$P_{F/H}$ PSIA	$\bar{F}/A$ 10^{-1}	$\frac{V_F}{V_c}$
14	1.53	608	163	2.81	--	.306	1.47	605	156	2.86	--	.324	15.20	.315	1.04
15	1.50	608	158	3.09	--	.343	1.45	605	153	3.01	--	.345	15.32	.345	1.03
16	2.56	624	279	4.80	--	.312	1.51	603	159	2.99	--	.330	15.25	.320	1.75
17	2.58	625	280	5.20	--	.336	1.53	604	160	3.26	--	.355	15.33	.343	1.75
18	1.51	610	161	--	2.88	.317	1.52	607	161	--	2.79	.306	15.26	.312	1.00
19	1.50	610	159	--	3.02	.335	1.49	608	157	--	3.08	.344	15.35	.340	1.01
20	2.48	626	271	--	4.46	.299	1.48	609	158	--	2.71	.305	15.20	.302	1.71
21	2.48	627	268	--	5.15	.346	1.46	607	153	--	3.03	.346	15.40	.346	1.75
22	1.56	611	167	1.42	1.40	.301	1.48	606	157	1.38	1.42	.315	15.22	.308	1.06
23	1.56	611	165	1.60	1.53	.334	1.47	606	154	1.58	1.50	.349	15.40	.342	1.07
24	2.60	626	284	2.43	2.38	.308	1.39	605	147	1.36	1.30	.318	15.22	.312	1.93
25	2.59	626	280	2.65	2.60	.338	1.40	606	147	1.40	1.44	.338	15.38	.338	1.90
26	1.53	612	162	2.10	1.07	.345	1.56	607	163	2.12	1.10	.344	15.42	.345	0.99
27	2.64	624	285	3.61	1.81	.342	1.48	605	155	2.02	1.01	.341	15.40	.342	1.84

(1) Premixed fuel injection (2) Local fuel injection

TABLE 4

TEST DATA

TEST SERIES - 3 FUEL - LIQUID-JP5 FLAMEHOLDER - "C"

Test No.	FAN (1)					CORE (1)					P_{FH} PSIA	$\overline{F}/A$ 10^{-1}	$\frac{V_F}{V_c}$
	$\dot{M}$ lb/s	T ^oR	V ft/s	$\dot{M}_F$ lb/m	F/A 10^{-1}	$\dot{M}$ lb/s	T ^oR	V ft/s	$\dot{M}_F$ lb/m	F/A 10^{-1}			
28	1.56	607	164	3.65	.389	1.48	1495	384	2.70	.304	15.39	.348	.427
29	1.54	598	159	4.11	.445	1.47	1524	387	3.02	.342	15.45	.395	.411
30	2.46	617	260	5.53	.374	1.52	1534	400	2.85	.312	15.55	.351	.650
31	2.45	619	260	6.64	.452	1.50	1517	390	2.89	.317	15.60	.402	.666
32	1.46	587	148	3.41	.389	1.51	1485	388	2.61	.288	15.40	.338	.381
33	1.52	594	156	4.01	.439	1.48	1502	383	3.17	.357	15.46	.399	.407
34	2.54	614	267	5.98	.392	1.45	1496	371	2.21	.254	15.59	.342	.719
35	2.54	620	267	6.85	.449	1.46	1518	376	2.70	.308	15.70	.407	.710
36	2.56	625	278	6.84	.445	1.12	1496	291	1.99	.296	15.35	.398	.939

(1) Tests 28 through 31 spray bar "A" located upstream; Tests 32 through 36 spray bar "A" located downstream.

TABLE 5

TEST DATA

TEST SERIES - 4 FUEL - LIQUID-JP5 FLAMEHOLDER - "C"

Test No.	FAN (1)					CORE (1)							
	$\dot{M}$ lb/s	T °R	V ft/s	$\dot{M}_F$ lb/m	F/A 10^{-1}	$\dot{M}$ lb/s	T °R	V ft/s	$\dot{M}_F$ lb/m	F/A 10^{-1}	P_{FH} PSIA	$\bar{F}/A$ 10^{-1}	$\frac{V_F}{V_c}$
40	1.48	598	154	3.36	.378	1.52	1457	385	2.61	.286	15.34	.332	.400
41	1.52	602	158	3.93	.431	1.50	1492	388	3.05	.339	15.40	.385	.407
42	2.61	624	281	5.87	.375	1.48	1521	388	2.23	.251	15.47	.330	.724
43	2.58	627	277	6.81	.439	1.49	1507	384	2.85	.319	15.58	.395	.721
44	1.52	599	158	3.46	.379	1.52	1493	394	2.41	.264	15.38	.322	.401
45	1.51	605	158	4.03	.445	1.52	1475	387	2.89	.316	15.45	.381	.408
46	2.48	623	265	5.58	.375	1.55	1502	399	2.03	.218	15.55	.315	.664
47	2.50	628	267	6.63	.442	1.56	1487	395	3.04	.325	15.67	.397	.675
48	2.52	631	274	6.63	.438	1.14	1492	294	2.17	.317	15.45	.401	.932

(1) Tests 40 through 43 spray bar "B" located upstream; Tests 44 through 48 spray bar "B" located downstream.

TABLE 6

TEST DATA

TEST SERIES - 5 & 6 | FUEL - LIQUID JP5 | FLAMEHOLDER - "A"

Test No.	FAN (1)					CORE (1)					P_{FH} PSIA	$\bar{F}/A$ 10^{-1}	$\frac{V_F}{V_c}$
	$\dot{M}$ lb/s	T °R	V ft/s	$\dot{M}_F$ lb/m	F/A 10^{-1}	$\dot{M}$ lb/s	T °R	V ft/s	$\dot{M}_F$ lb/m	F/A 10^{-1}			
50	1.62	589	165	4.39	.452	1.56	1435	389	2.99	.319	15.36	.387	.424
51	2.57	617	274	7.04	.456	1.48	1474	377	2.67	.300	15.42	.399	.727
52	2.58	624	282	6.48	.418	1.47	1162	299	3.00	.340	15.22	.390	.943
53	1.56	592	160	4.29	.458	1.52	1472	389	2.90	.310	15.35	.389	.411
54	2.61	623	281	7.17	.458	1.51	1456	381	2.52	.278	15.40	.392	.737
55	2.58	629	284	6.62	.427	1.61	1135	319	3.33	.344	15.25	.396	.890
56	1.52	598	158	4.08	.447	1.49	1487	385	2.82	.316	15.34	.382	.410
57	2.54	625	274	6.98	.458	1.50	1466	380	2.64	.293	15.42	.397	.721
58	2.56	630	283	6.60	.429	1.57	1152	317	3.16	.336	15.19	.394	.892
60	1.49	602	156	4.04	.452	1.58	1438	394	3.08	.325	15.36	.386	.396
61	2.58	631	281	7.12	.460	1.56	1456	393	2.61	.278	15.41	.392	.715
62	2.57	628	282	6.63	.430	1.61	1124	317	3.12	.323	15.23	.389	.889

(1) Tests 50-52 spray bar "B" downstream; Tests 53-55 spray bar "B" upstream.
Tests 56-58 spray bar "A" upstream; Tests 60-62 spray bar "A" downstream.

TABLE 7

TEST DATA

TEST SERIES - 7 FUEL - LIQUID JP5 FLAMEHOLDER - "C"

Test No.	FAN $\dot{M}$ lb/s	FAN T °R	FAN V ft/s	FAN (1) $\dot{M}_F$ lb/m	FAN F/A 10^{-1}	CORE $\dot{M}$ lb/s	CORE T °R	CORE V ft/s	CORE (1) $\dot{M}_F$ lb/m	CORE F/A 10^{-1}	P_{FH} PSIA	$\overline{F}/A$ 10^{-1}	$\frac{V_F}{V_c}$
65	1.62	588	166	4.06	.417	1.48	1436	370	2.97	.334	15.33	.378	.448
66	2.54	629	276	6.32	.414	1.45	1442	361	2.90	.333	15.45	.385	.764
67	2.50	632	274	6.10	.406	1.13	1432	280	2.20	.325	15.38	.381	.978
68	1.51	592	156	3.95	.436	1.54	1106	298	3.10	.335	15.25	.385	.523
69	2.48	631	271	6.19	.416	1.52	1092	288	2.95	.323	15.38	.381	.941
70	2.53	634	279	6.16	.406	1.09	1084	205	2.22	.339	15.35	.386	1.36

(1) Tests 65 through 70 spray bar "A" downstream.

TABLE 8

TEST DATA

TEST SERIES - 8 FUEL - LIQUID JP5 FLAMEHOLDER - "VEE"

Test No.	FAN (1)					CORE (1)							
	$\dot{M}$ lb/s	T ^{o}R	V ft/s	$\dot{M}_F$ lb/m	F/A 10^{-1}	$\dot{M}$ lb/s	T ^{o}R	V ft/s	$\dot{M}_F$ lb/m	F/A 10^{-1}	P_{FH} PSIA	$\bar{F}/A$ 10^{-1}	$\frac{V_F}{V_c}$
76	1.62	589	166	3.87	.398	1.51	1432	375	2.70	.298	15.36	.350	.442
77	1.57	597	162	4.22	.448	1.48	1420	364	2.95	.332	15.39	.392	.445
78	2.48	624	266	5.48	.368	1.47	1458	368	2.77	.314	15.53	.348	.722
79	2.54	631	274	6.60	.433	1.45	1445	359	3.00	.345	15.58	.401	.763
80	1.48	601	154	3.82	.430	1.58	1422	389	2.77	.292	15.40	.359	.396
81	1.50	603	156	4.15	.461	1.56	1434	386	2.99	.319	15.45	.389	.404
82	2.59	626	278	5.97	.384	1.52	1409	367	2.59	.284	15.54	.347	.757
83	2.54	632	274	6.93	.454	1.57	1420	381	2.98	.316	15.60	.402	.720

(1) Tests 76 through 79 spray bar "A" located downstream; Tests 80 through 83 spray bar "A" located upstream.

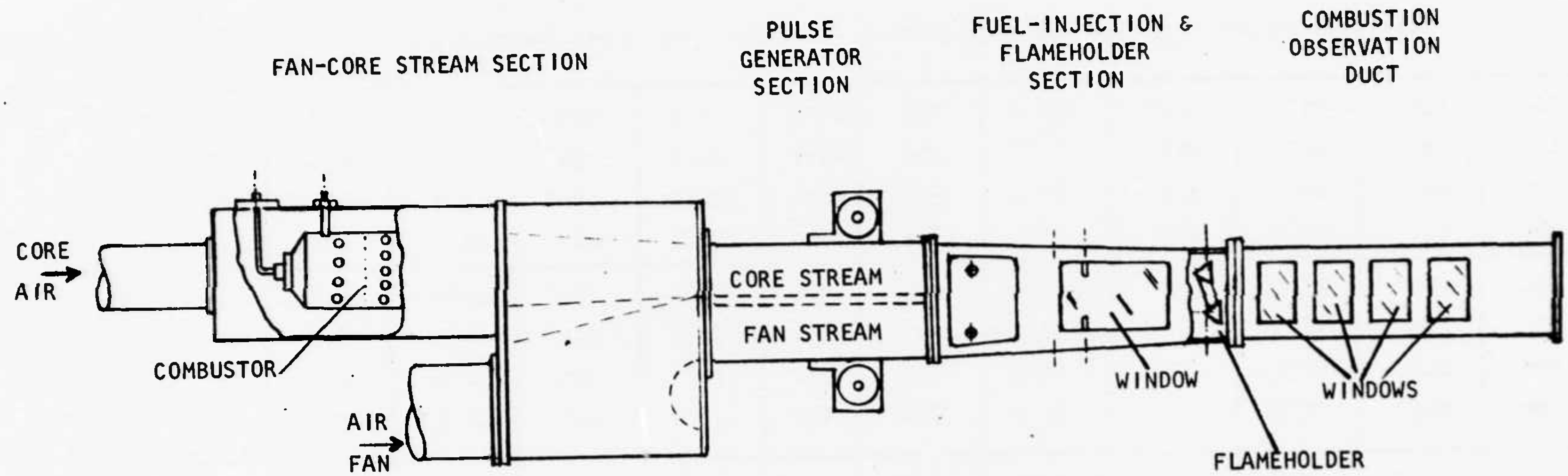

Figure 1. Flameholder Test Rig Assembly

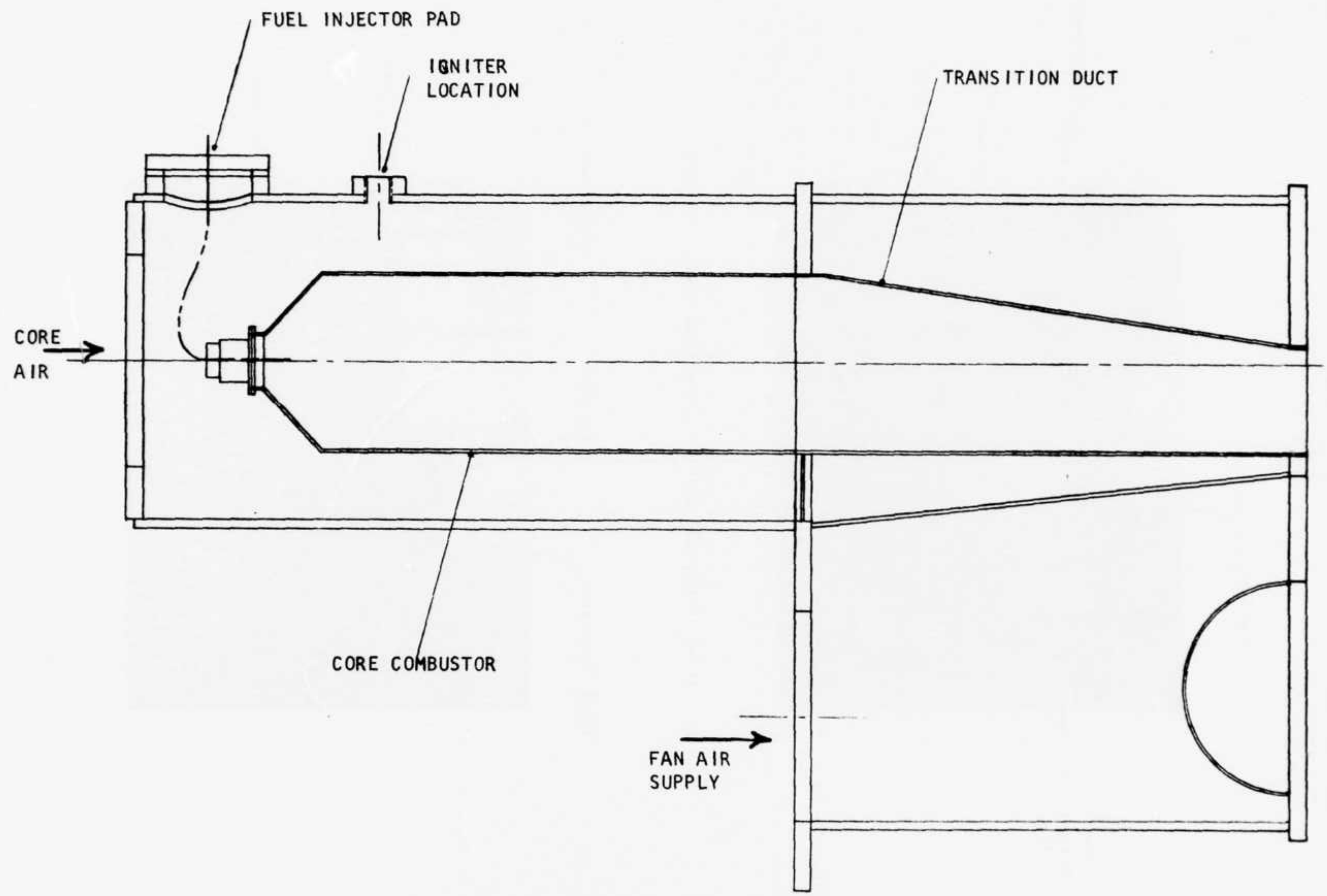

Figure 2. Fan–Core Stream Section

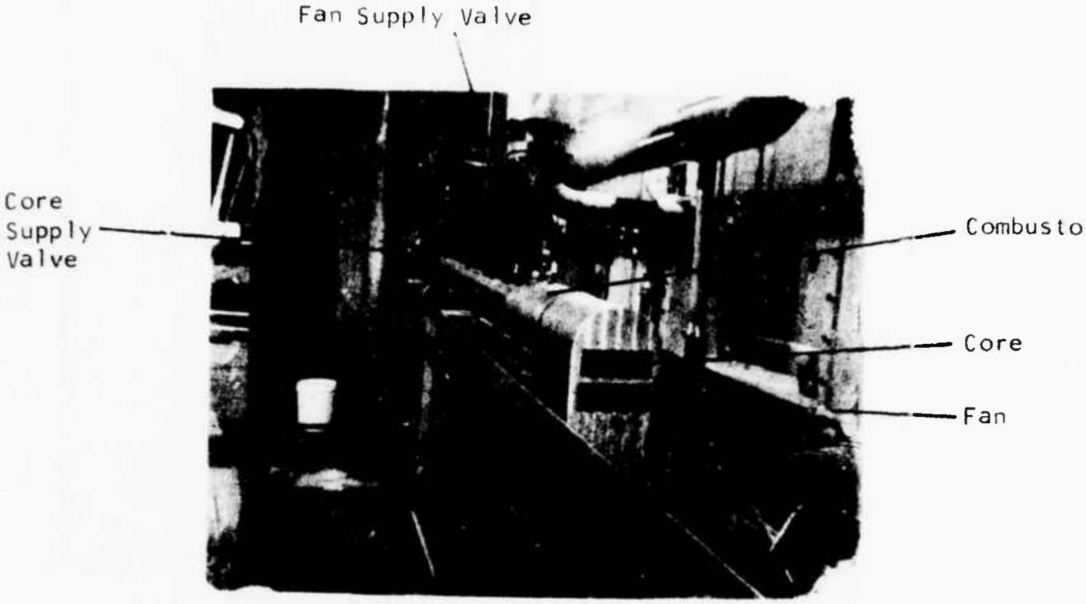

a. Inlet fan/core section connected to air supply

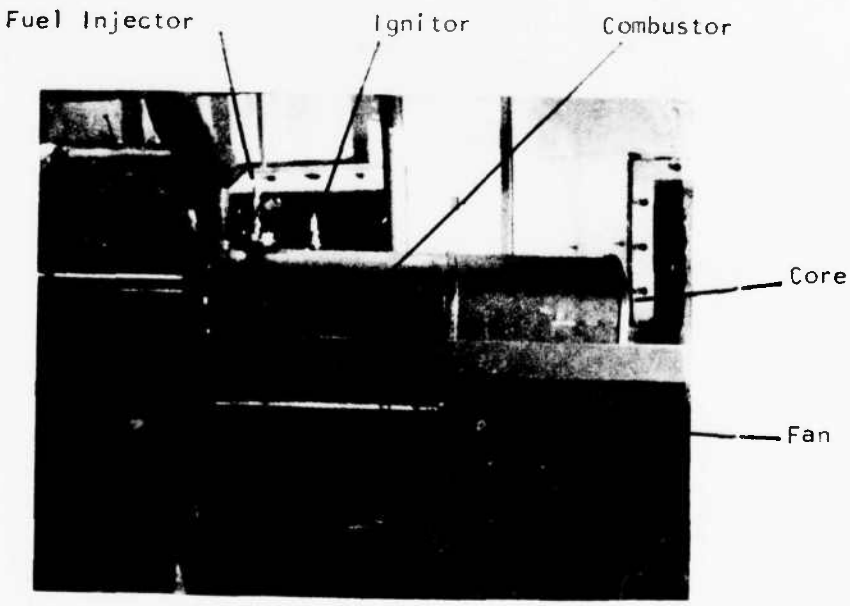

b. Side view of inlet fan/core section

Figure 3. Test Rig Inlet Fan/Core Section

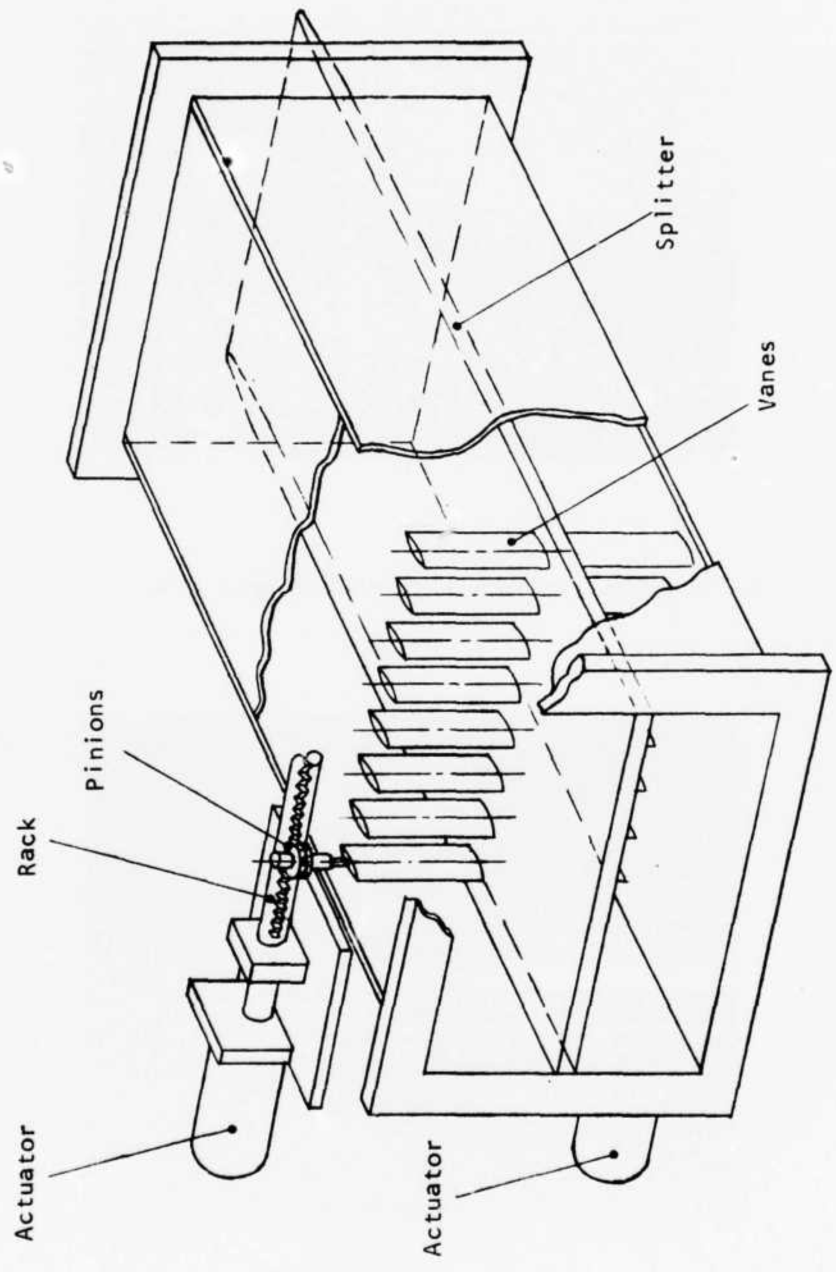

Figure 4. Pulse Generator Section

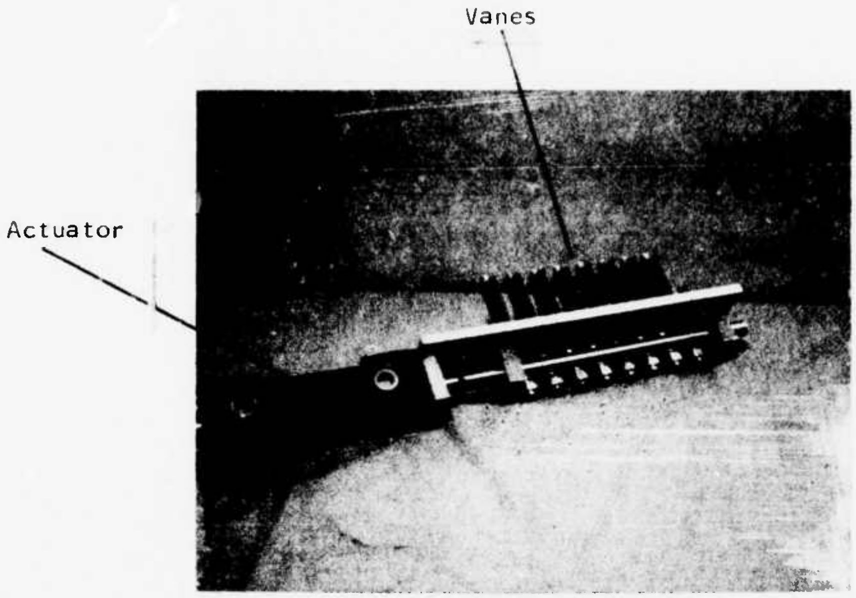

a. Core stream vane and actuator assembly

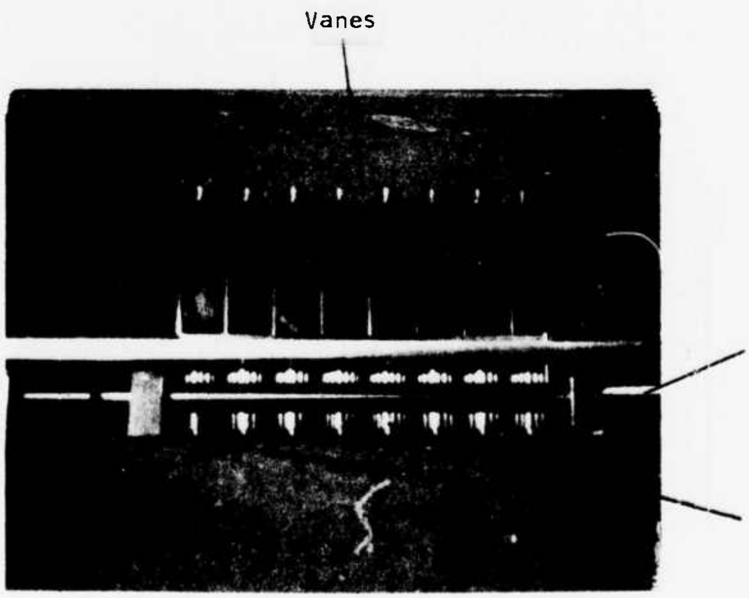

b. Vane assembly with rack and pinion grive

Figure 5. Pulse Generator Vane Assembly

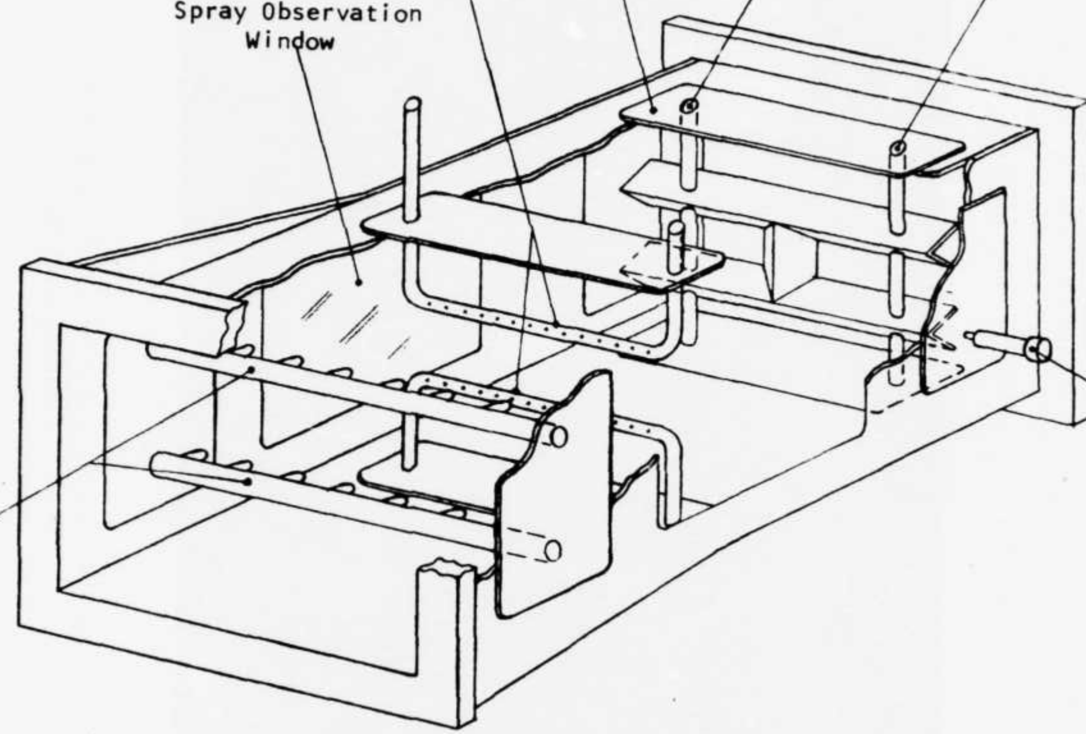

Figure 6. Fuel Injection and Flameholder Section

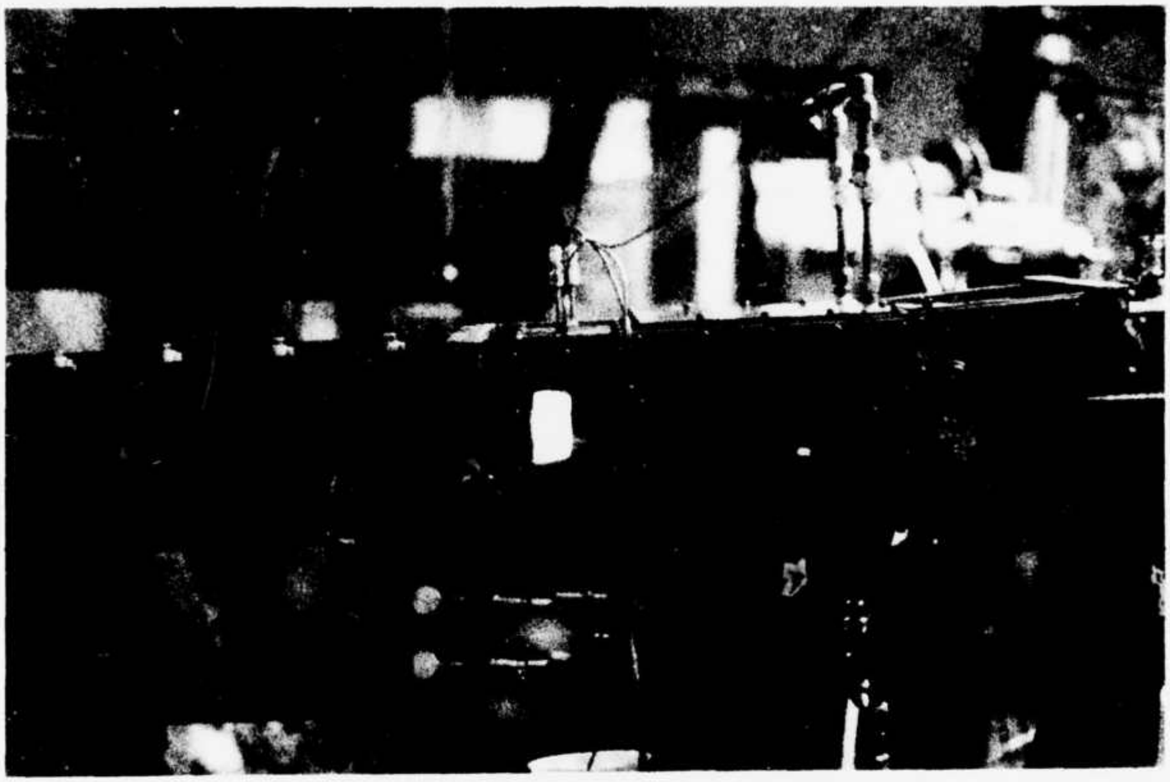

Figure 7. Fuel Injection And Flameholder Section
(Torch Operation)

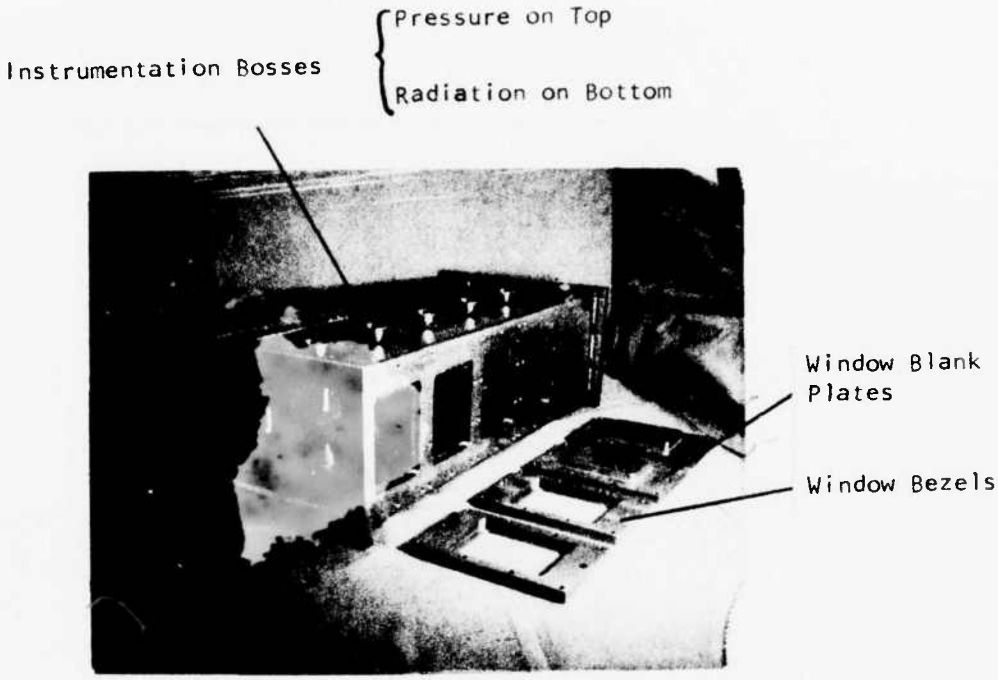

Figure 8. Combustion Observation Section

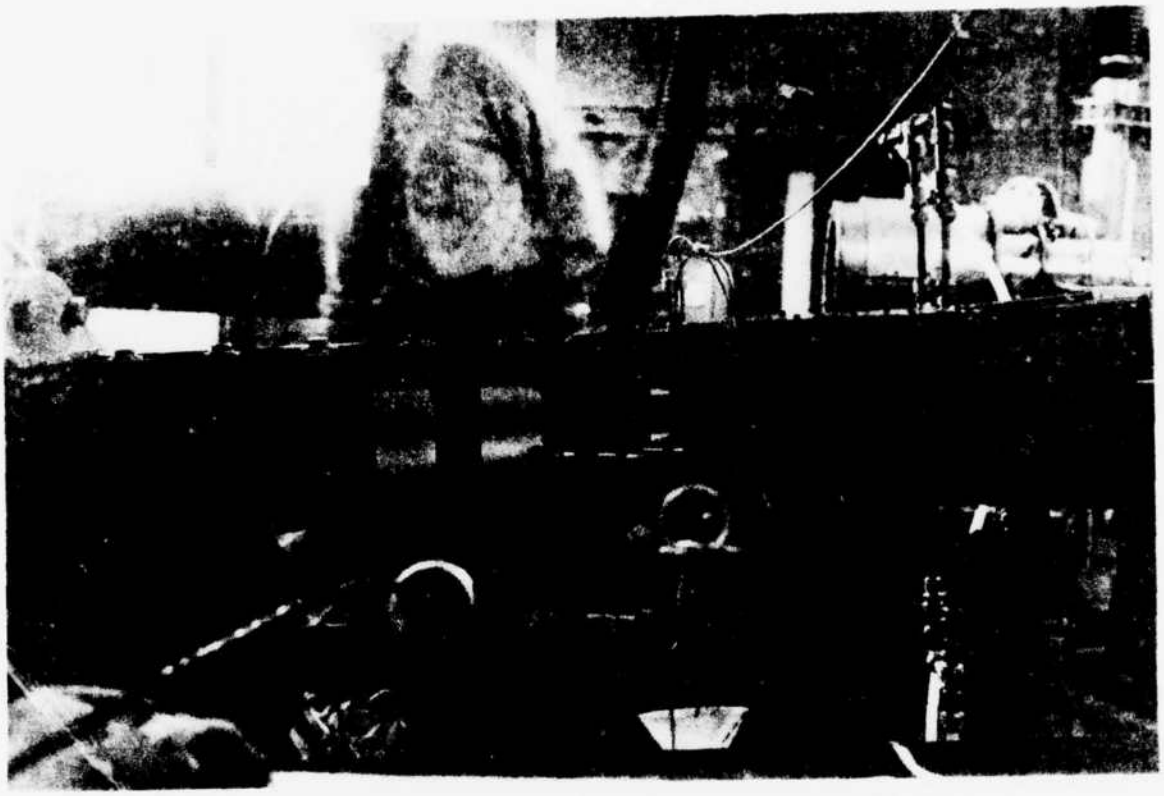

Figure 9. Local Gas Burning in Observation Section

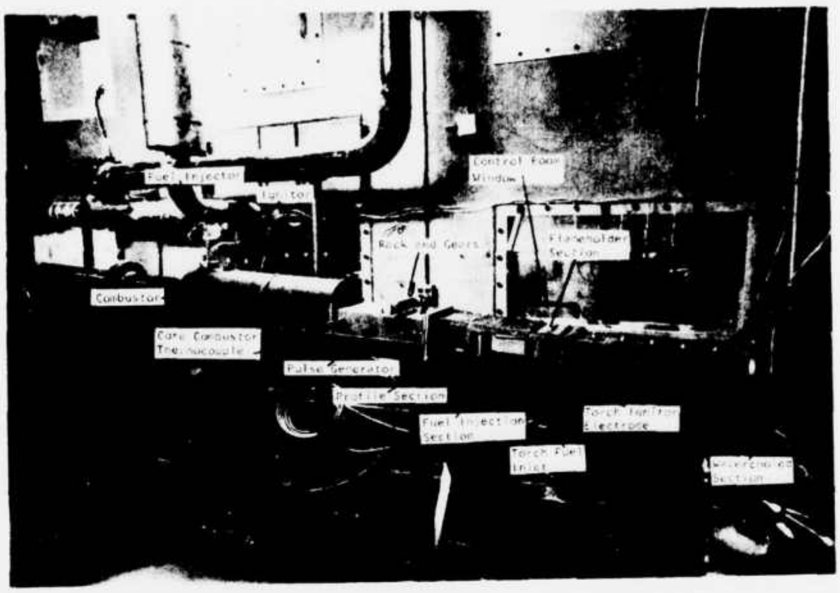

Figure 10. Combustion Test Rig Assembly

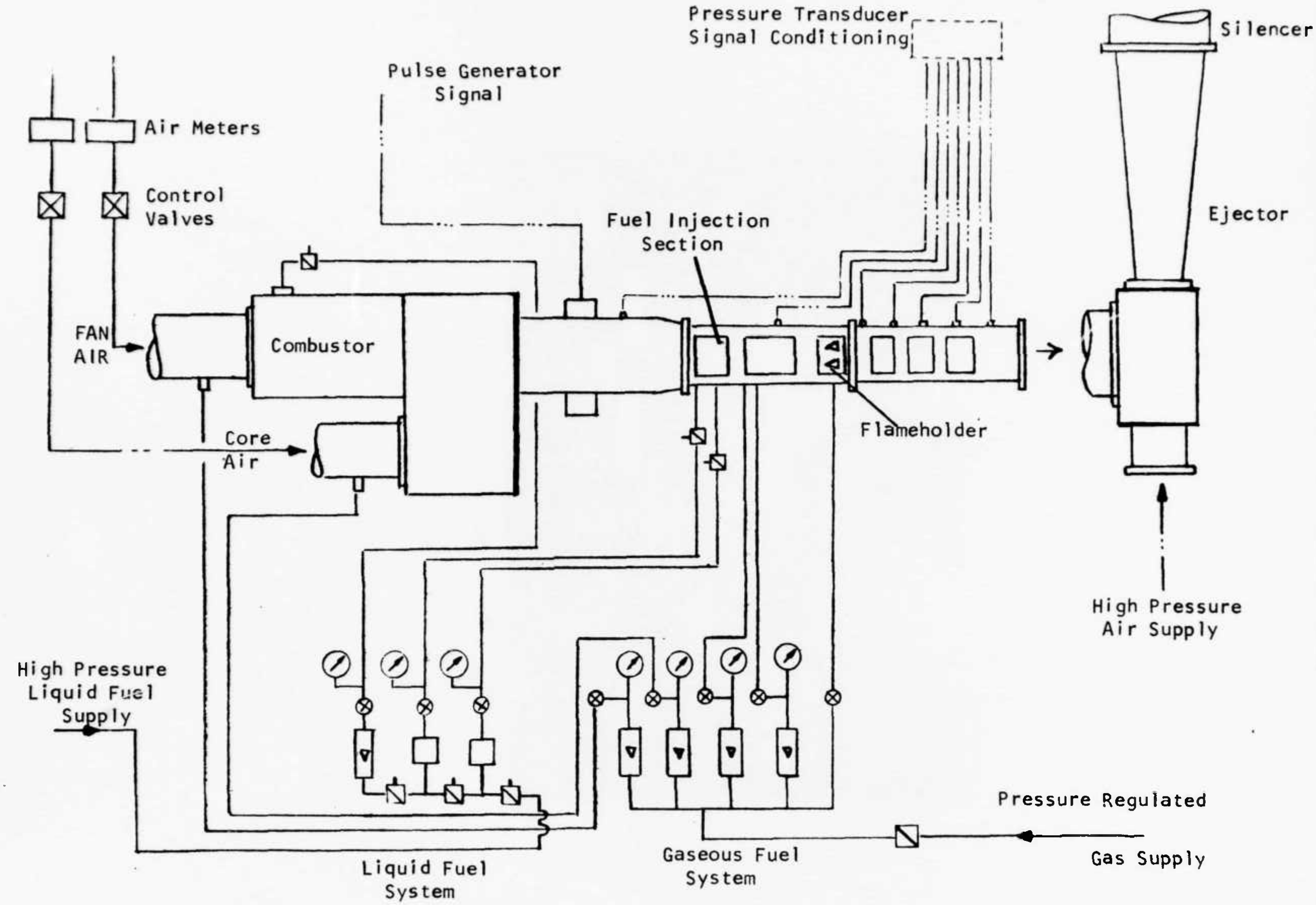

Figure 11. Overall Test Rig Arrangement

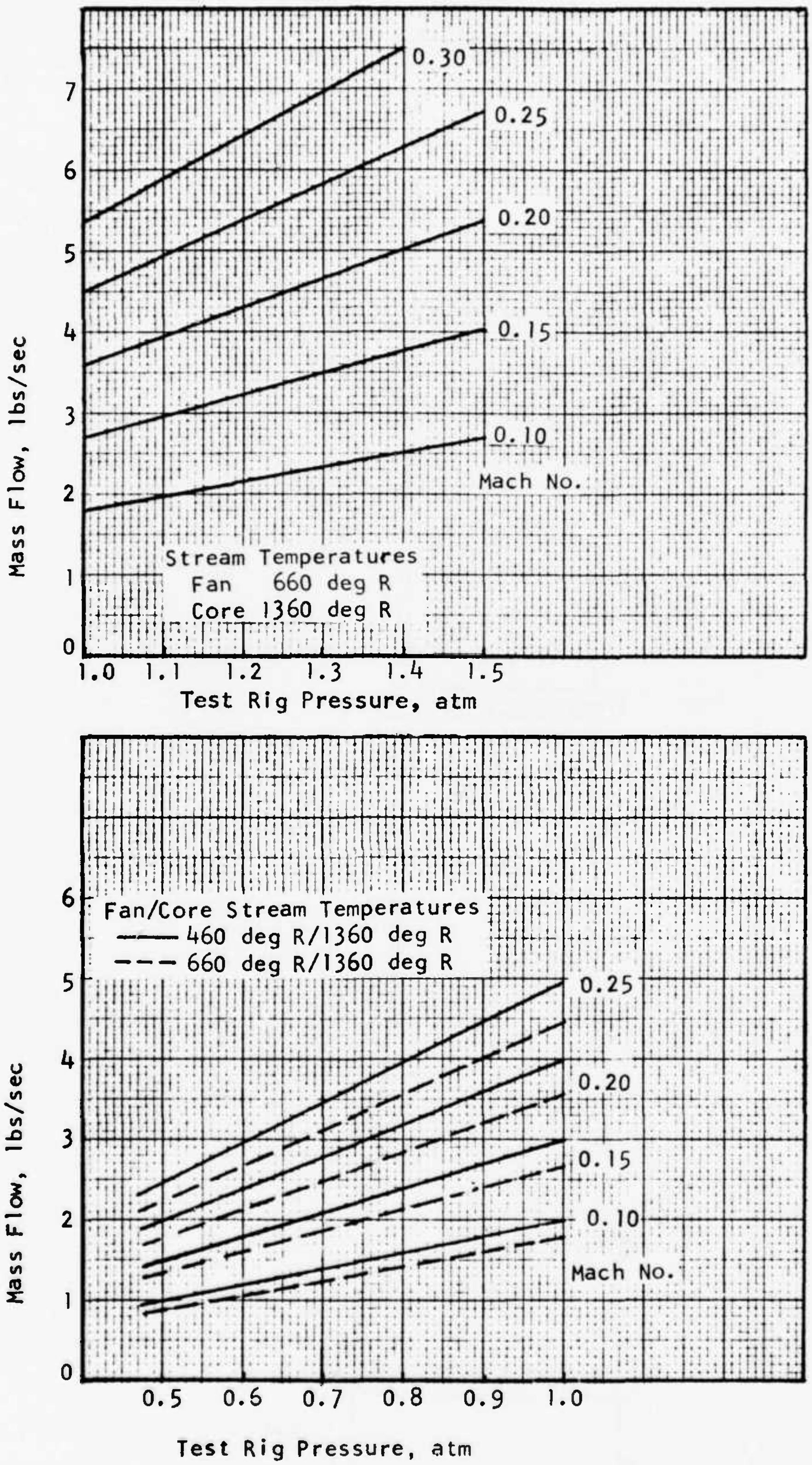

Figure 12. Test Rig Air Flow Rates

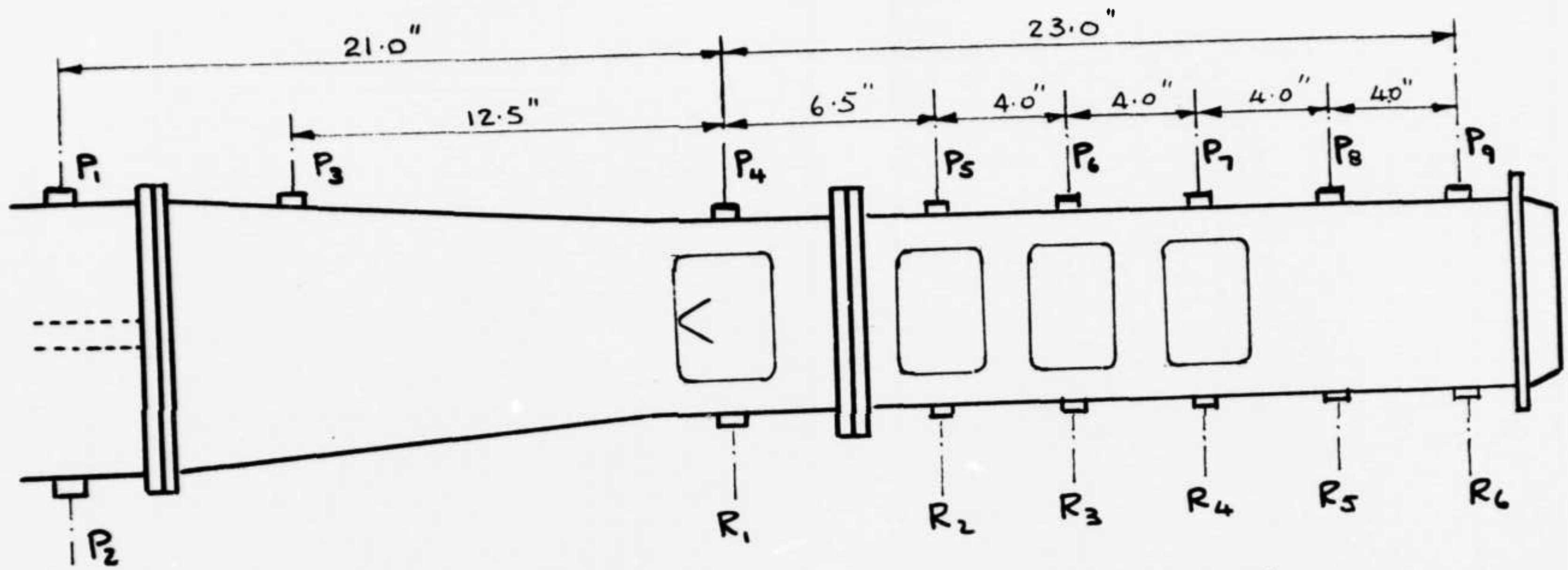

Figure 13. Pressure And Radiation Transducer Locations In Flameholder Rig

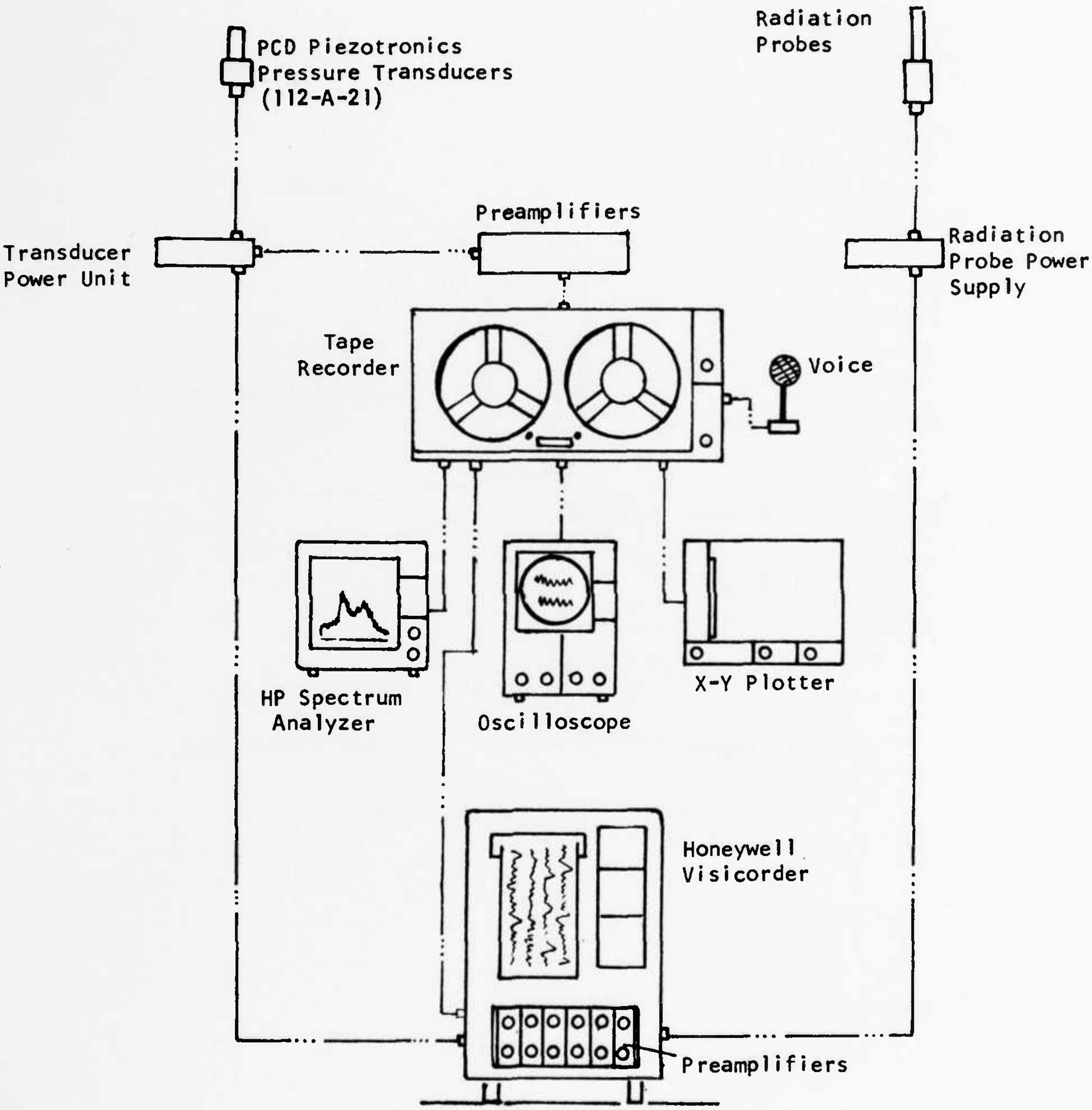

Figure 14. Dynamic Recording Instrumentation

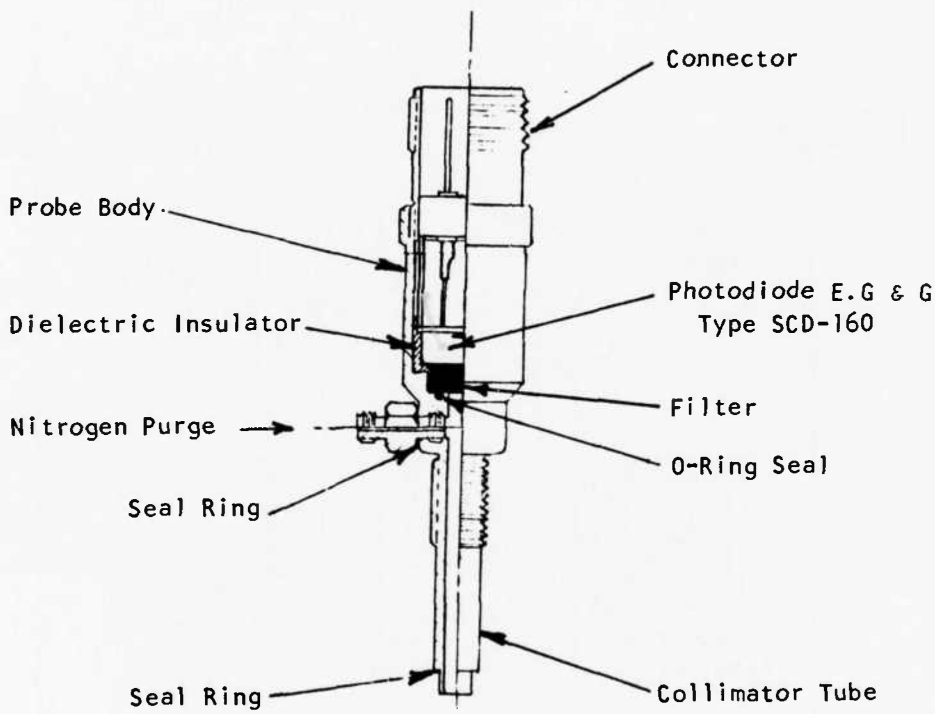

Figure 15. Radiation Probe

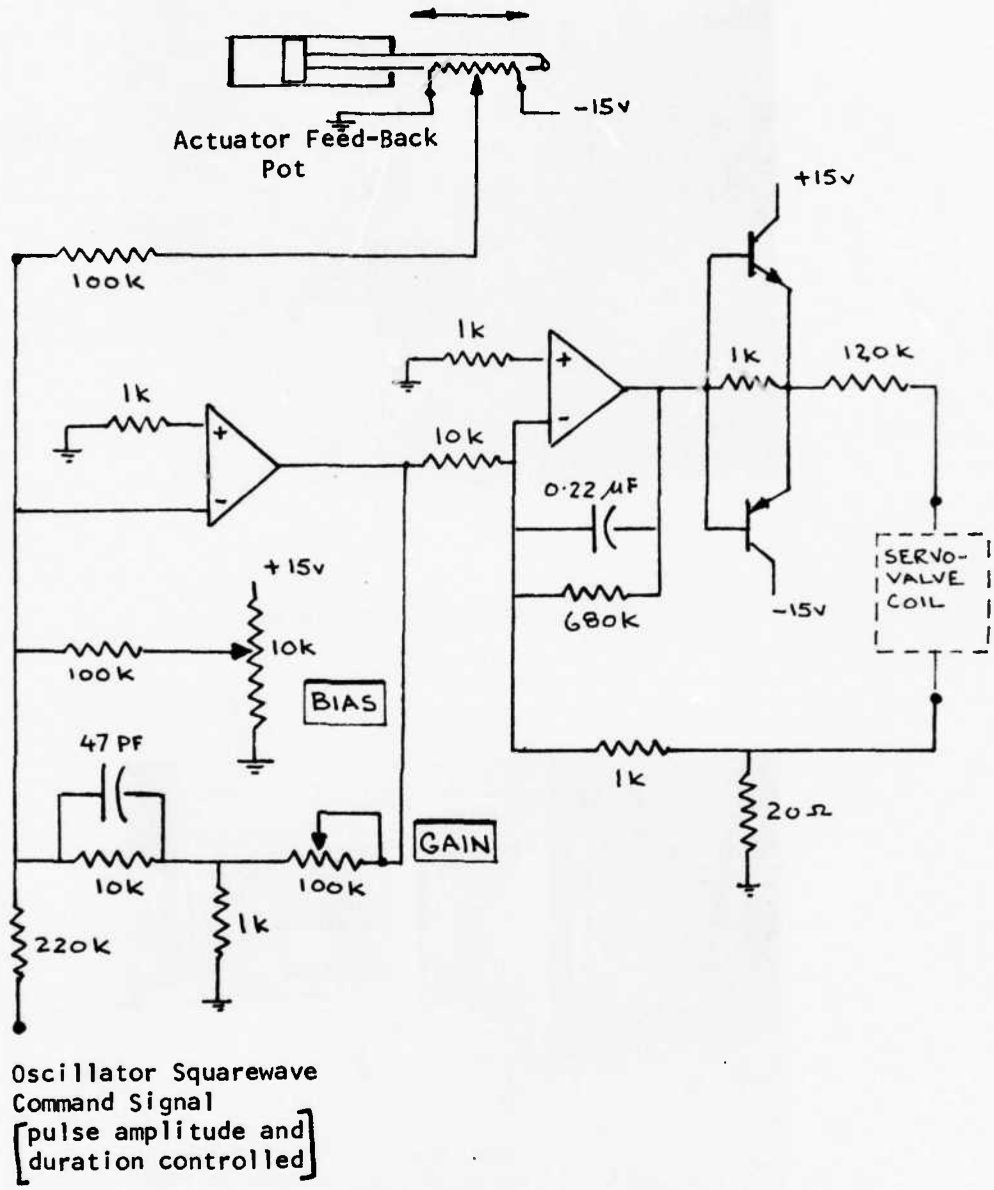

Figure 16. Electronic Servo-Controller For Pulse Generator

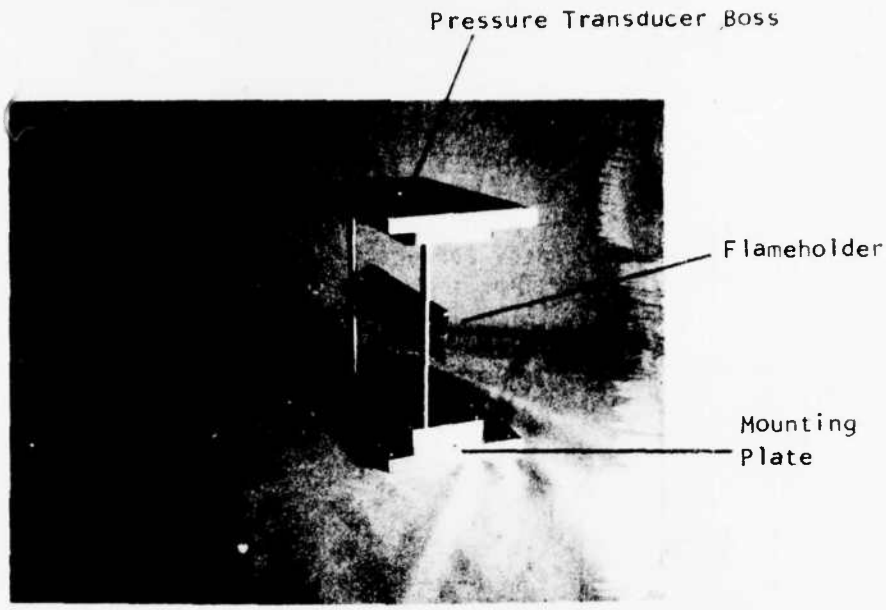

a. Flameholder and mounting plates

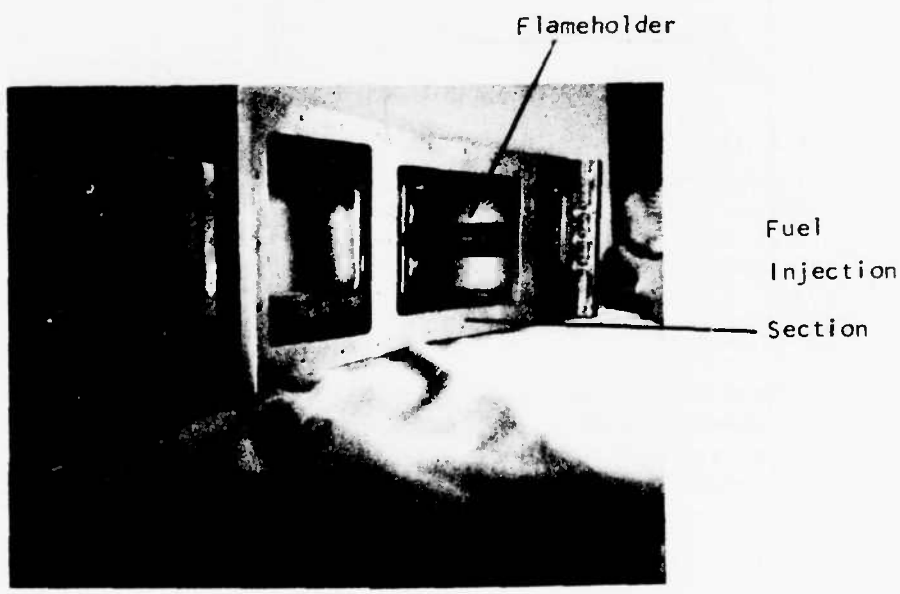

b. Flameholder installed in fuel injection section

Figure 17. Flameholder Assembly

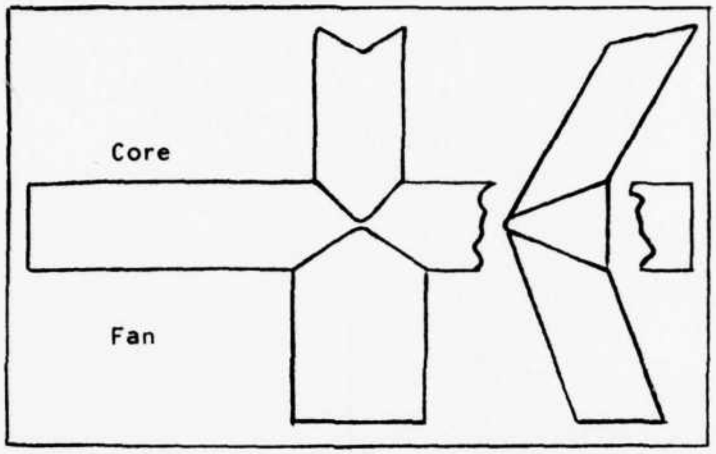

Type A

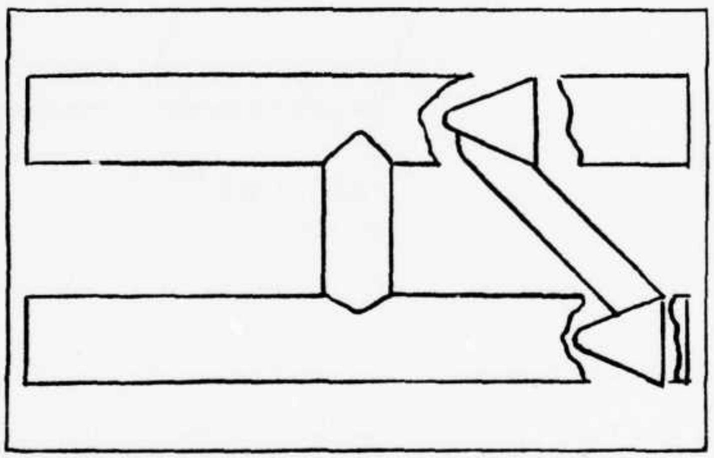

Type C (Double Gutter)

Figure 18. Preliminary Flameholders Configurations

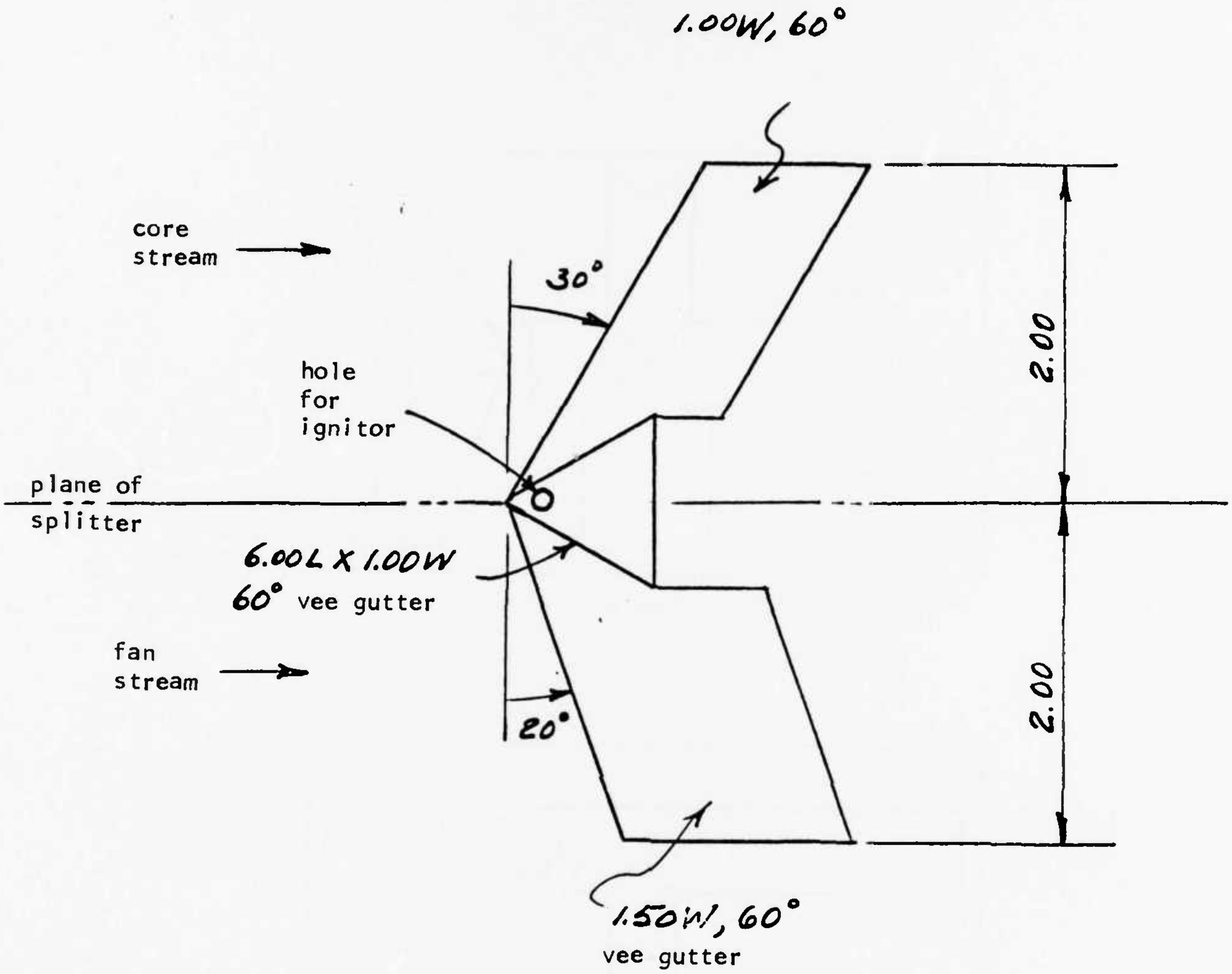

1. Weld End Plates On All Gutters.
2. Mount With Rod and Tube/Support As Was Simple Vee Gutter.

Figure 19. Type A Flameholder Configuration

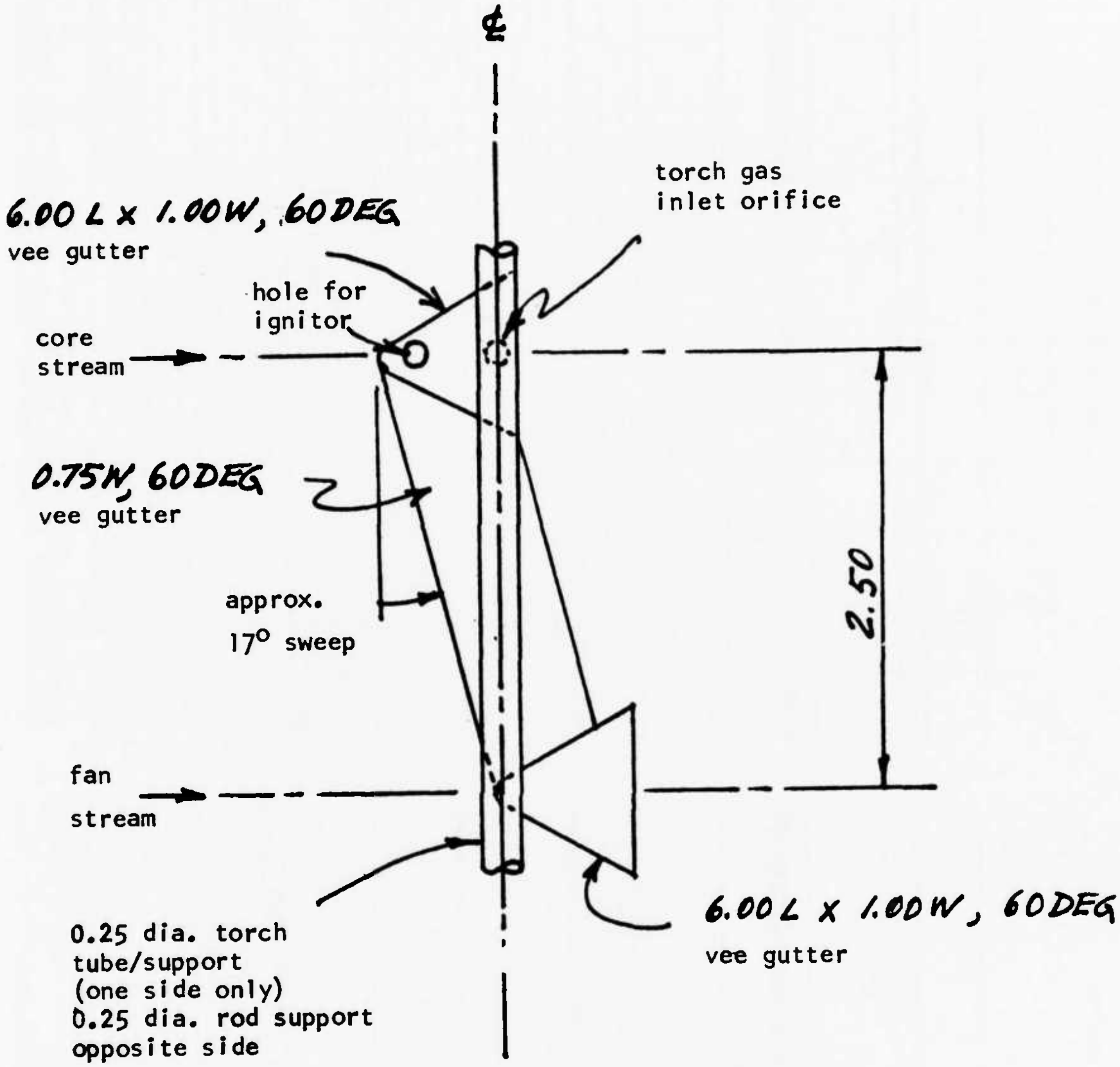

Figure 20. Type C Flameholder Configuration

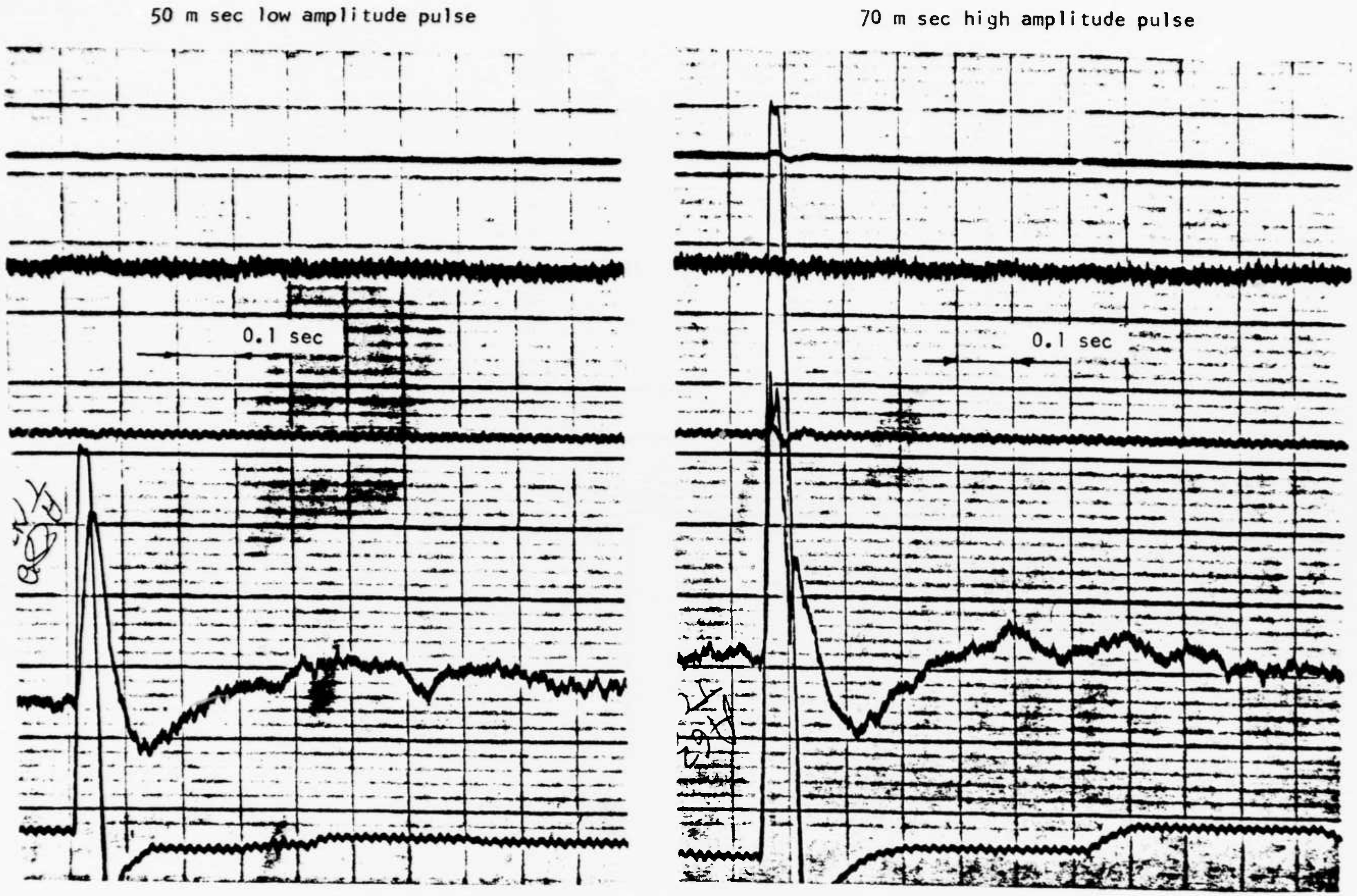

Figure 21. Typical Pressure Pulses

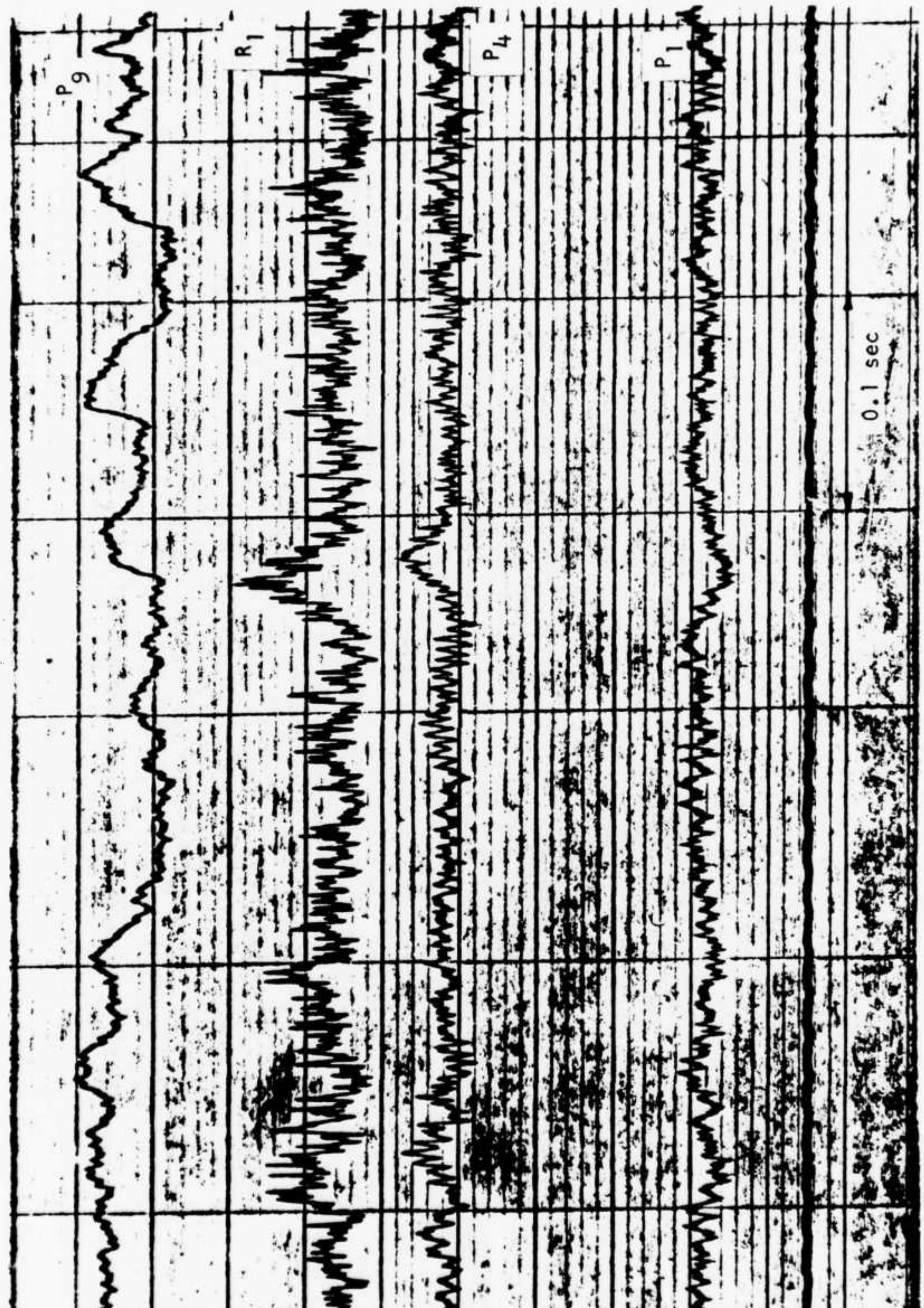

Figure 22. Unsteady Pressure and Radiation Characteristics
Series 1, Test 1

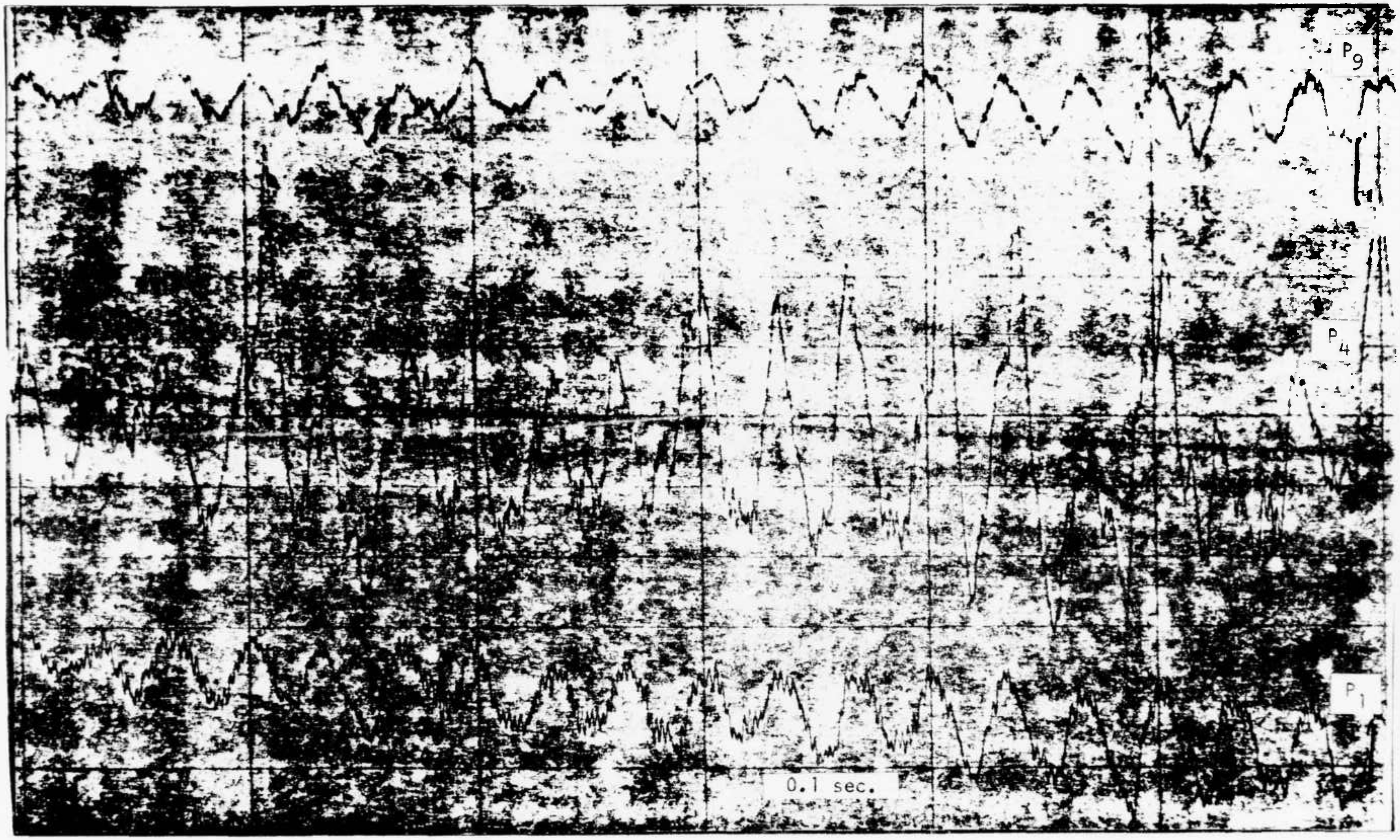

Figure 23. Unsteady Pressure and Radiation Characteristics
Series 1, Test 5

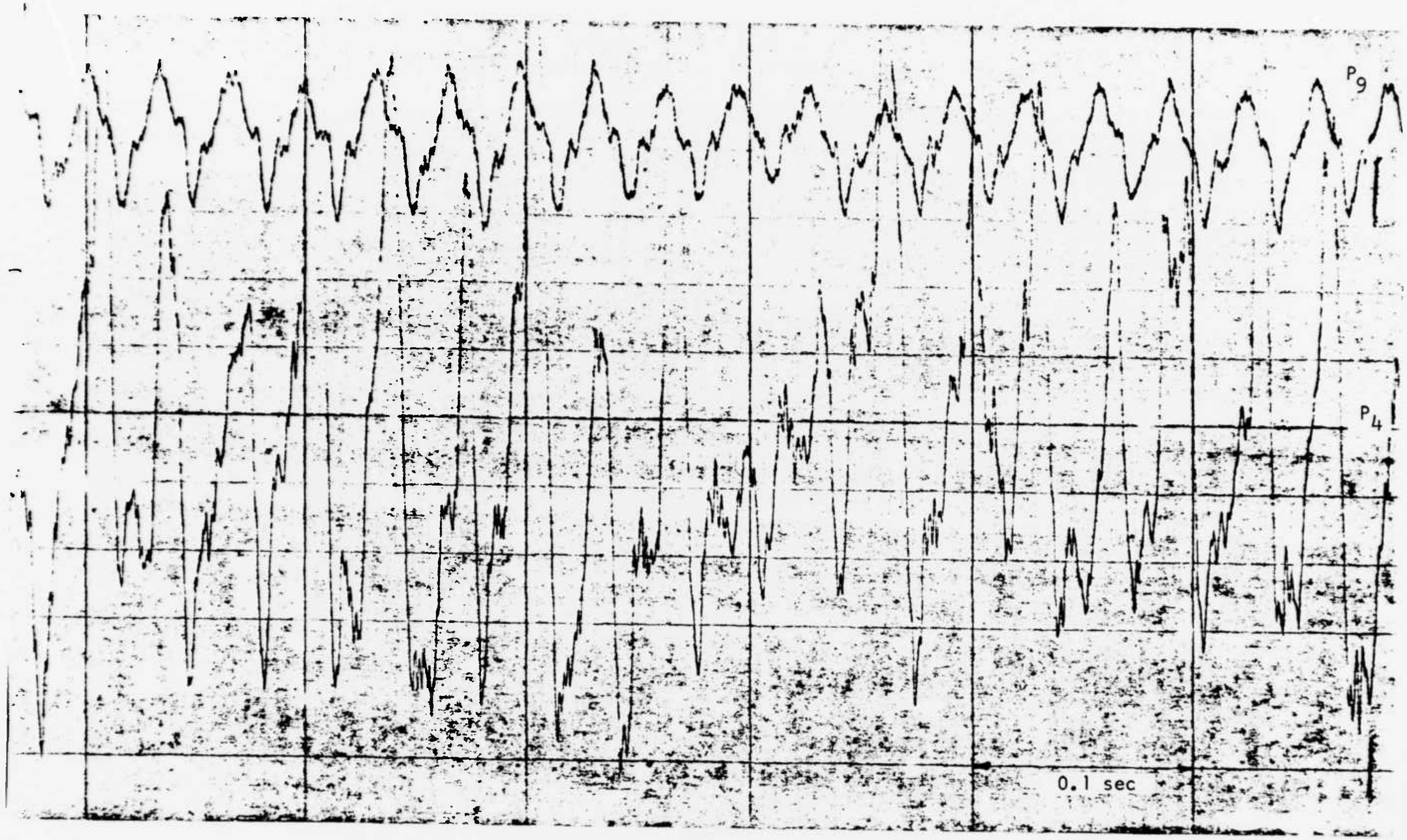

Figure 24. Unsteady Pressure and Radiation Characteristics
Series 1, Test 6

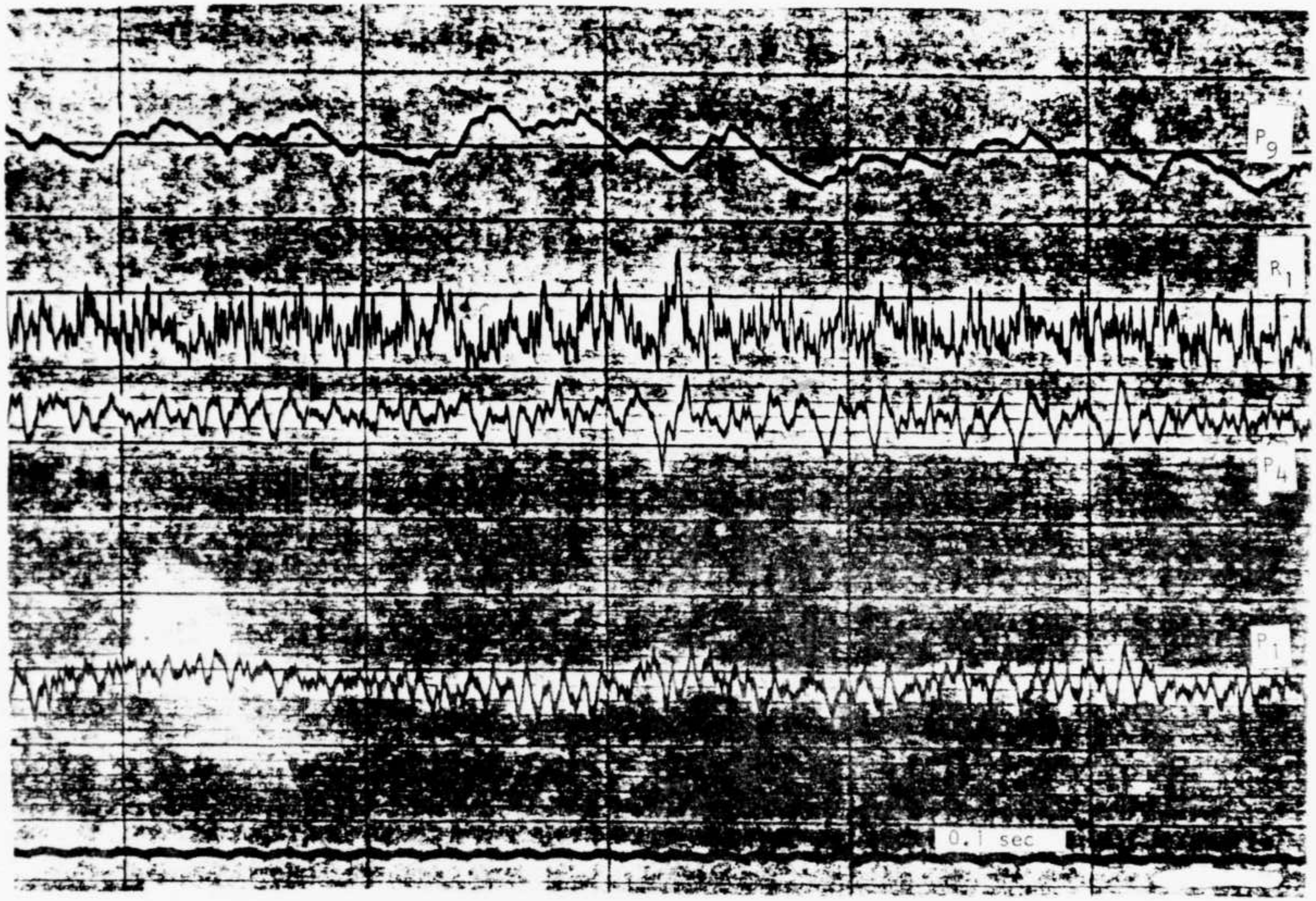

Figure 25. Unsteady Pressure and Radiation Characteristics
Series 1, Test 8-No Pulse

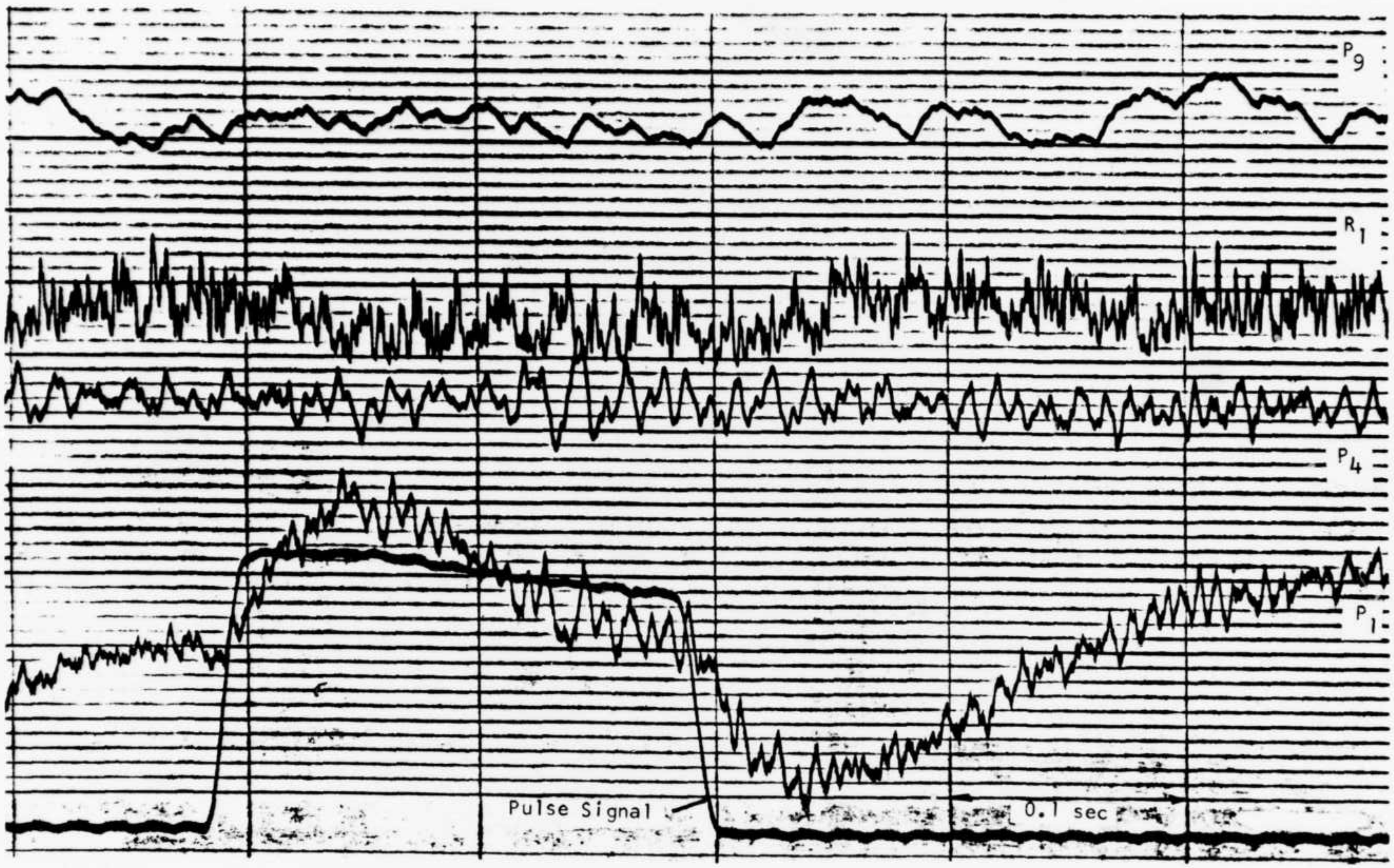

Figure 26. Unsteady Pressure and Radiation Characteristics
Series 1, Test 8-200 msec Pulse

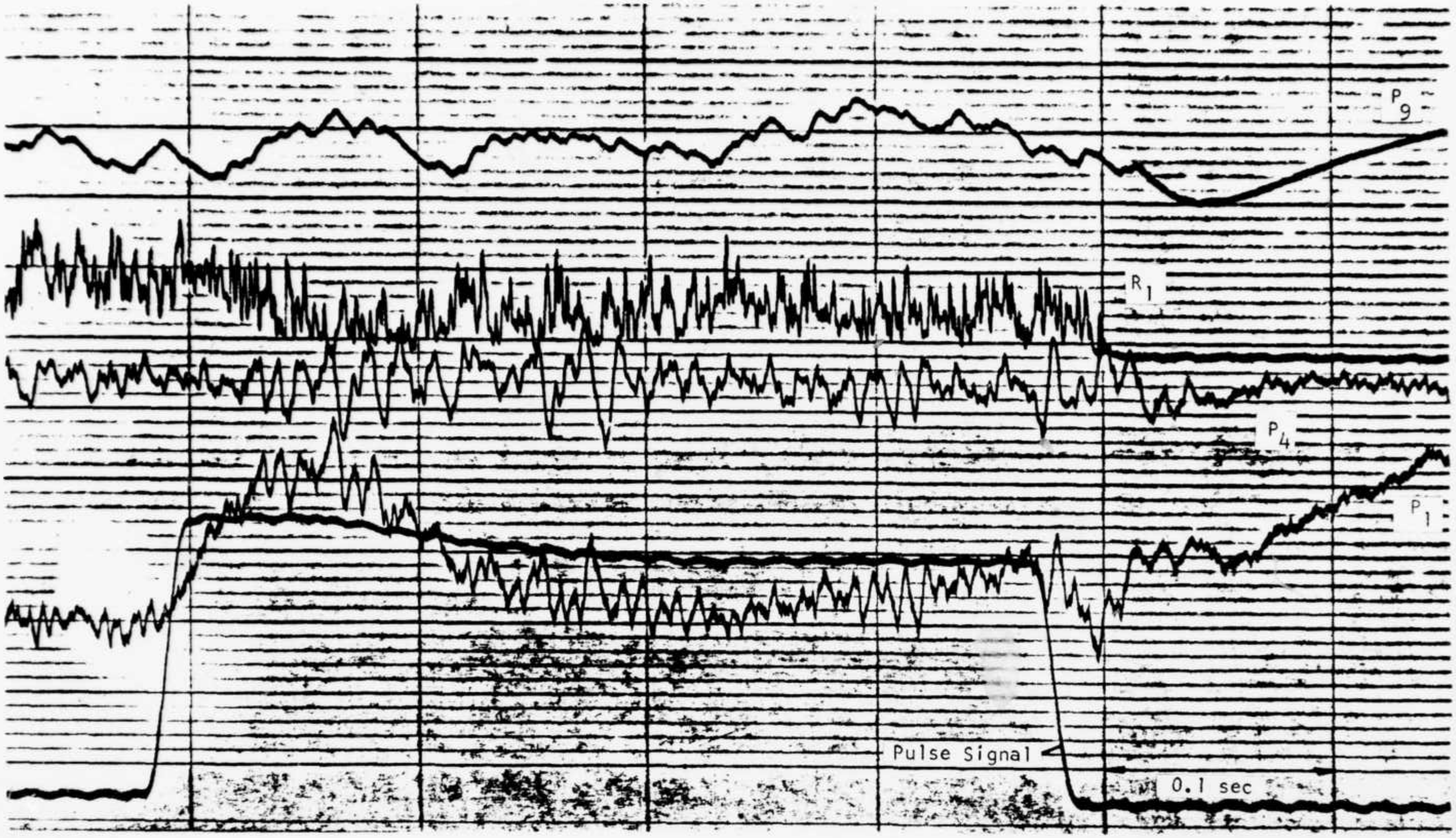

Figure 27. Unsteady Pressure and Radiation Characteristics
Series 1, Test 8-400 msec Pulse

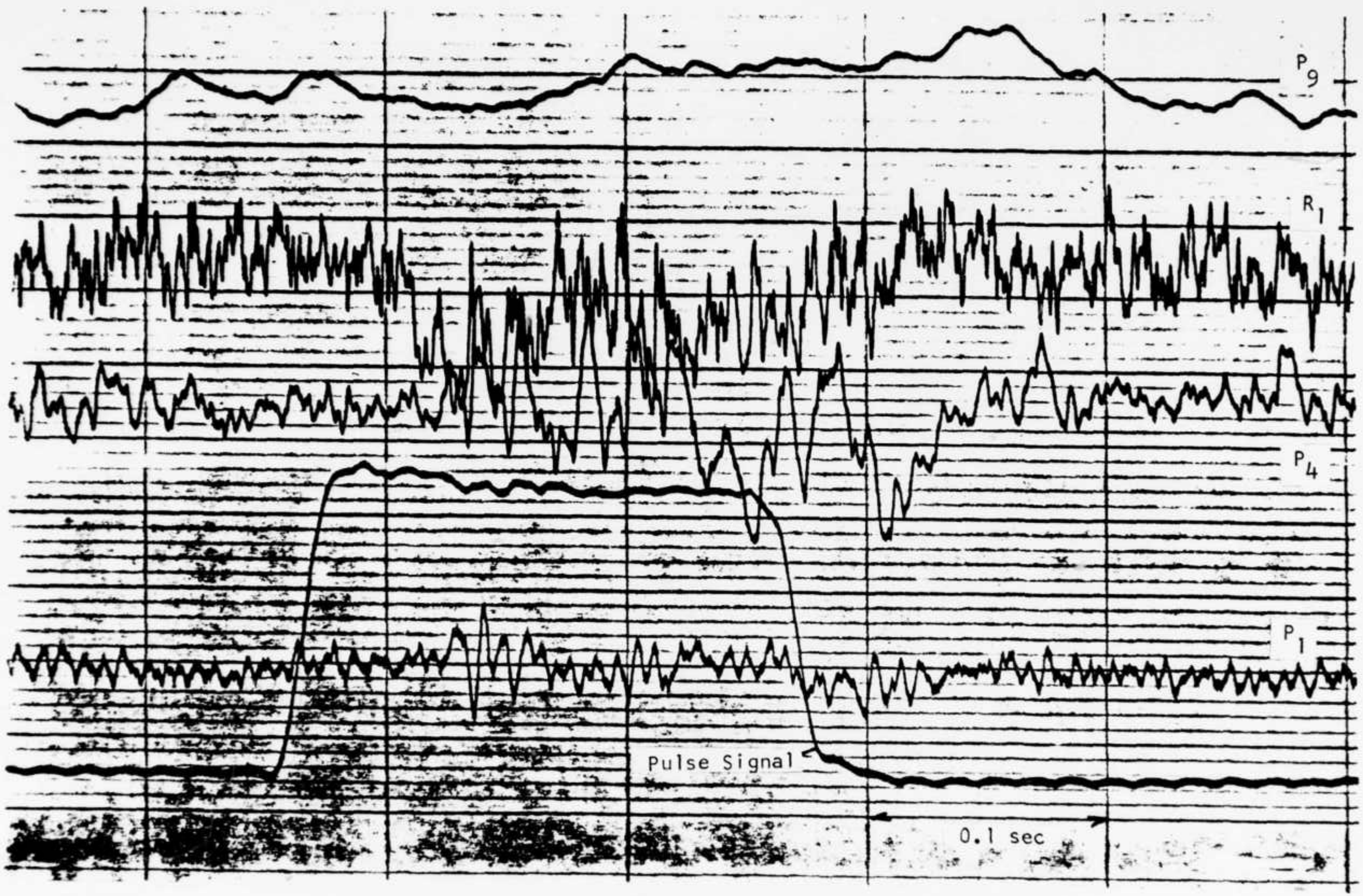

Figure 28. Unsteady Pressure and Radiation Characteristics
Series 1, Test 11

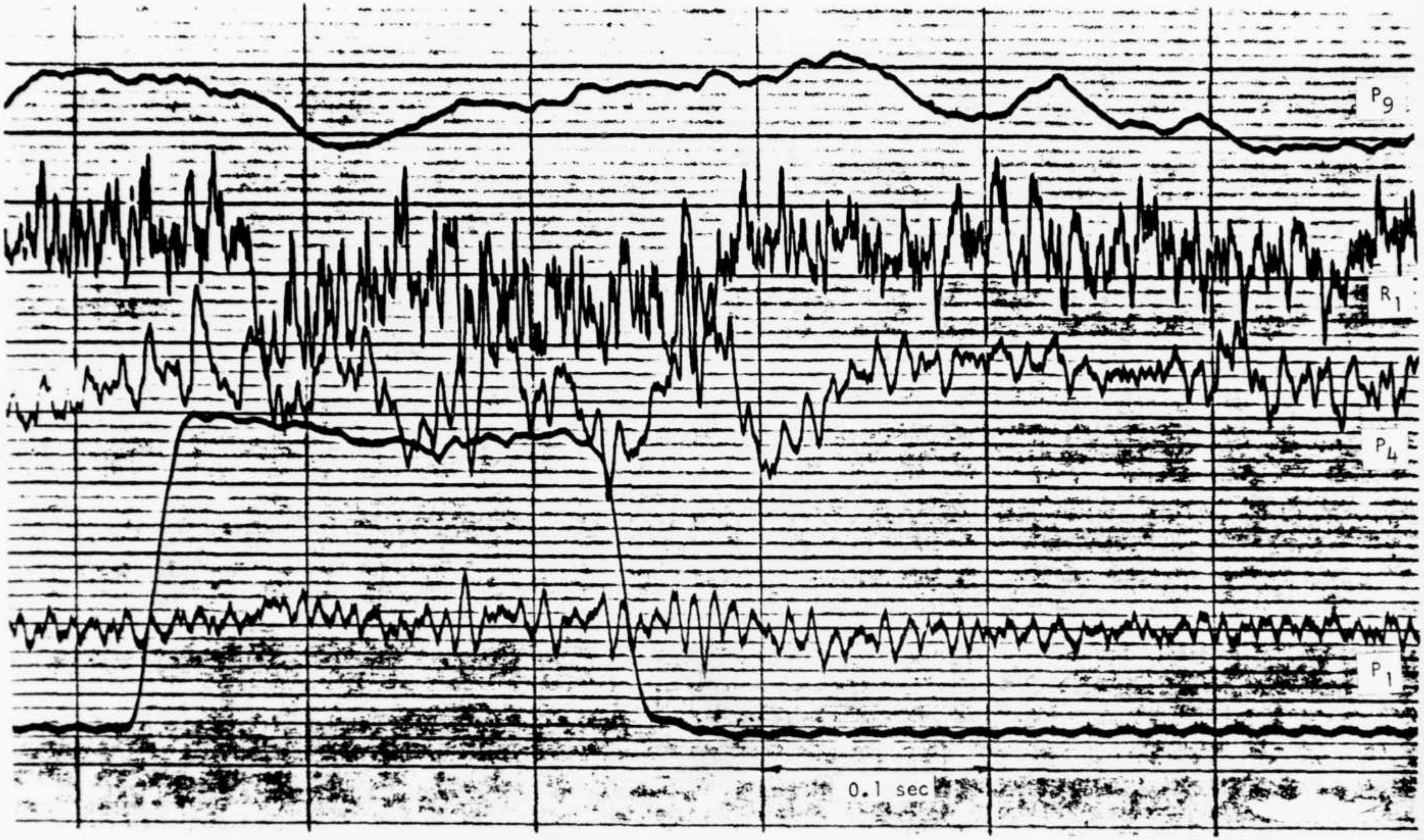

Figure 29. Unsteady Pressure and Radiation Characteristics
Series 1, Test 13

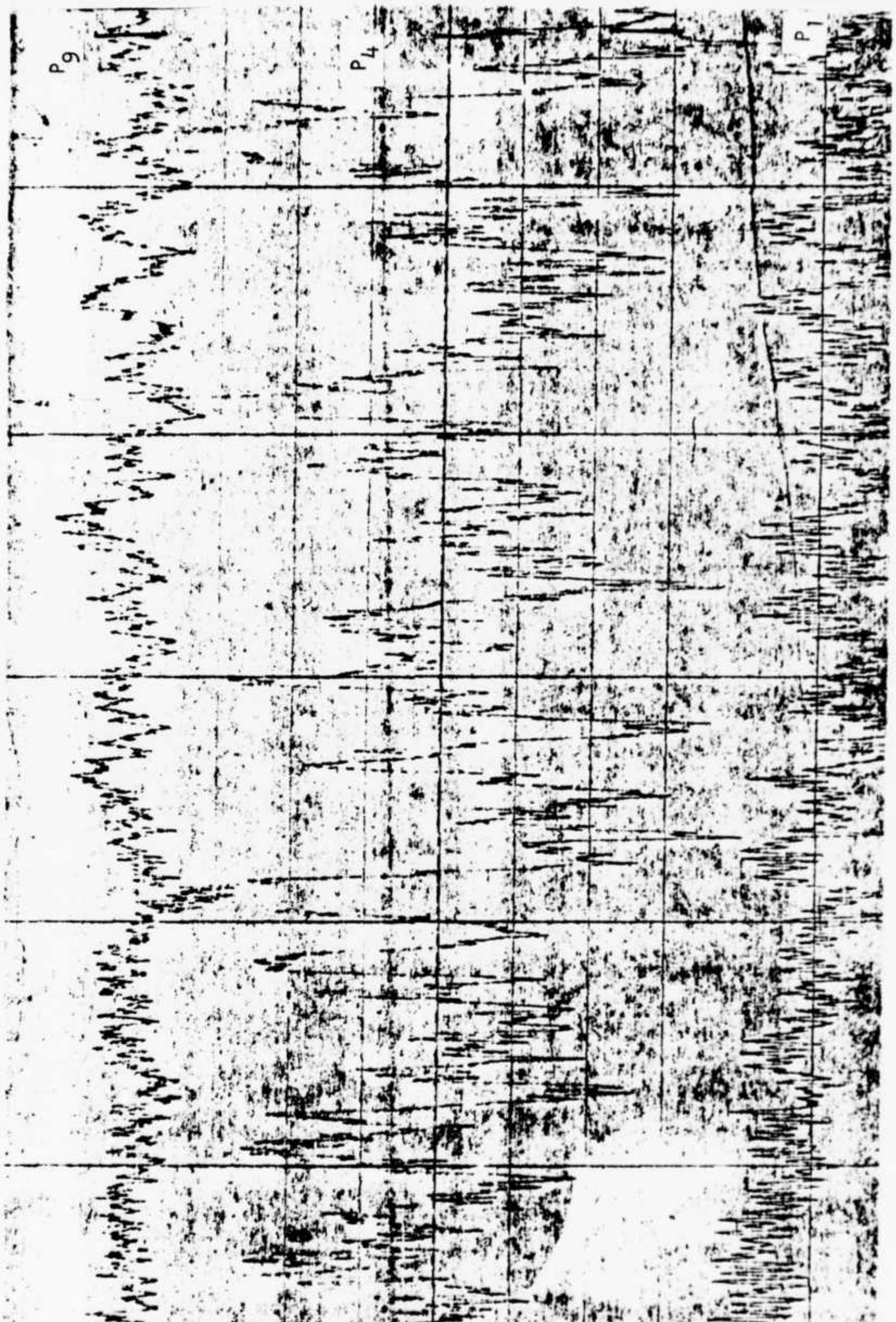

Figure 30. Unsteady Pressure and Radiation Characteristics
Series 2, Test 15

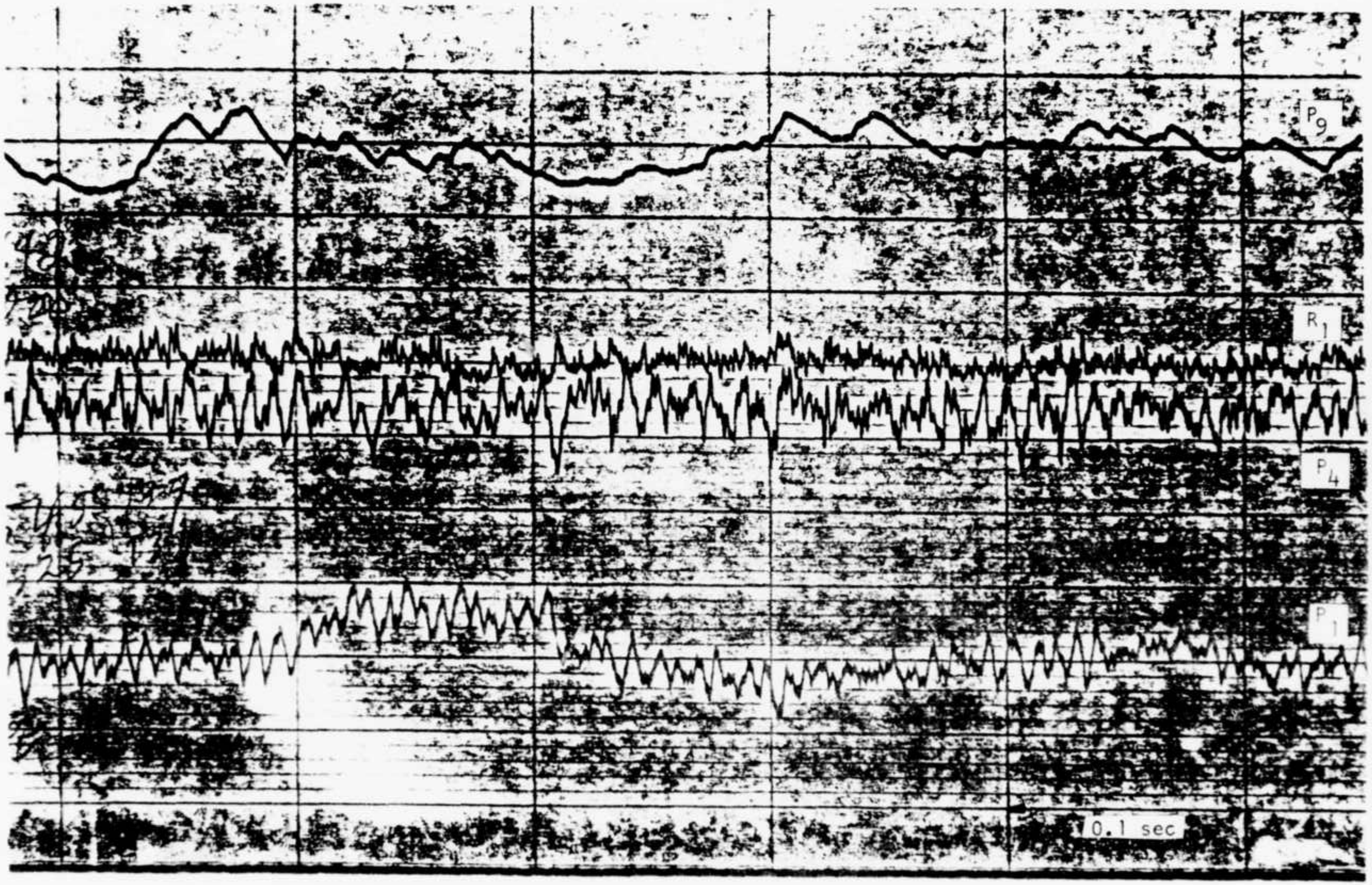

Figure 31. Unsteady Pressure and Radiation Characteristics
Series 2, Test 19-Small Pulse Amplitude

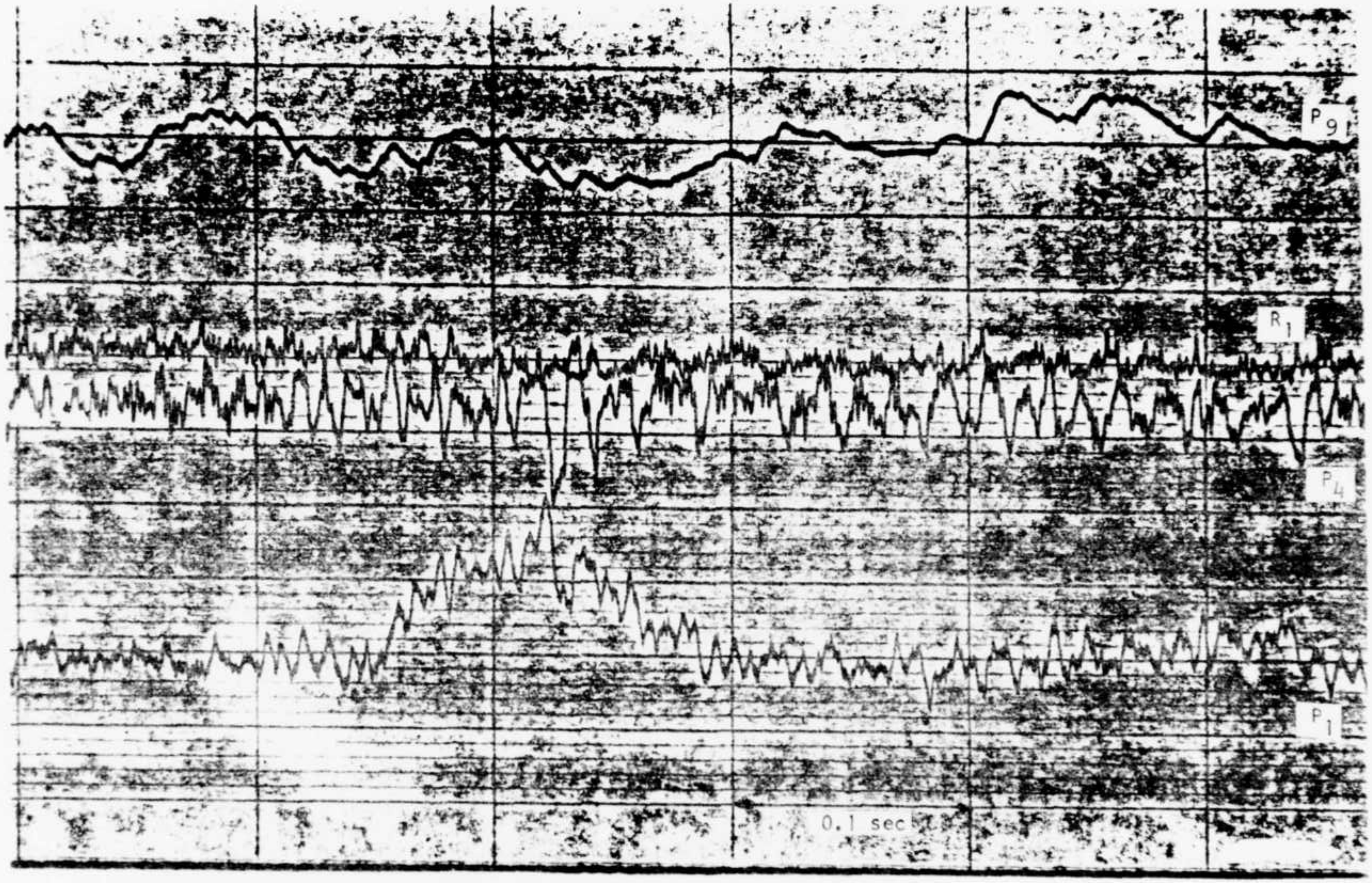

Figure 32. Unsteady Pressure and Radiation Characteristics
Series 2, Test 19-Medium Pulse Amplitude

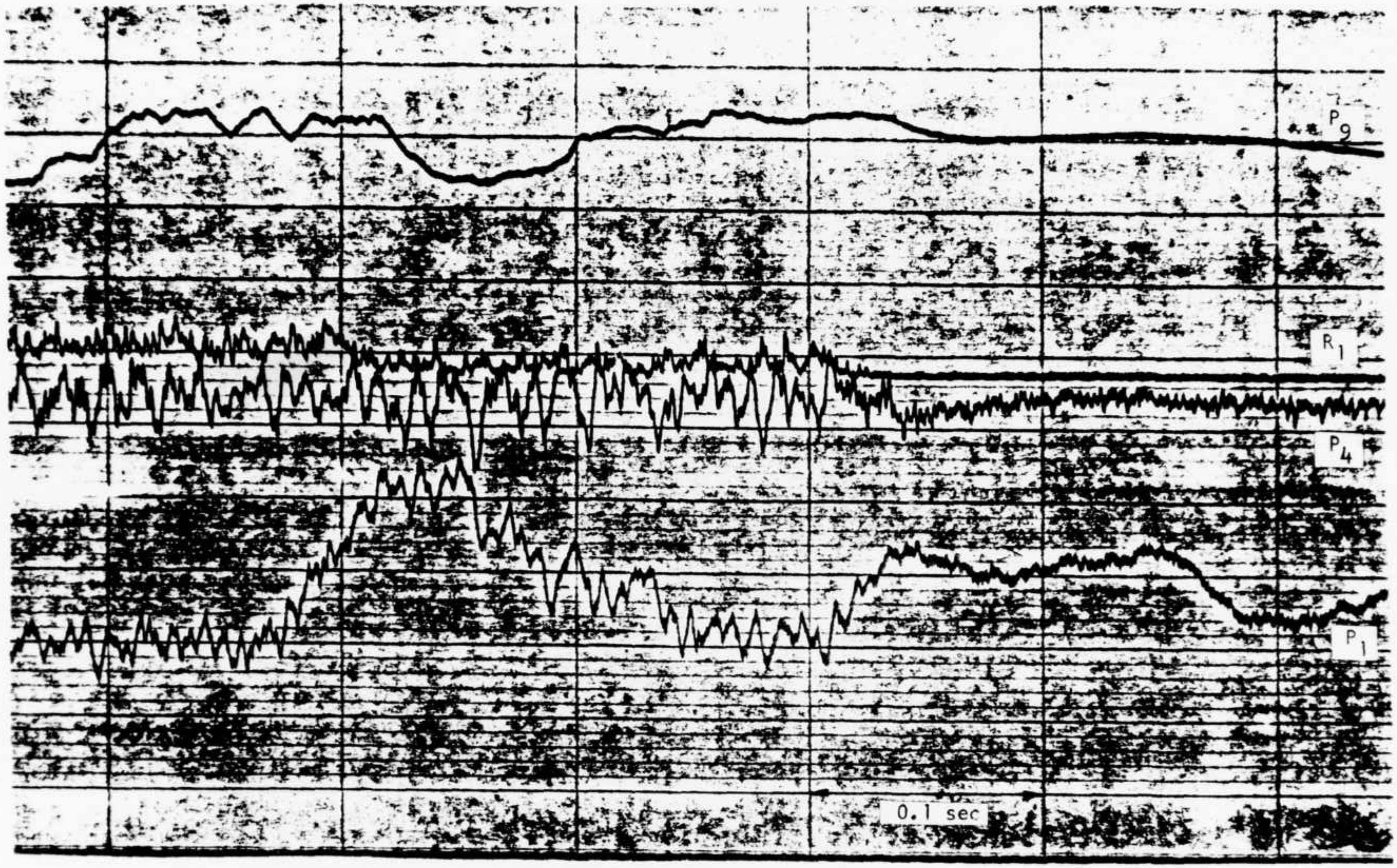

Figure 33. Unsteady Pressure and Radiation Characteristics
Series 2, Test 19-Large Pulse Amplitude

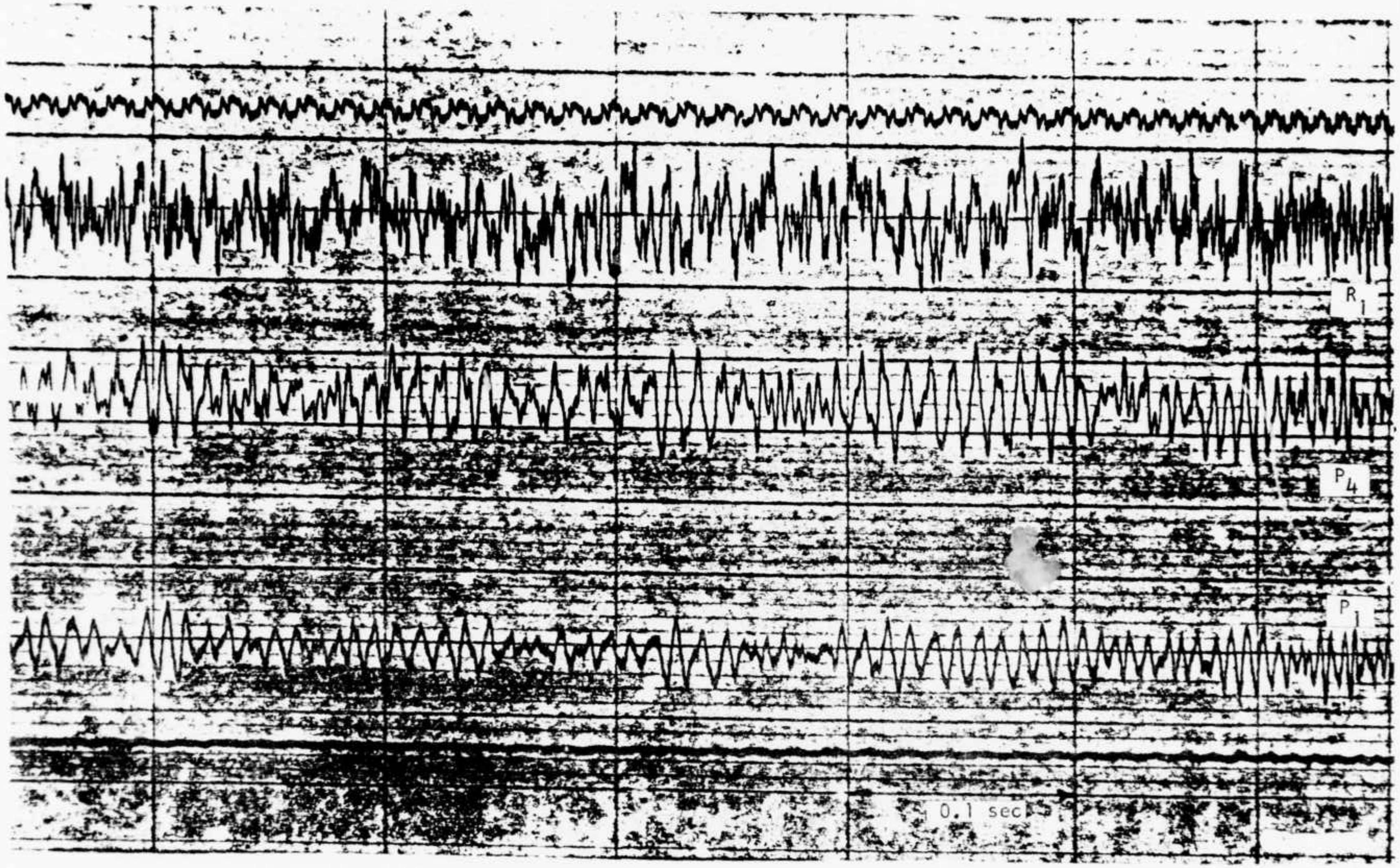

Figure 34. Unsteady Pressure and Radiation Characteristics
Series 2, Test 23

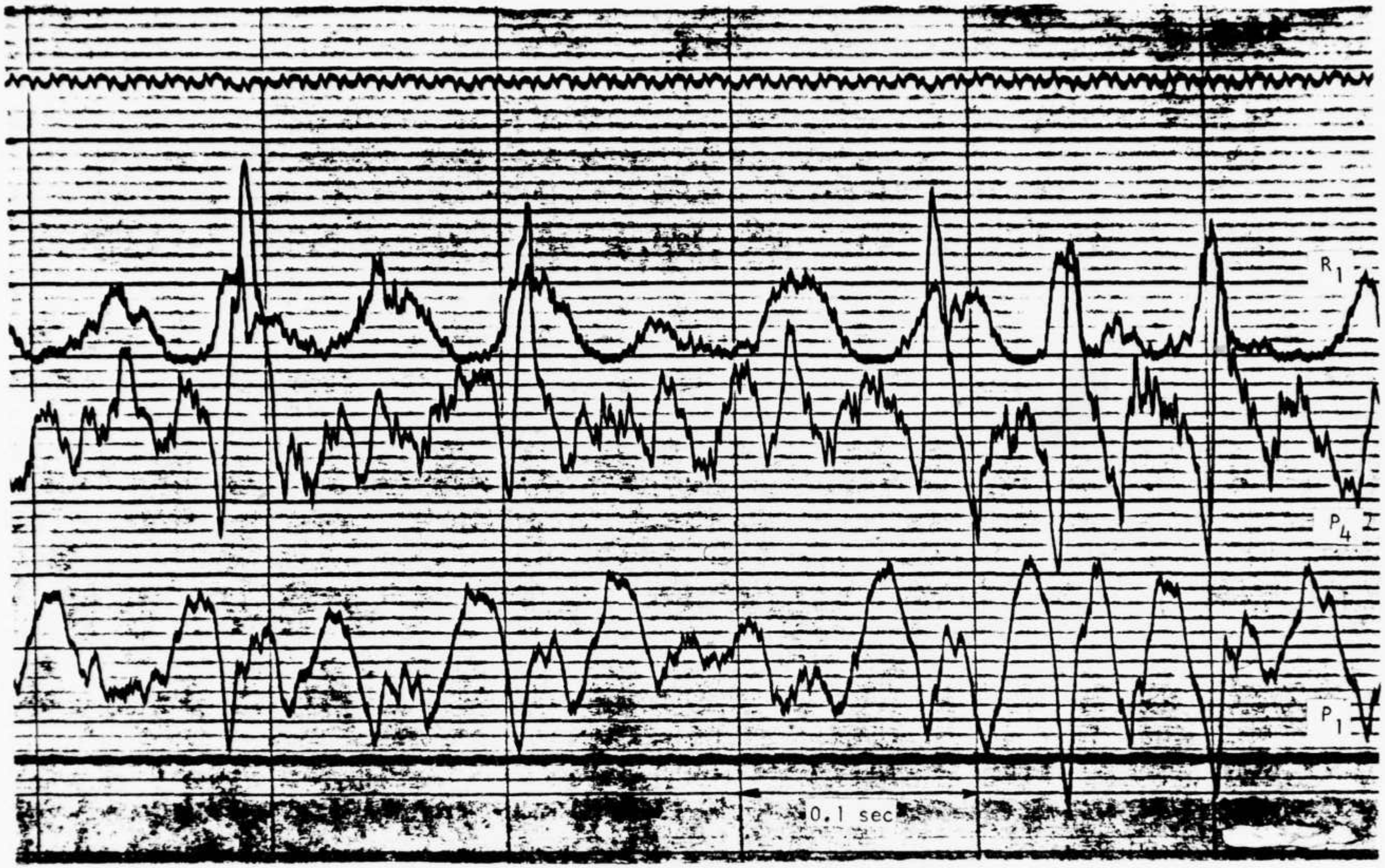

Figure 35. Unsteady Pressure and Radiation Characteristics
Series 2, Test 25

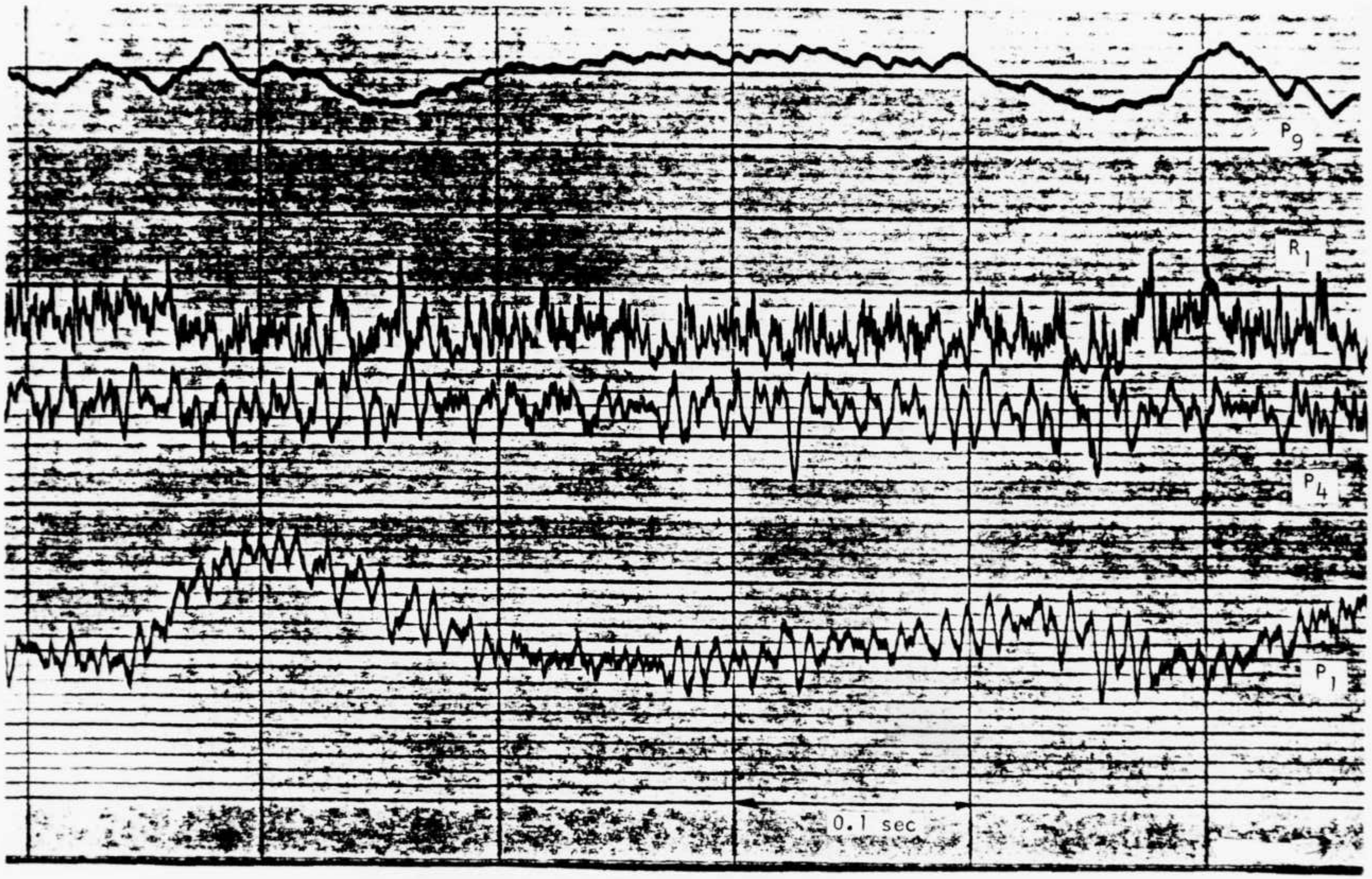

Figure 36. Unsteady Pressure and Radiation Characteristics
Series 3, Test 29

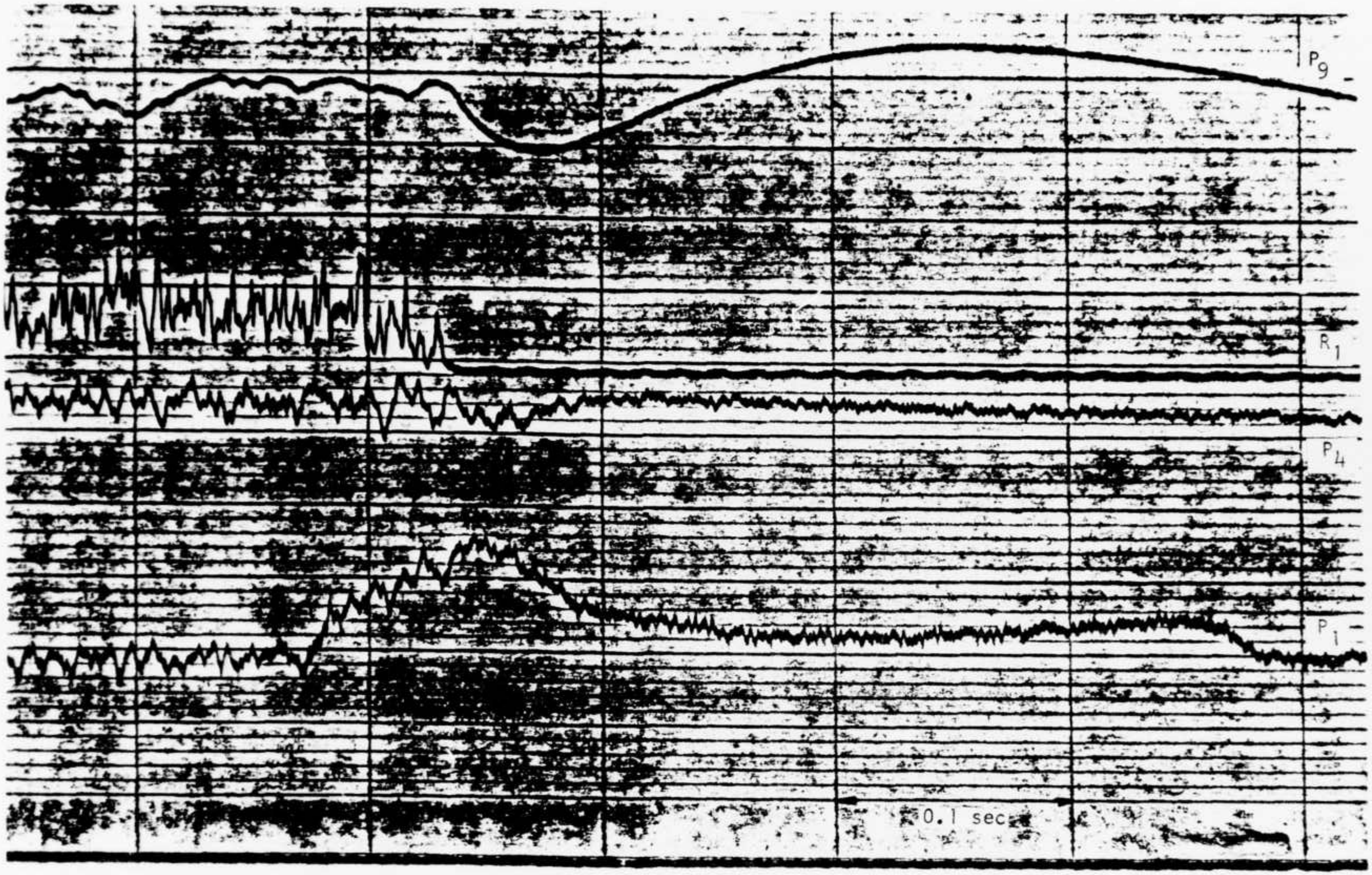

Figure 37. Unsteady Pressure and Radiation Characteristics
Series 3, Test 30

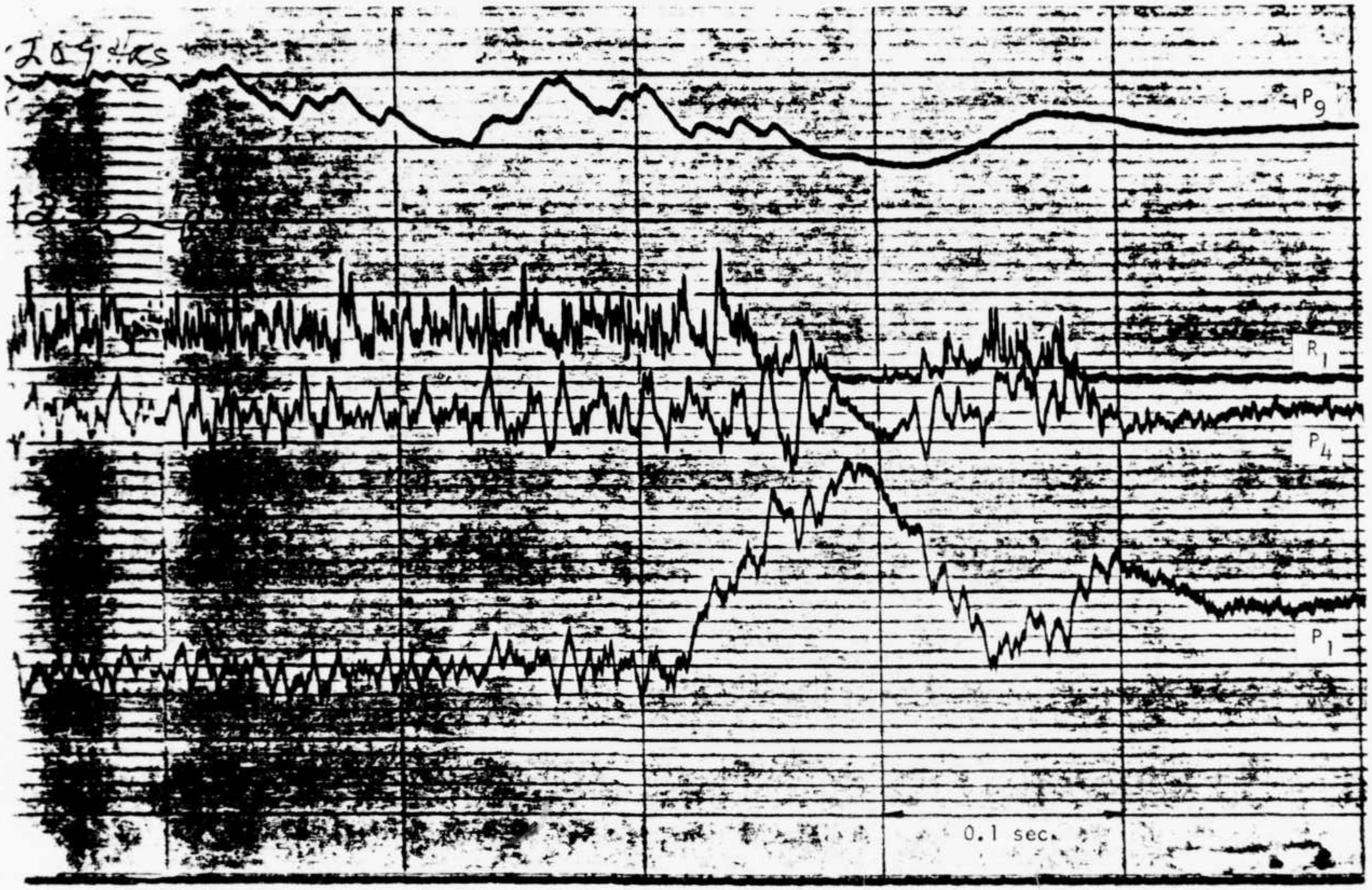

Figure 38. Unsteady Pressure and Radiation Characteristics
Series 3, Test 33

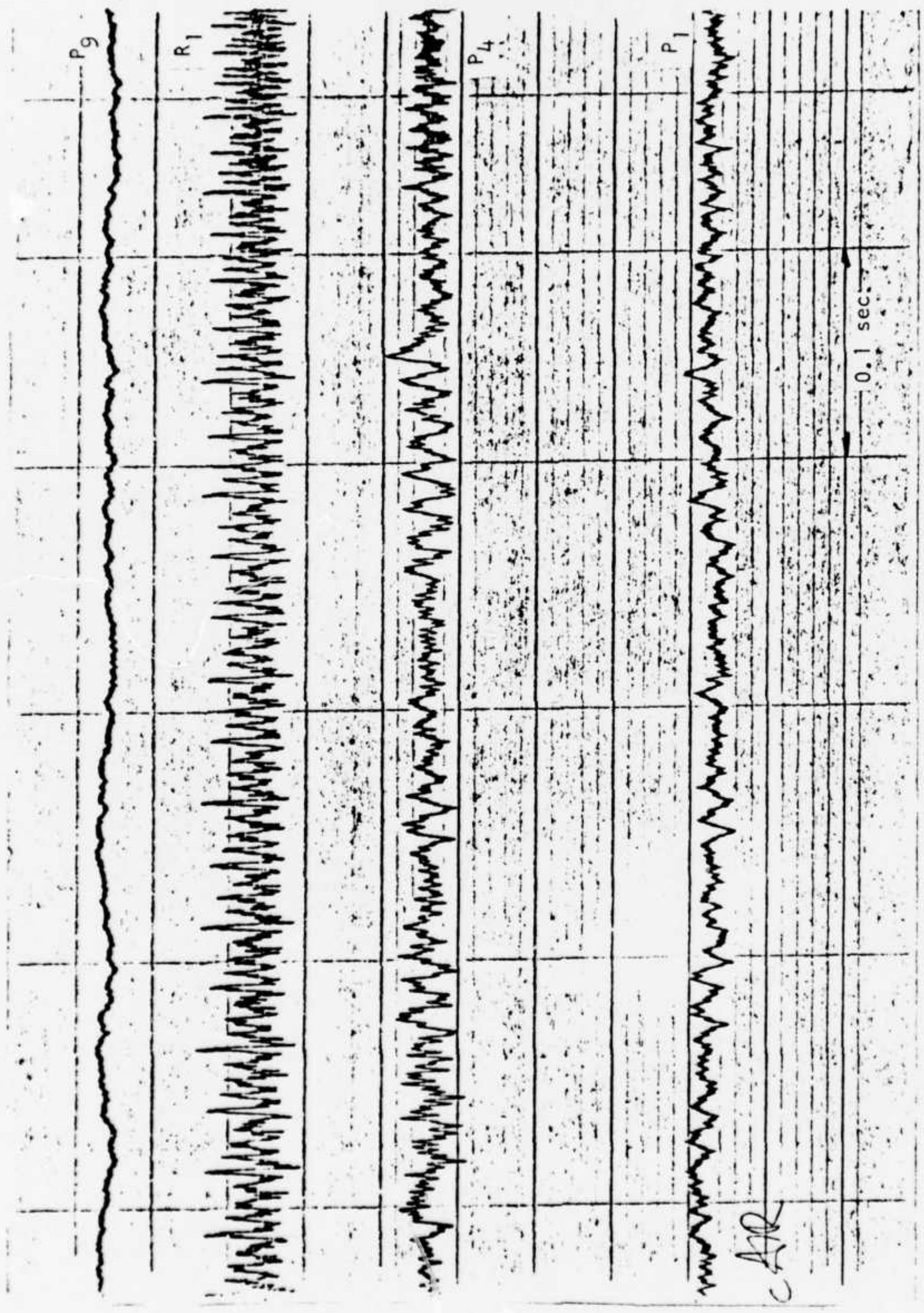

Figure 39. Unsteady Pressure and Radiation Characteristics
Series 4, Test 44

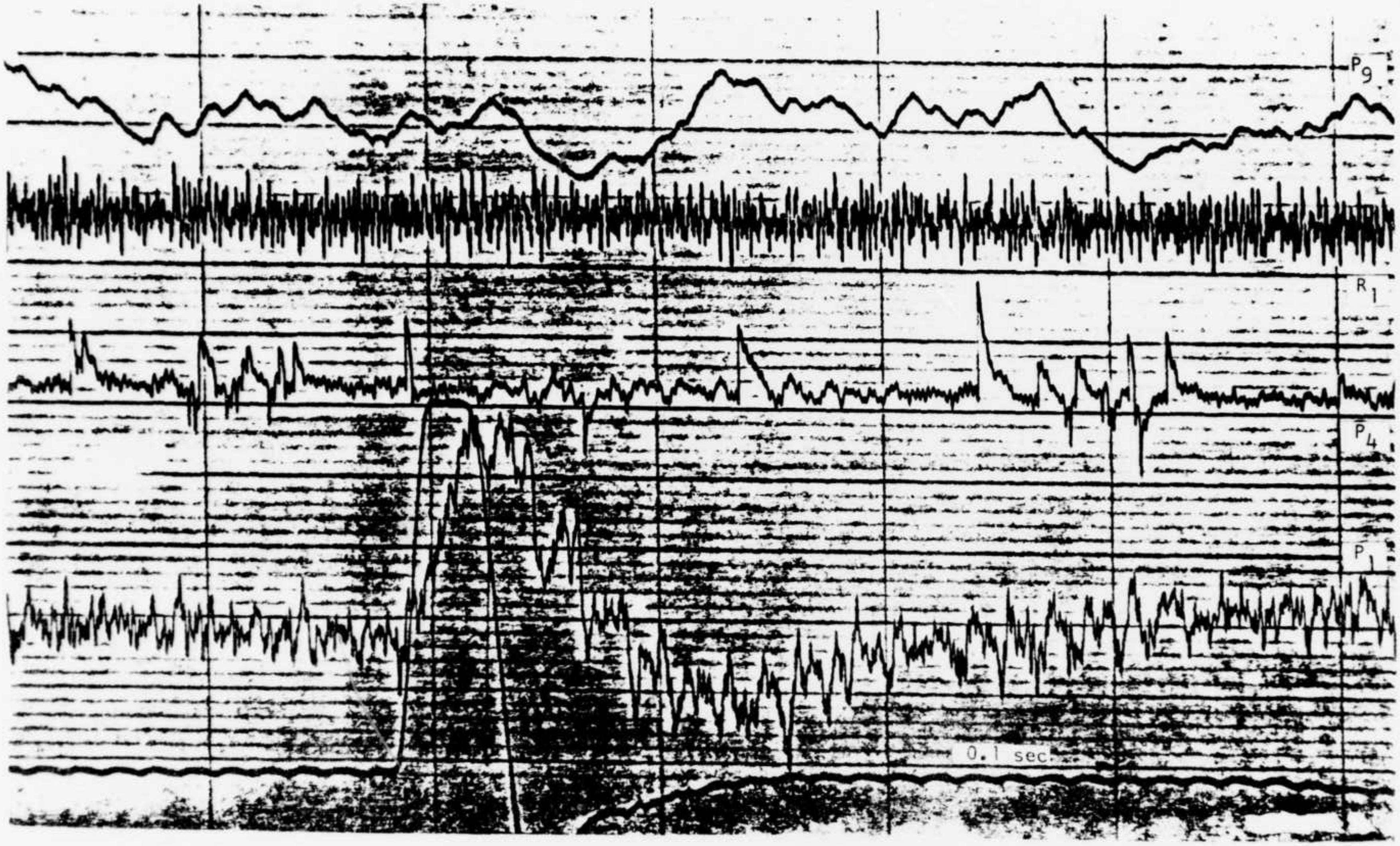

Figure 40. Unsteady Pressure and Radiation Characteristics
Series 4, Test 45

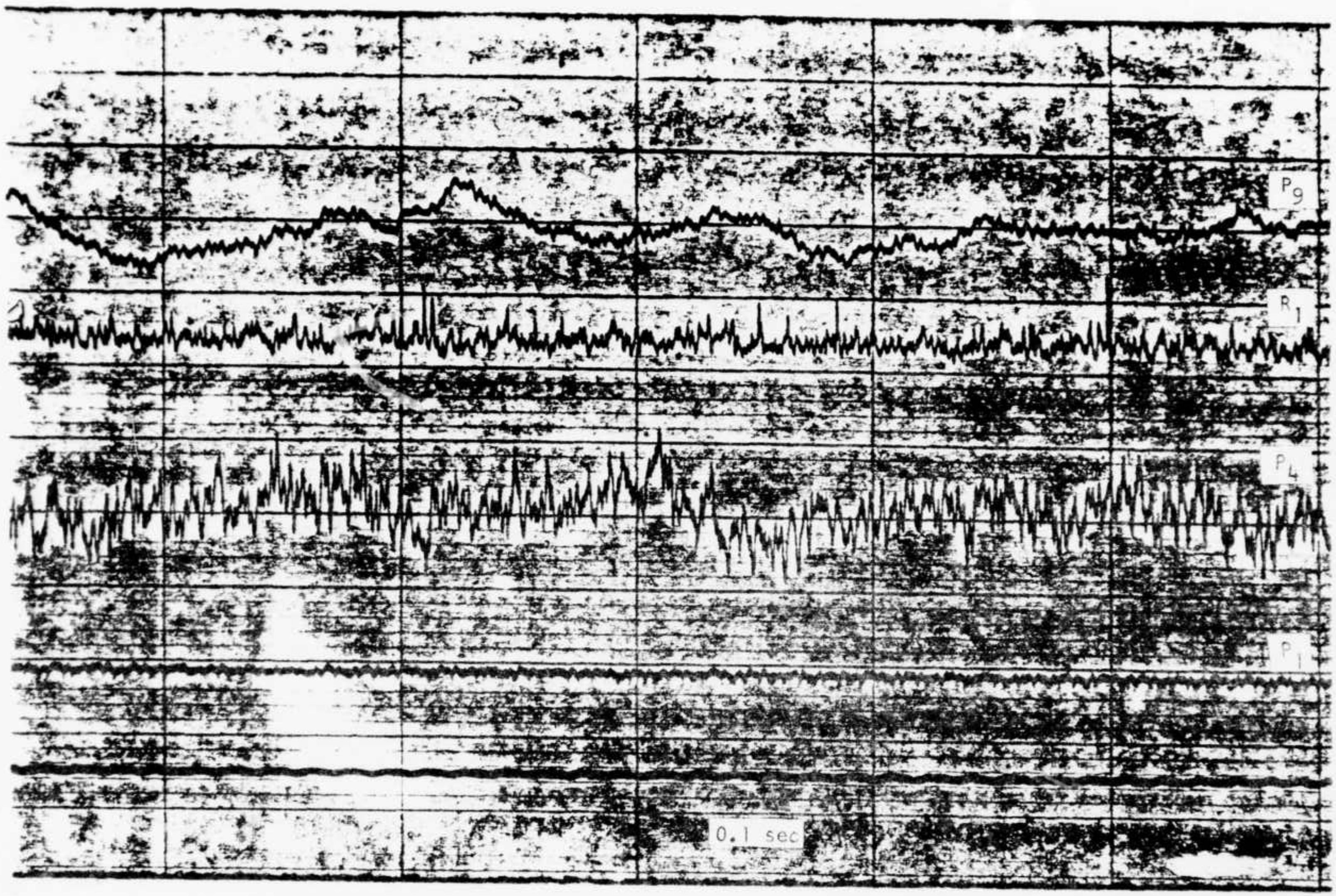

Figure 41. Unsteady Pressure and Radiation Characteristics
Series 5, Test 51-No Pulse

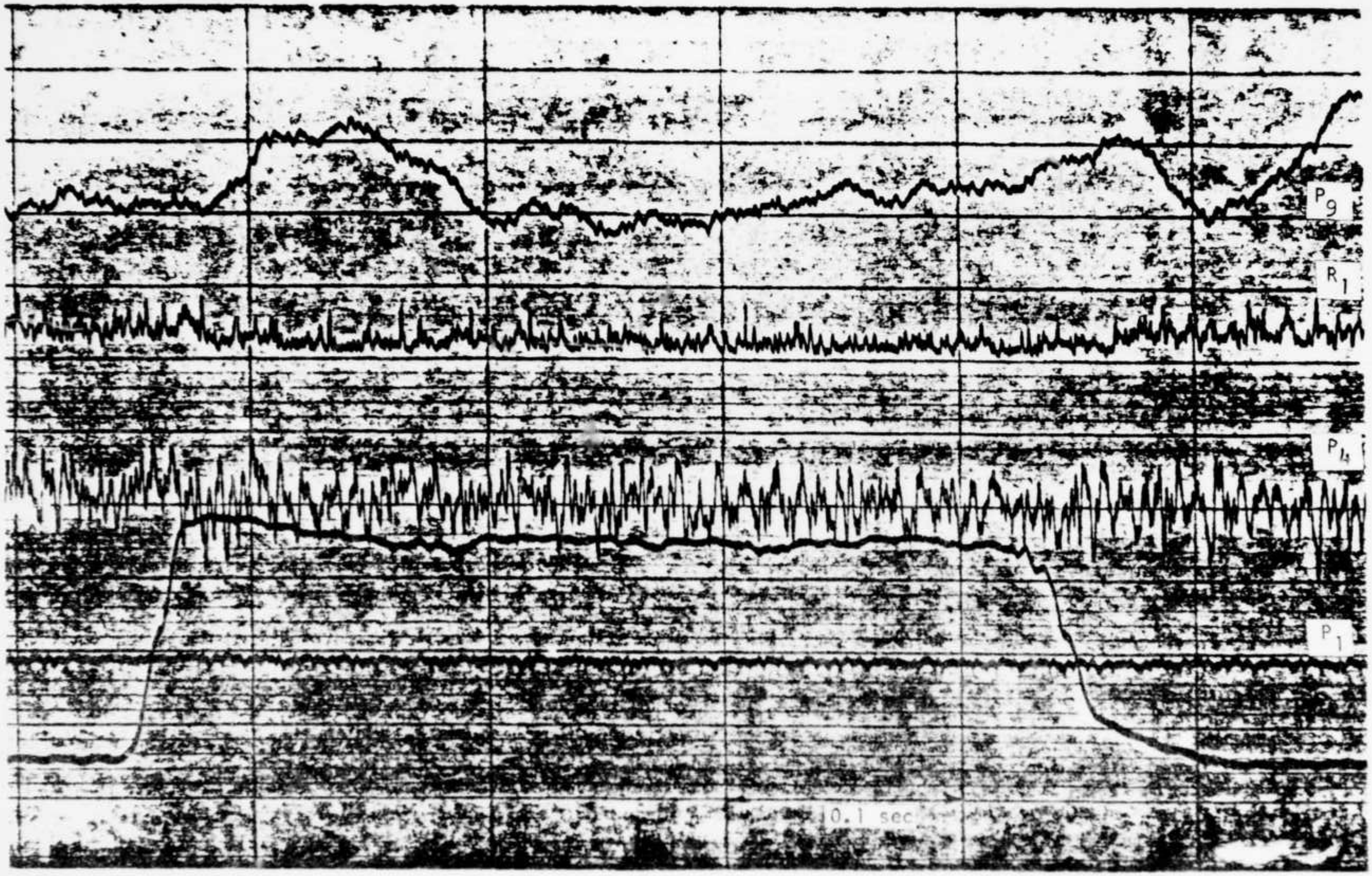

Figure 42. Unsteady Pressure and Radiation Characteristics
Series 5, Test 51-400 msec Small Amplitude Pulse

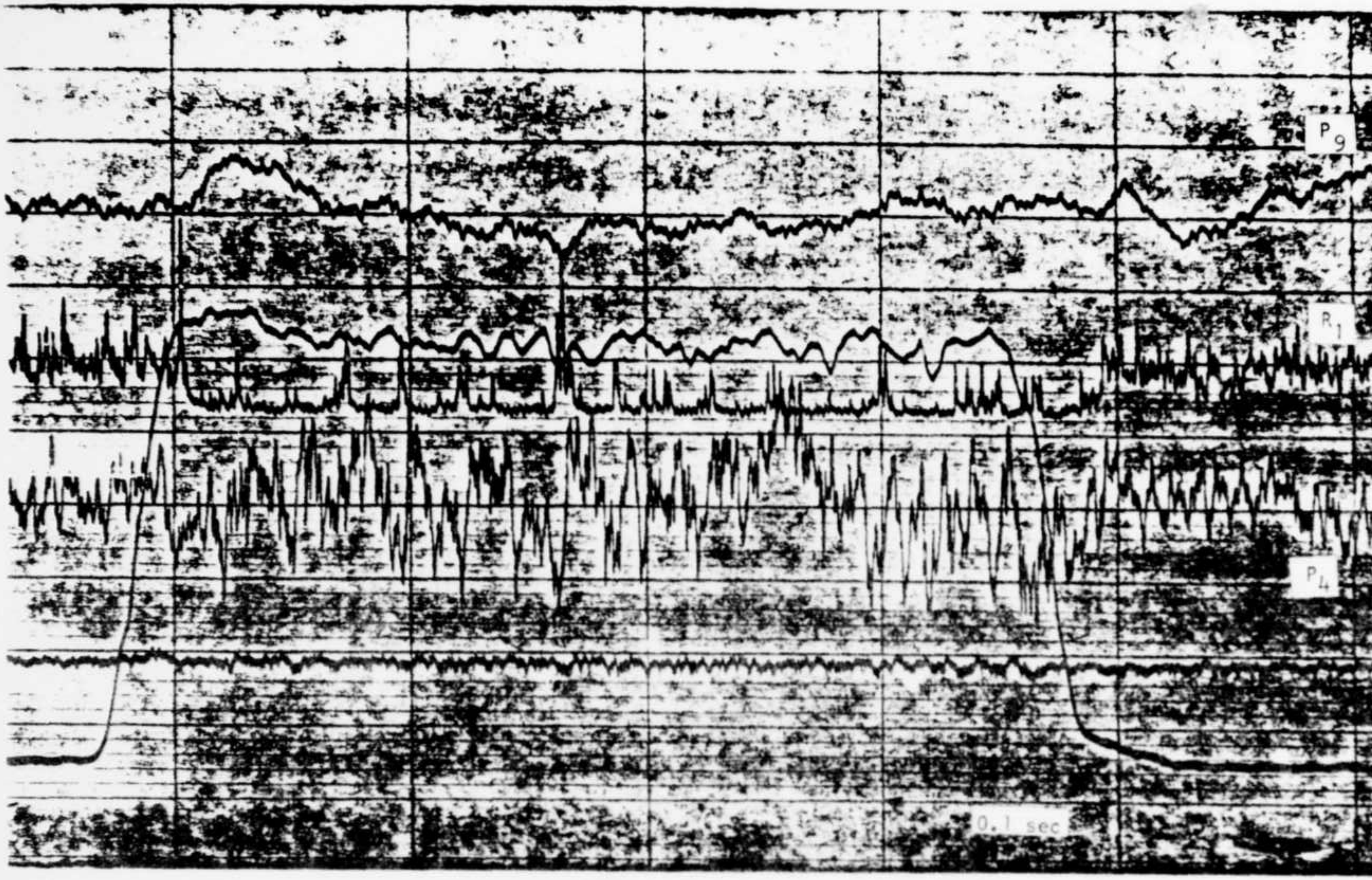

Figure 43. Unsteady Pressure and Radiation Characteristics
Series 5, Test 51-400 msec Larger Amplitude Pulse

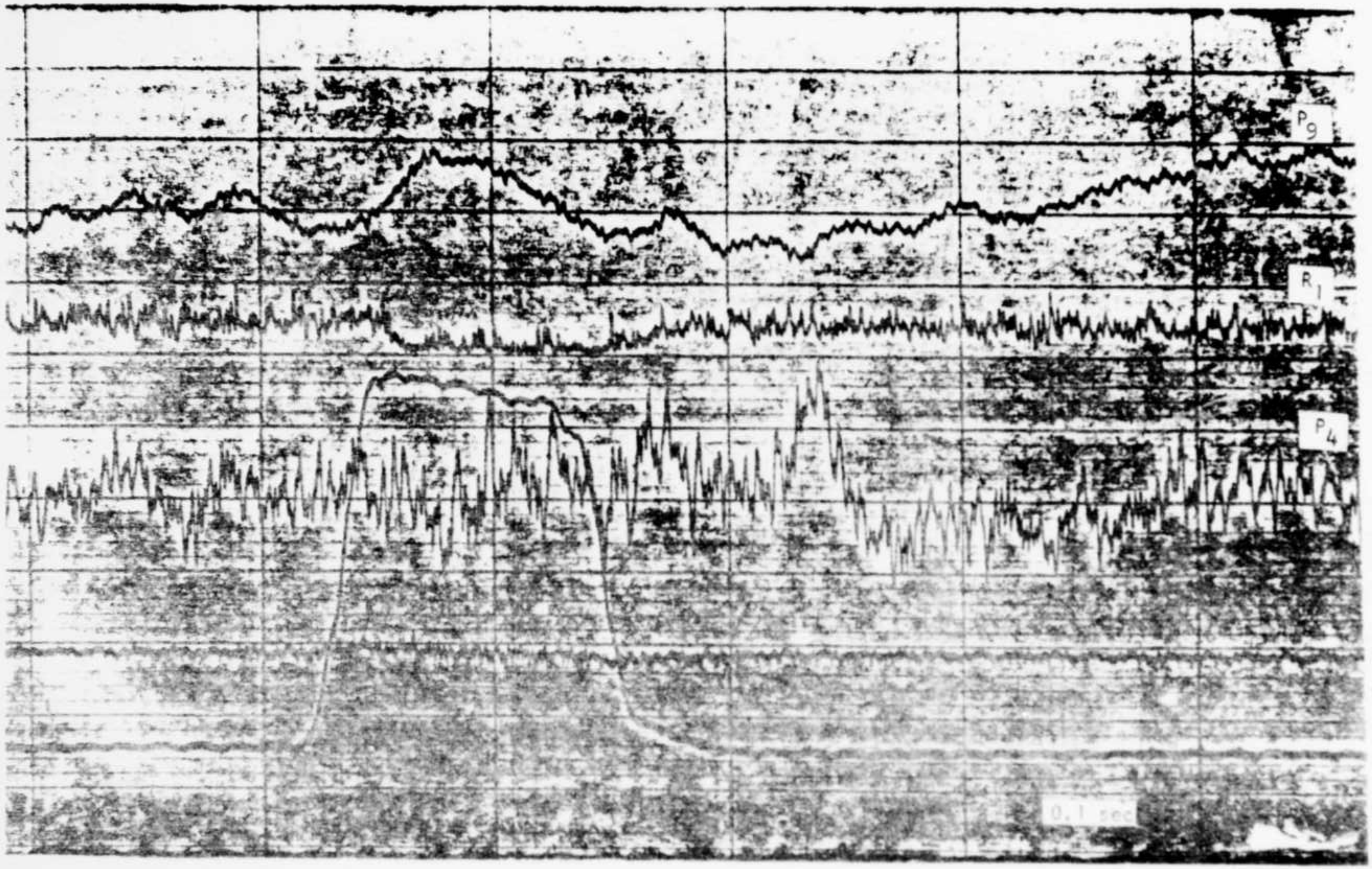

Figure 44. Unsteady Pressure and Radiation Characteristics
Series 5, Test 41-100 msec Pulse

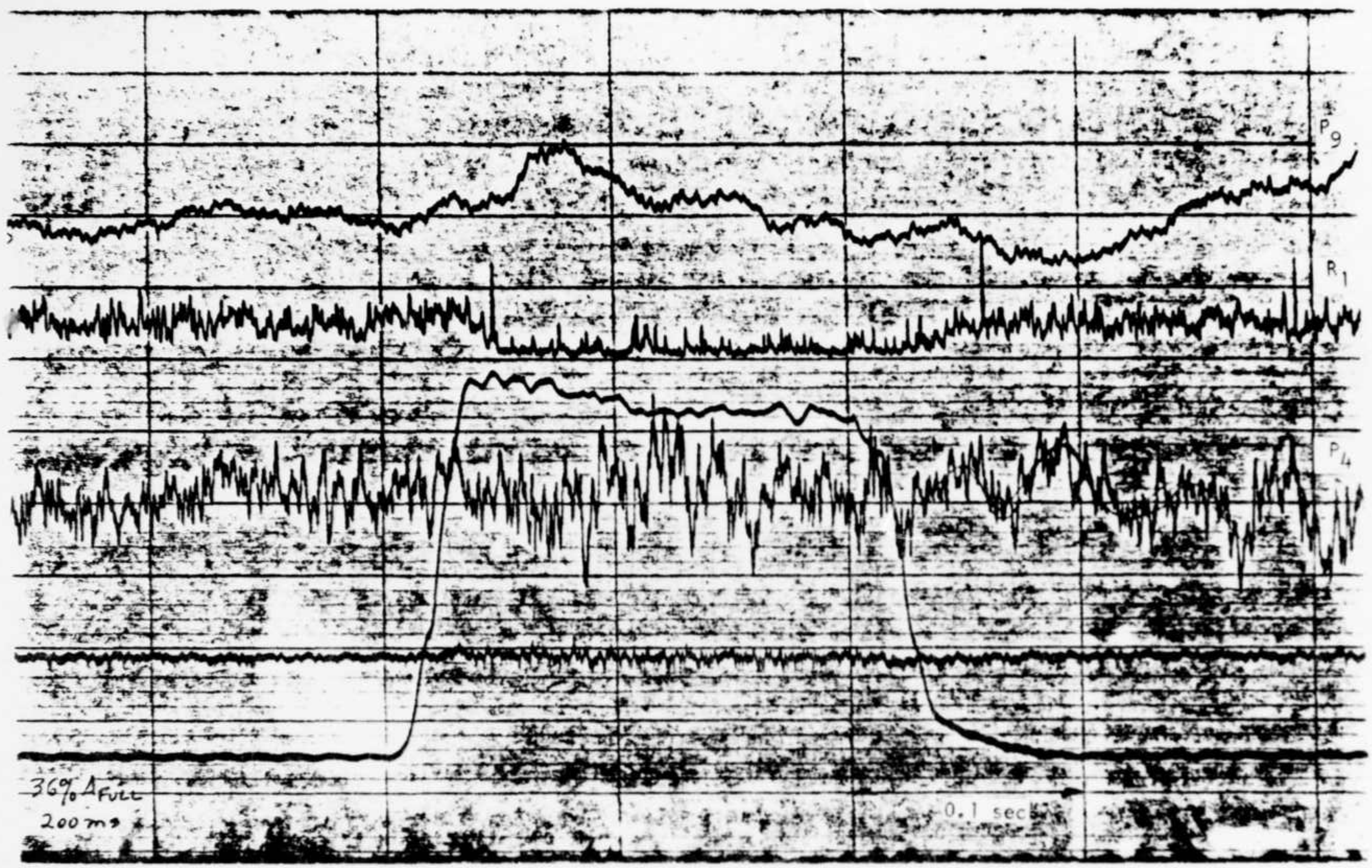

Figure 45. Unsteady Pressure and Radiation Characteristics
Series 5, Test 51-200 msec Pulse

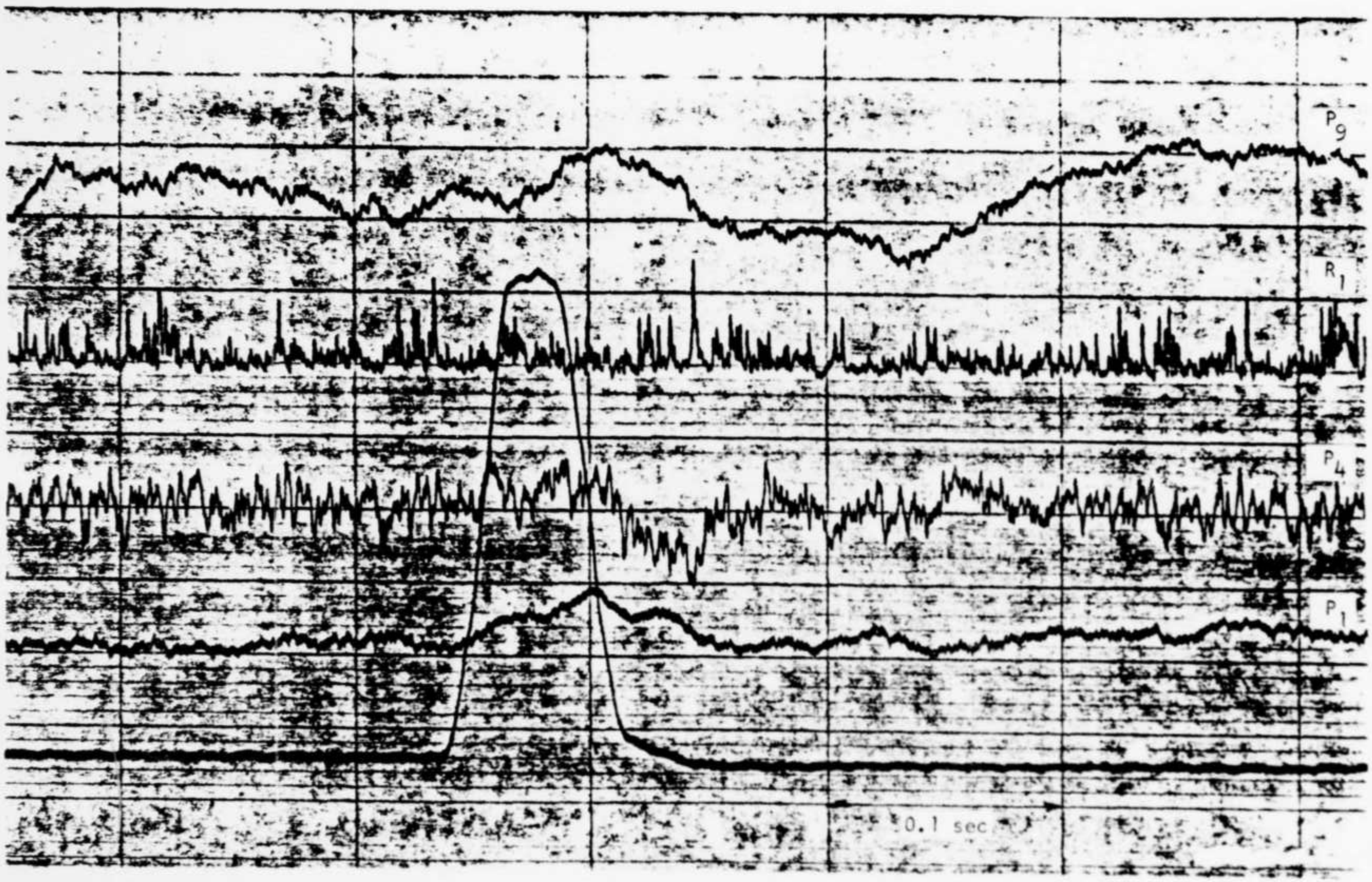

Figure 46. Unsteady Pressure and Radiation Characteristics
Series 6, Test 57-Short Duration Pulse

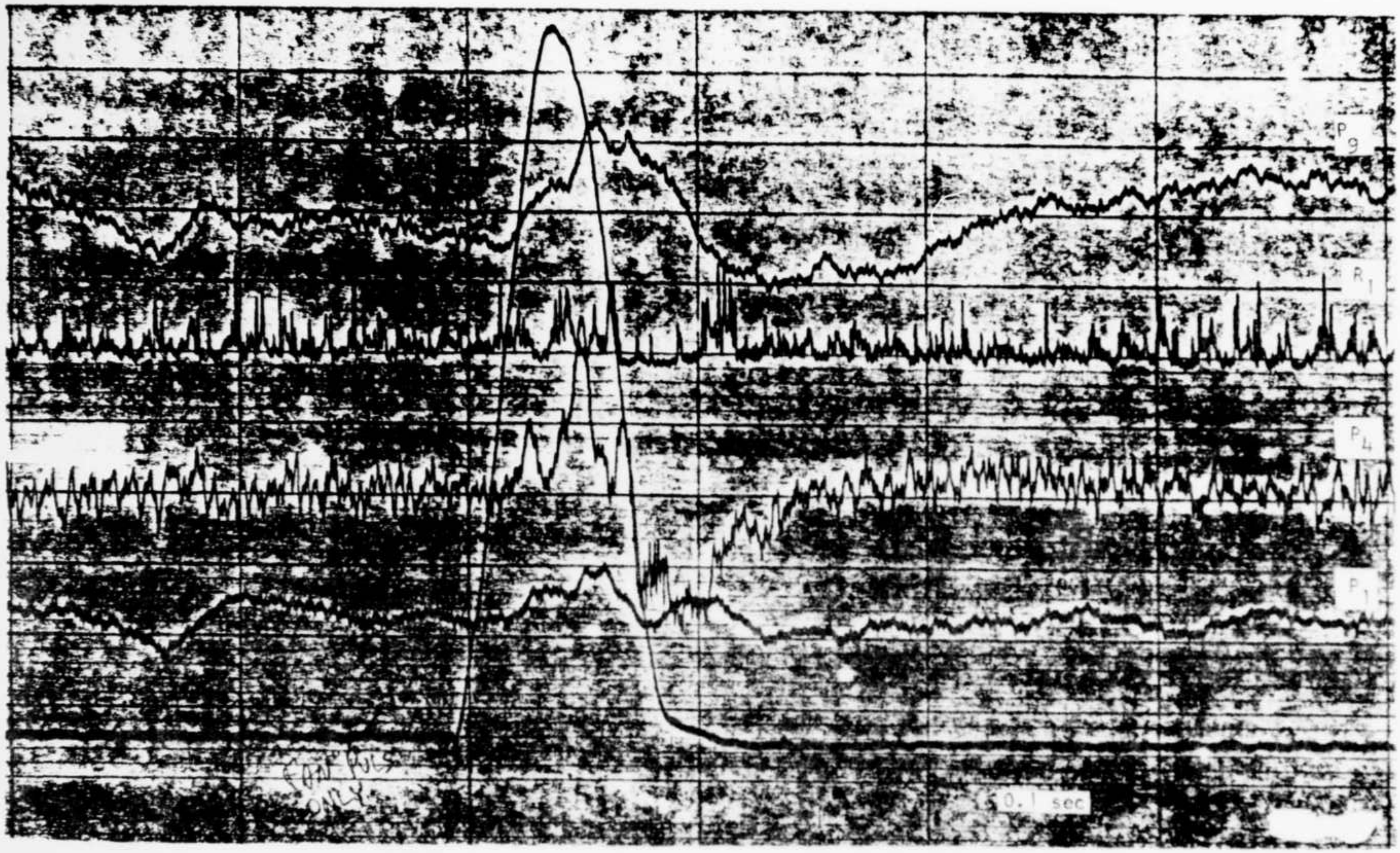

Figure 47. Unsteady Pressure and Radiation Characteristics
Series 6, Test 57-Larger Amplitude Pulse

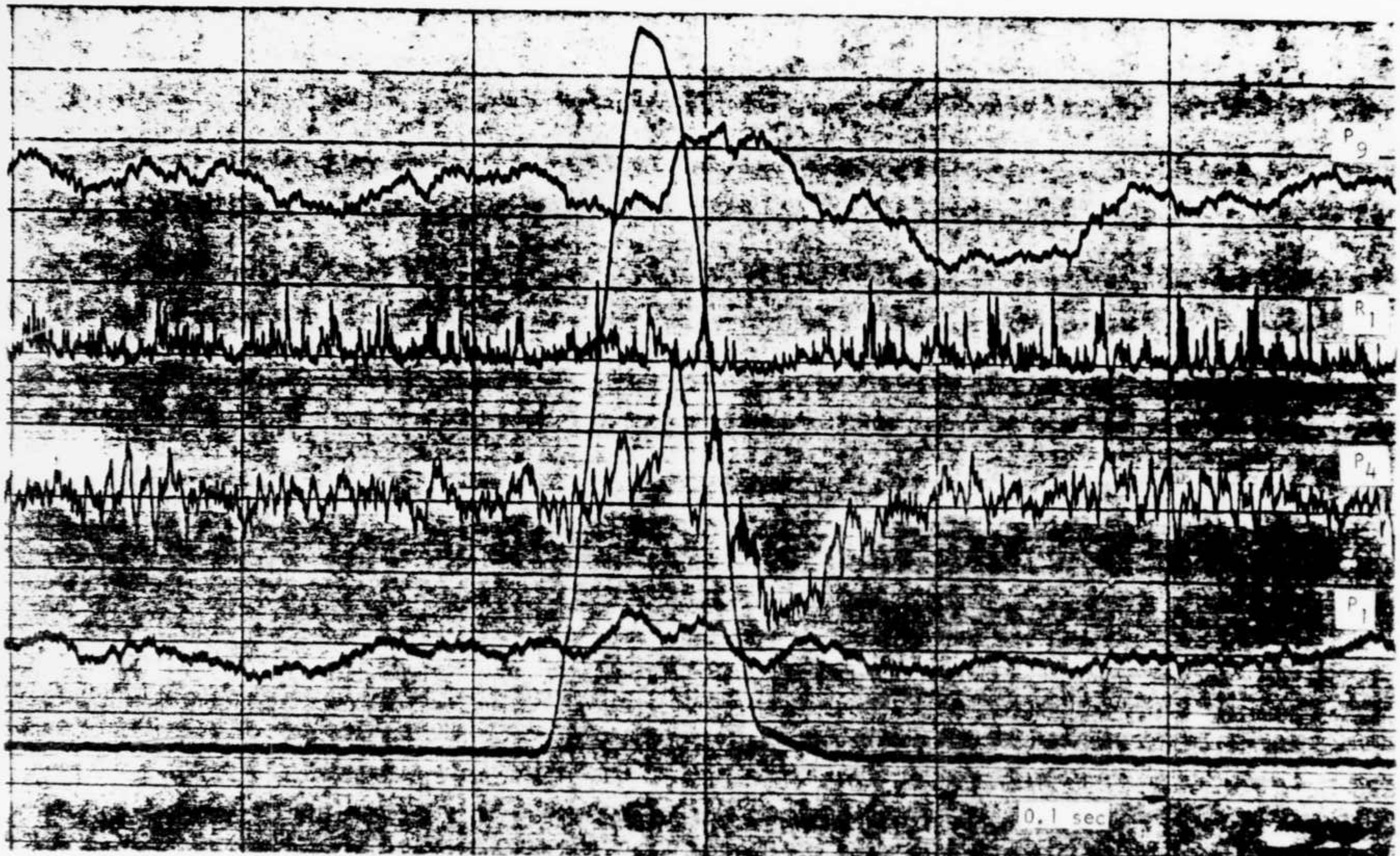

Figure 48. Unsteady Pressure and Radiation Characteristics
Series 6, Test 57-Larger Amplitude Pulse

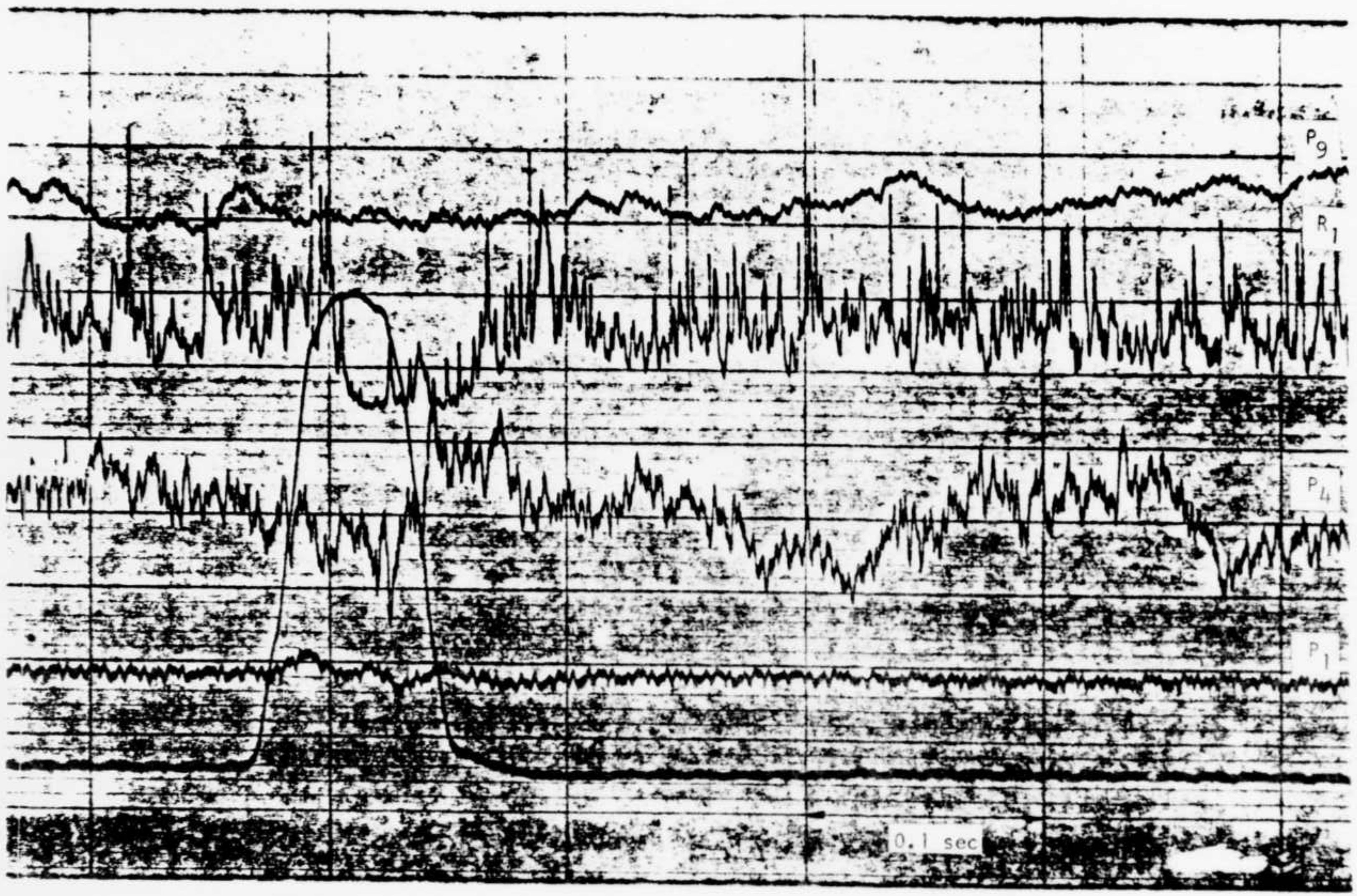

Figure 49. Unsteady Pressure and Radiation Characteristics
Series 7, Test 65

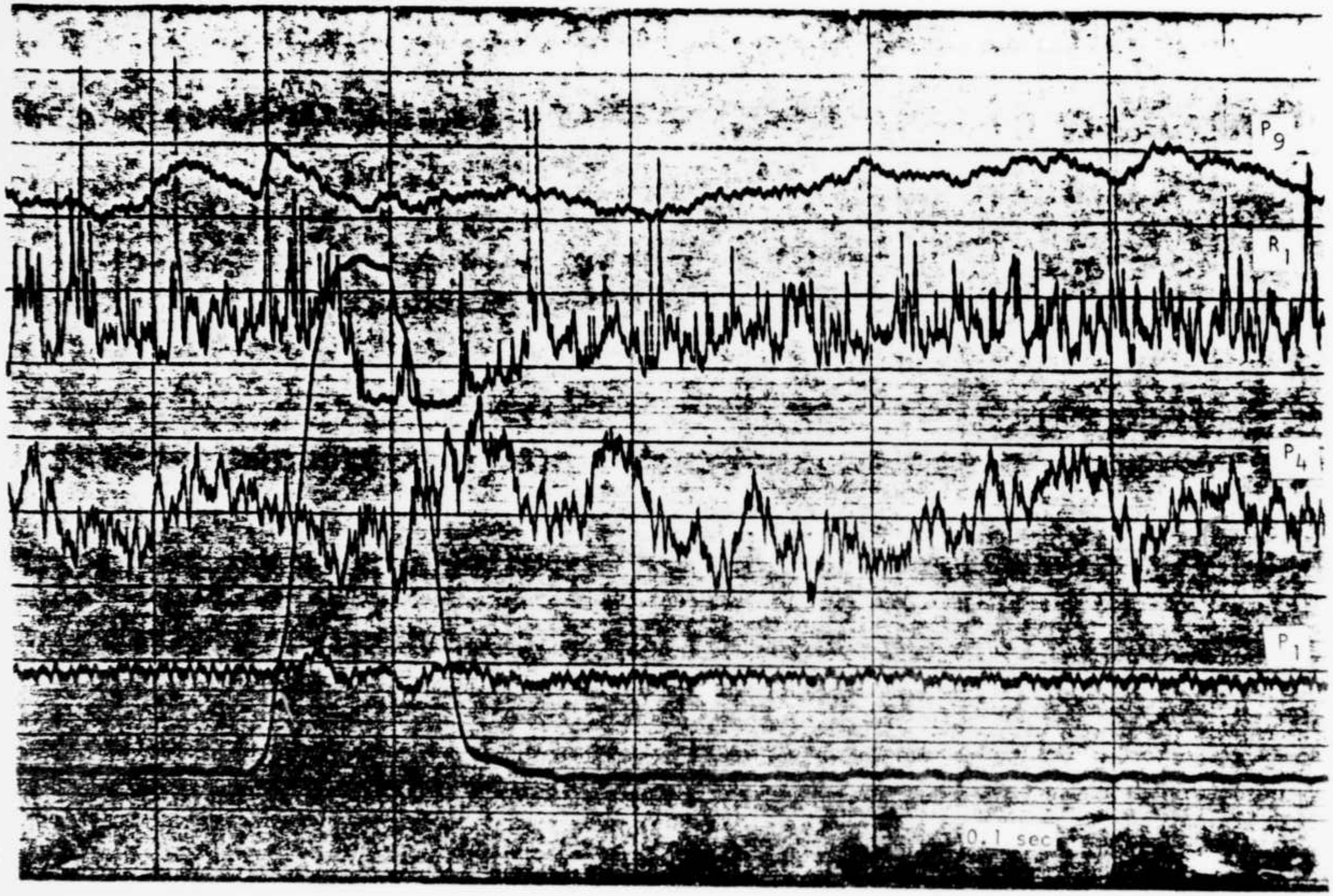

Figure 50. Unsteady Pressure and Radiation Characteristics
Series 7, Test 66

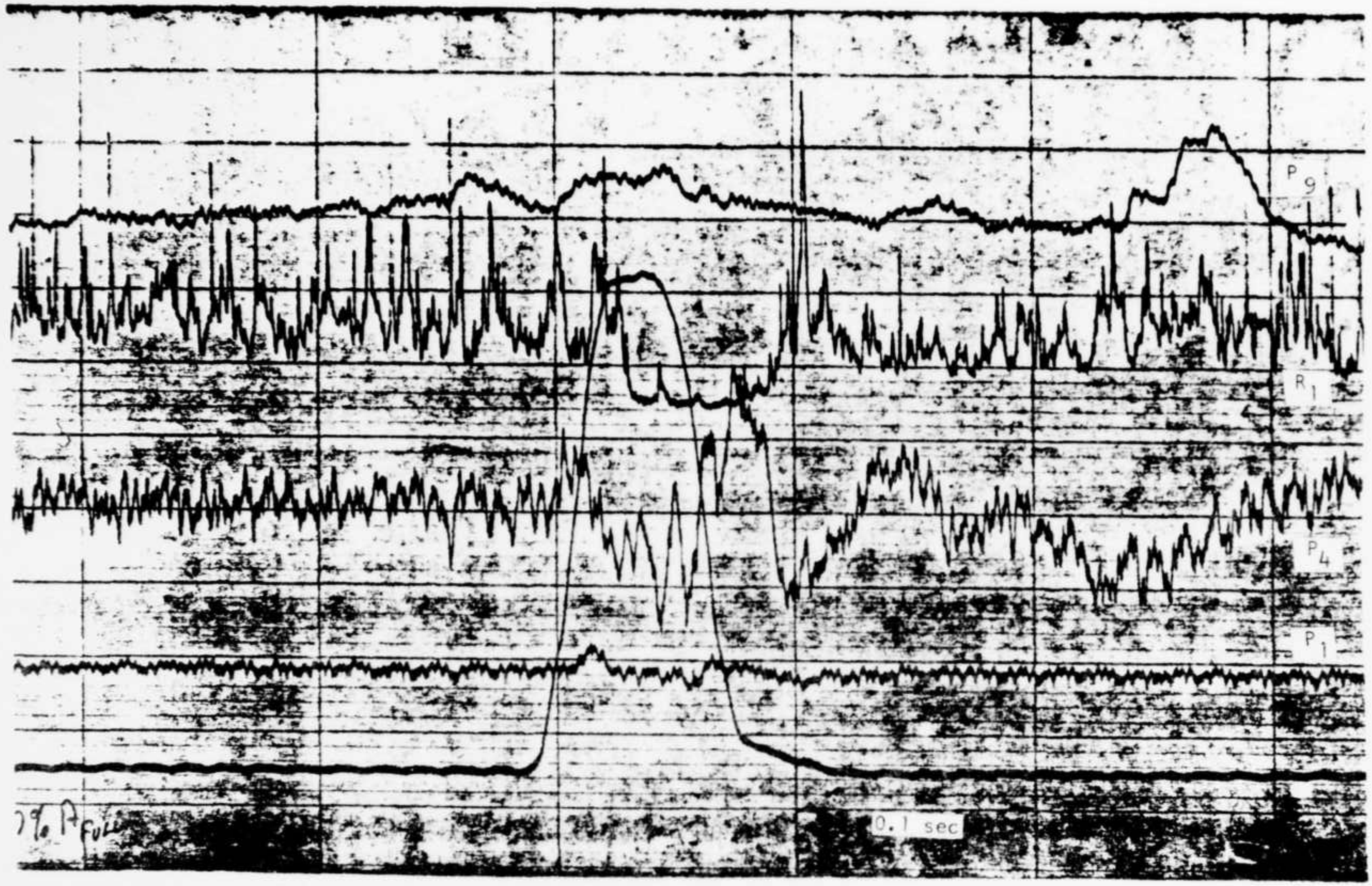

Figure 51. Unsteady Pressure and Radiation Characteristics
Series 7, Test 67-74 msec Pulse

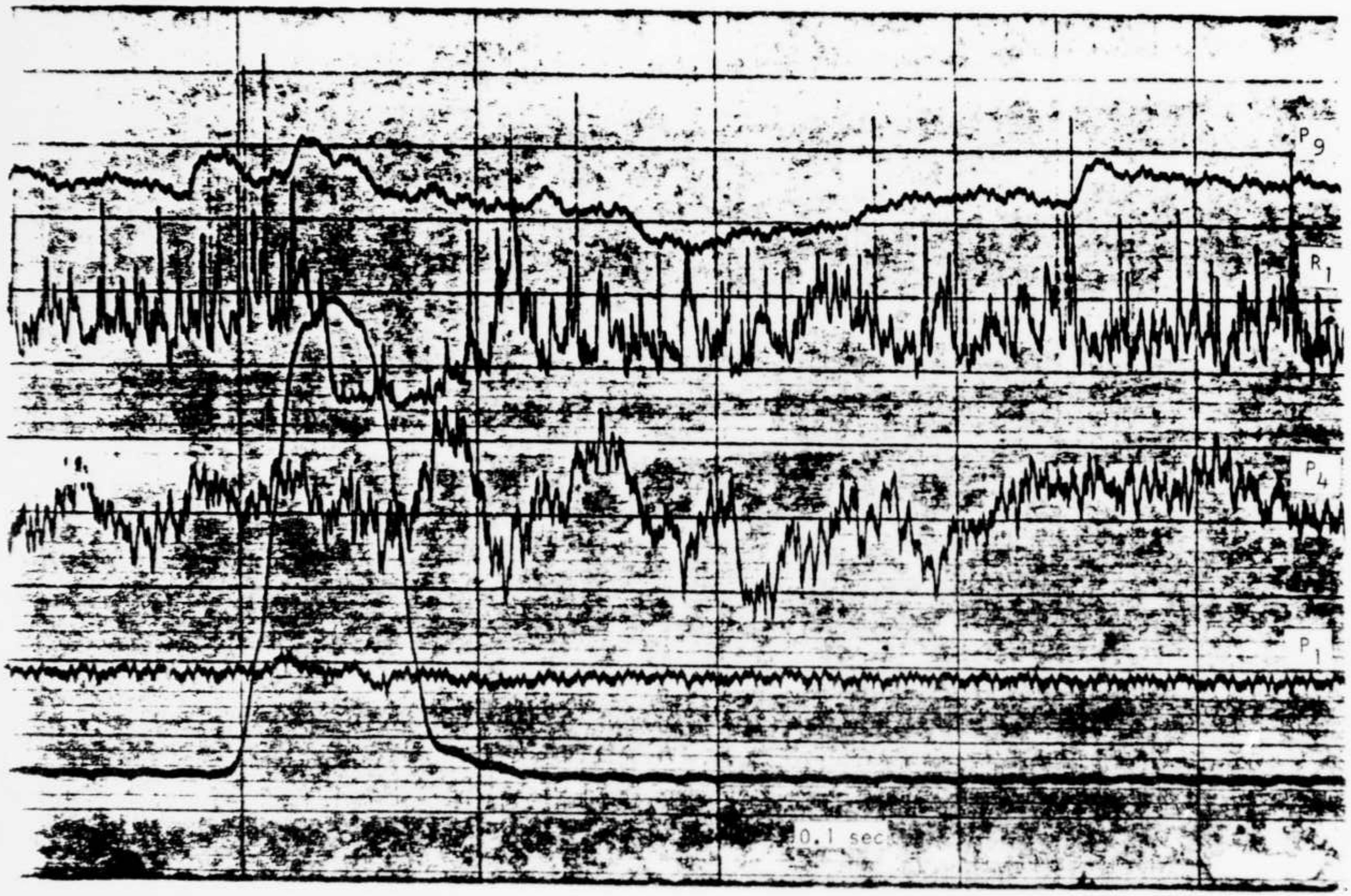

Figure 52. Unsteady Pressure and Radiation Characteristics
Series 7, Test 68

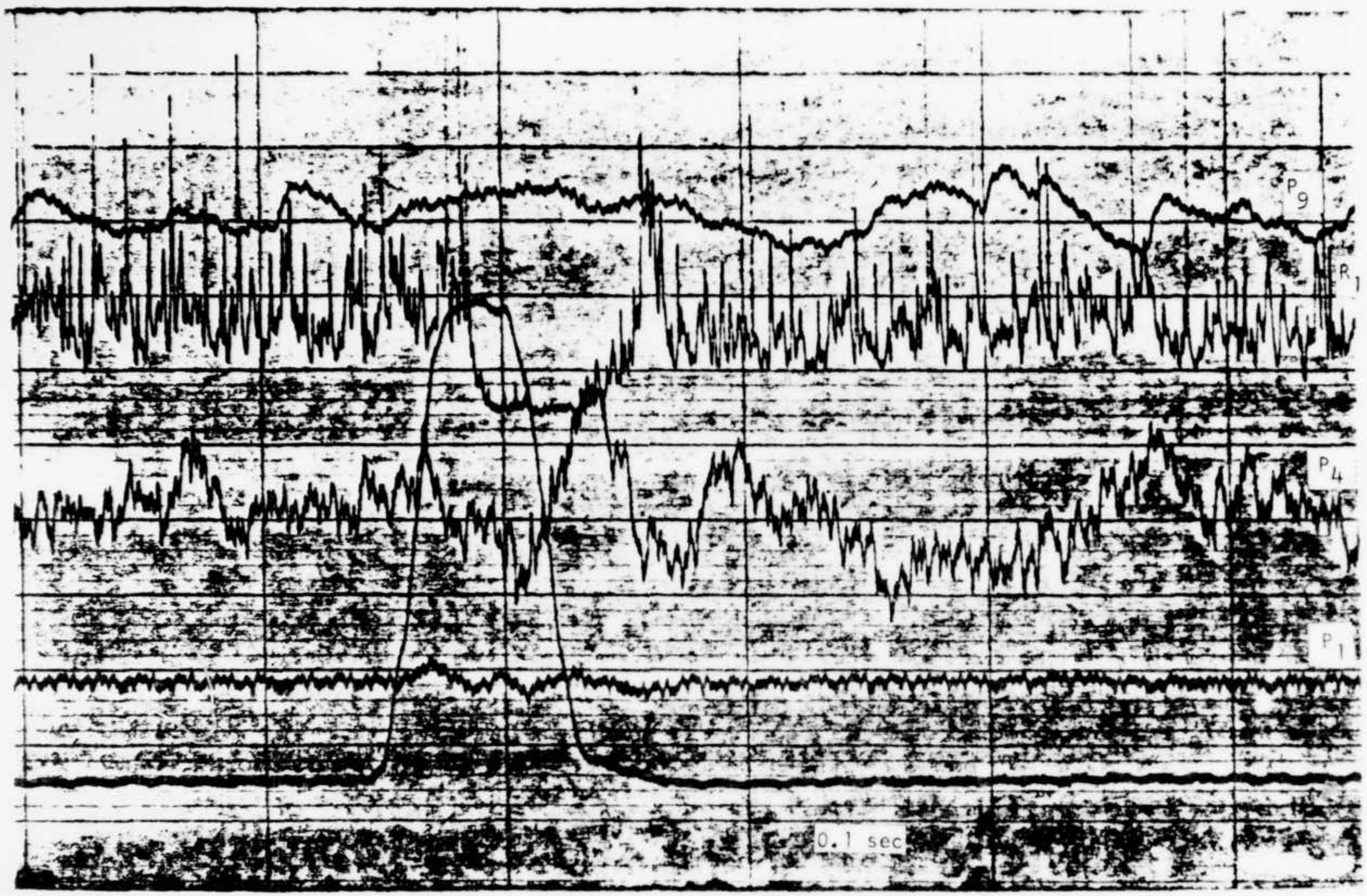

Figure 53. Unsteady Pressure and Radiation Characteristics
Series 7, Test 69

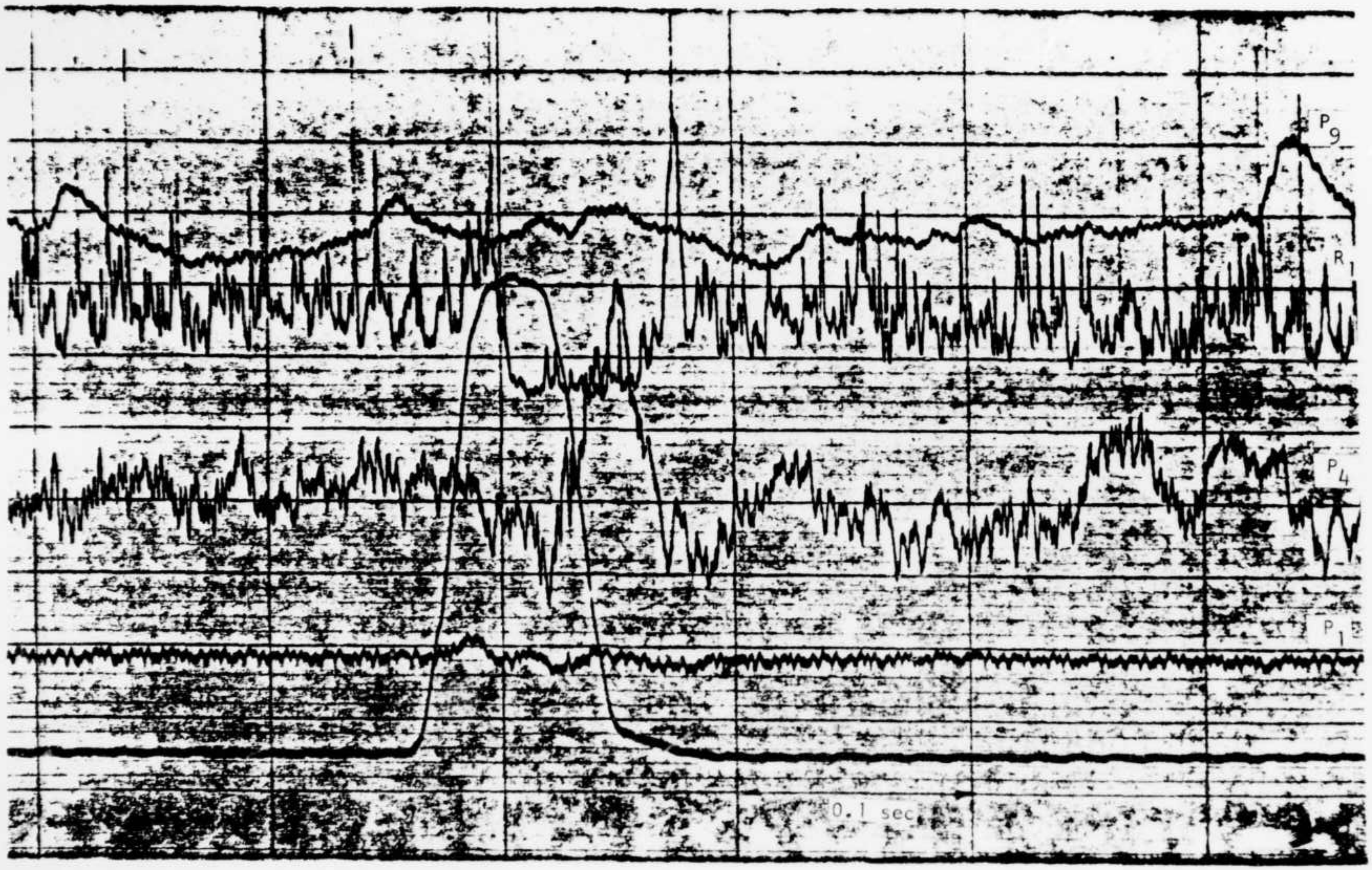

Figure 54. Unsteady Pressure and Radiation Characteristics
Series 7, Test 70-75 msec Pulse

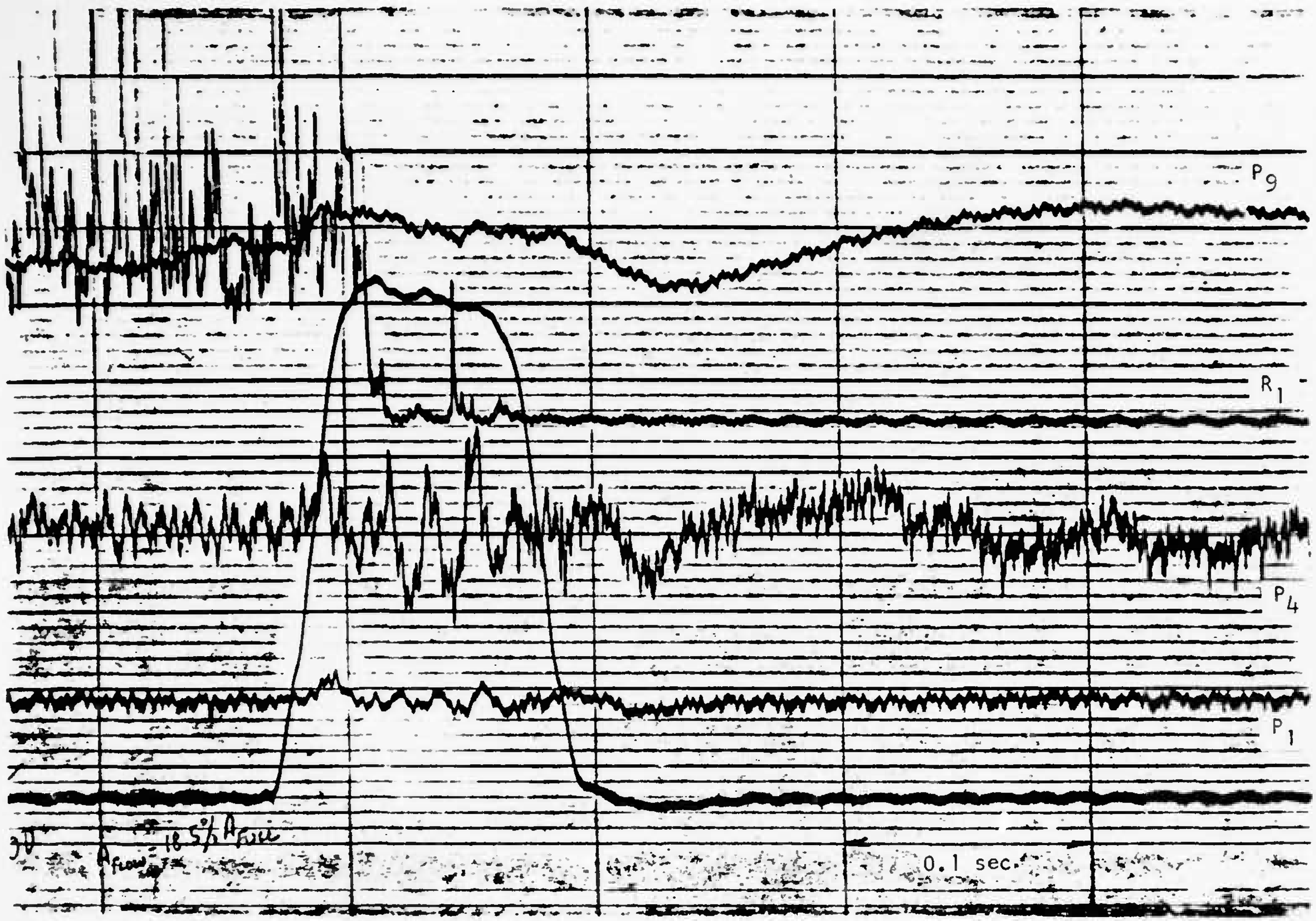

Figure 55. Unsteady Pressure and Radiation Characteristics
Series 7, Test 67-100 msec Pulse

AD-A059 847 NORTHERN RESEARCH AND ENGINEERING CORP CAMBRIDGE MASS F/G 21/2
FLAMEHOLDER COMBUSTION INSTABILITY STUDY. VOLUME II. EXPERIMENT--ETC(U)
MAY 78 E R NORSTER F33615-76-C-2112
UNCLASSIFIED NREC-1294-2 AFAPL-TR-78-27-VOL-2 NL

2 OF 2
AD
A059847

END
DATE
FILMED
12-78
DDC

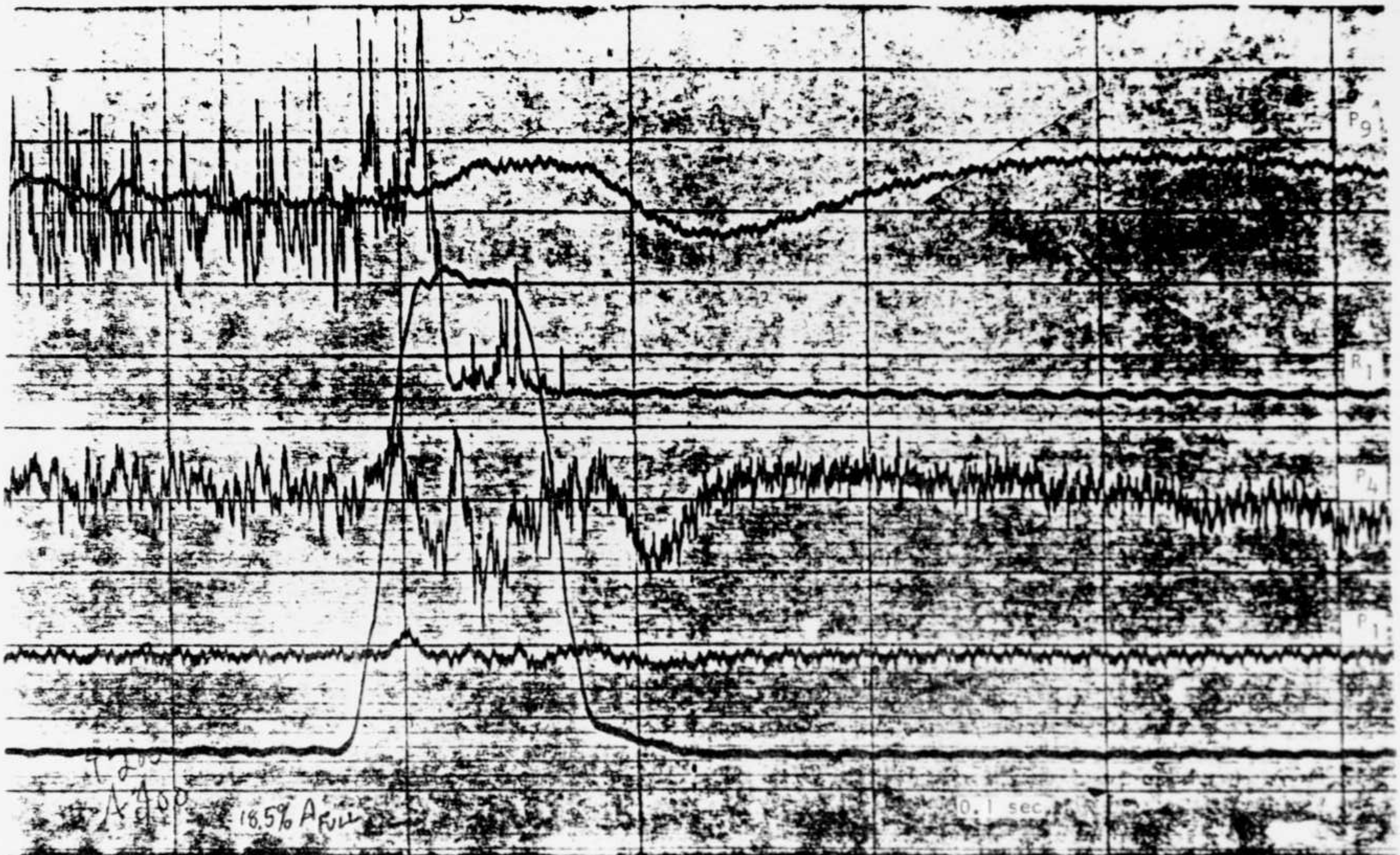

Figure 56. Unsteady Pressure and Radiation Characteristics
Series 7, Test 70-100 msec Pulse

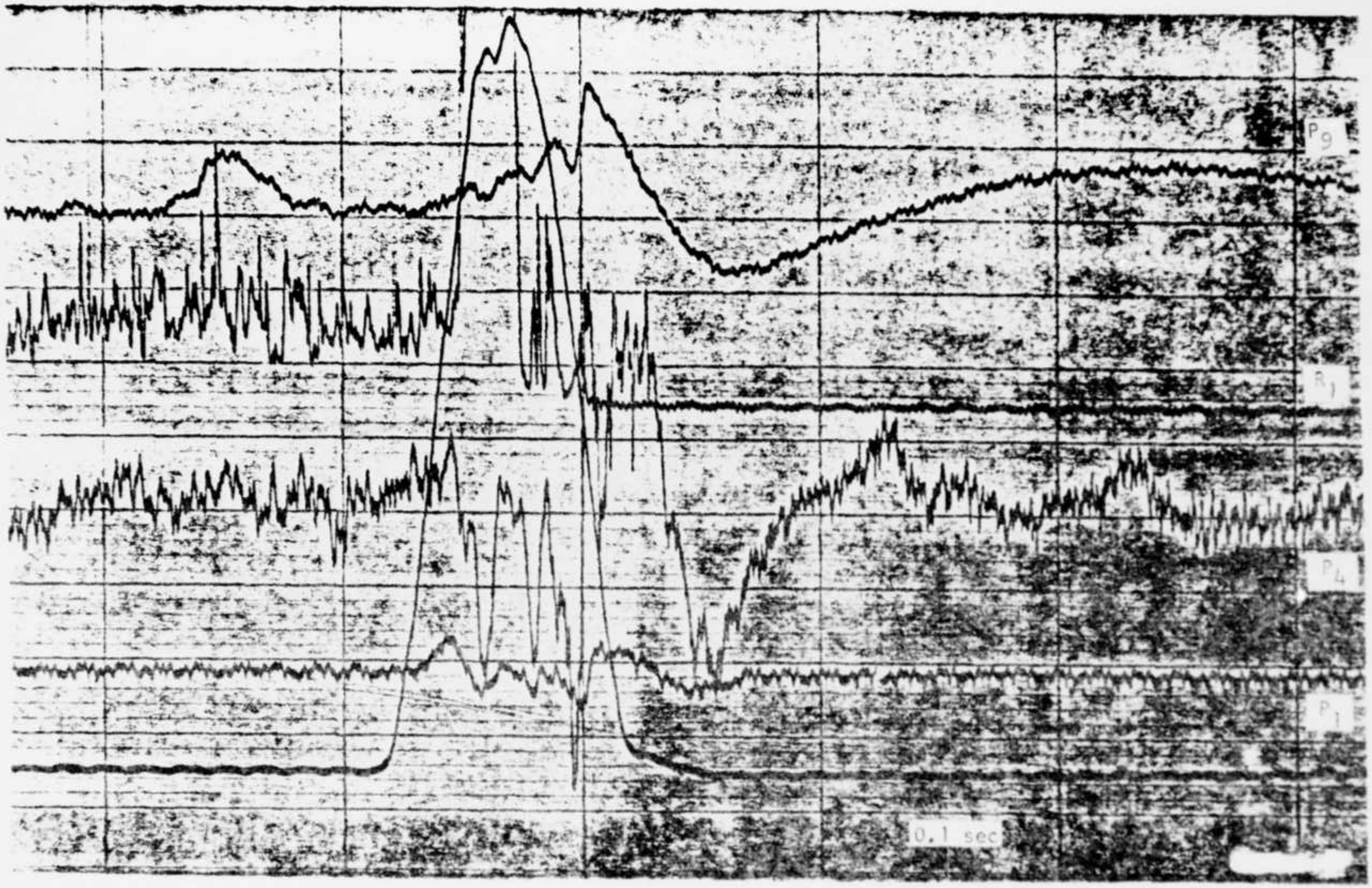

Figure 57. Unsteady Pressure and Radiation Characteristics
Series 7, Test 70-Large Amplitude 100 msec Pulse

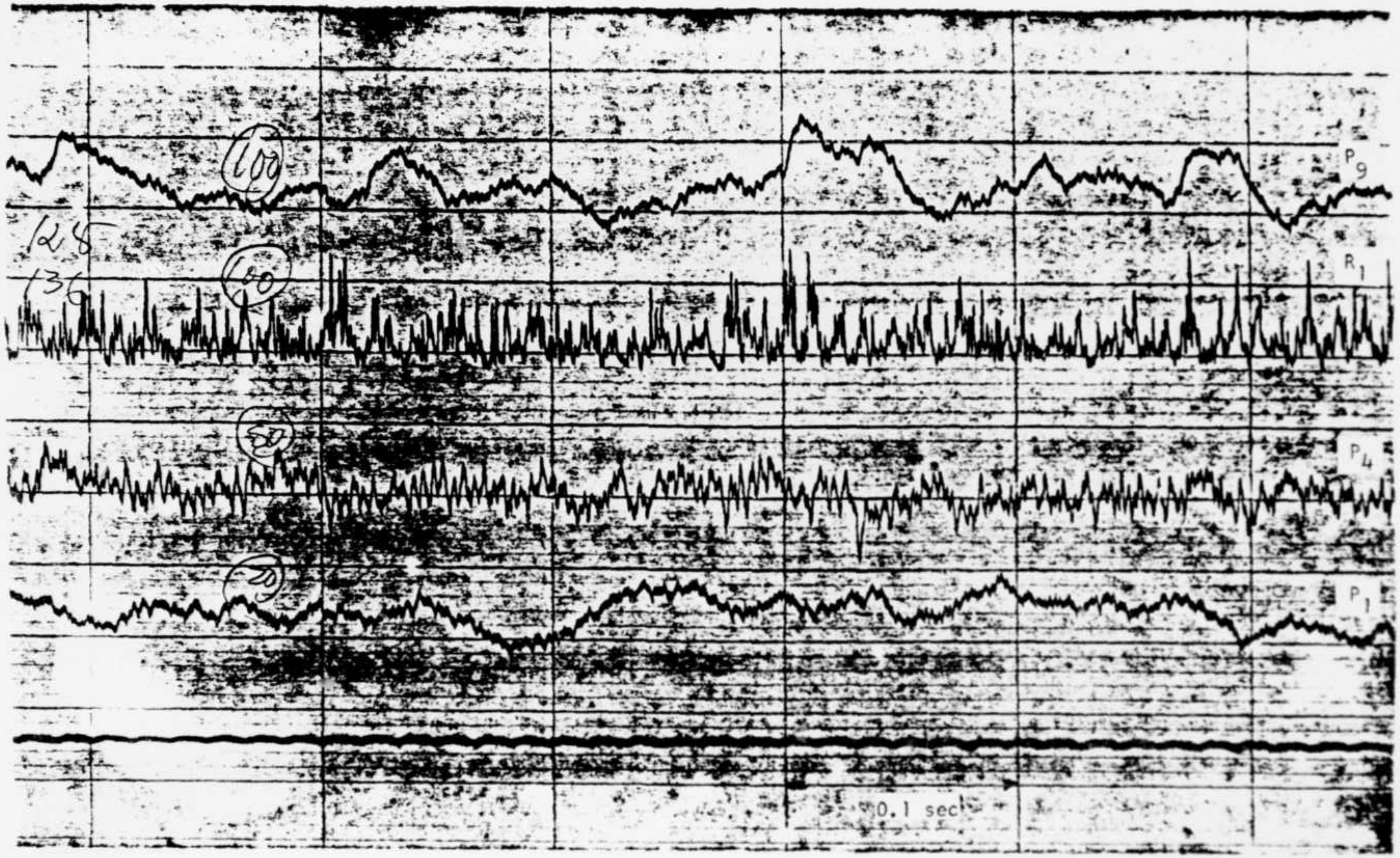

Figure 58. Unsteady Pressure and Radiation Characteristics
Series 8, Test 76

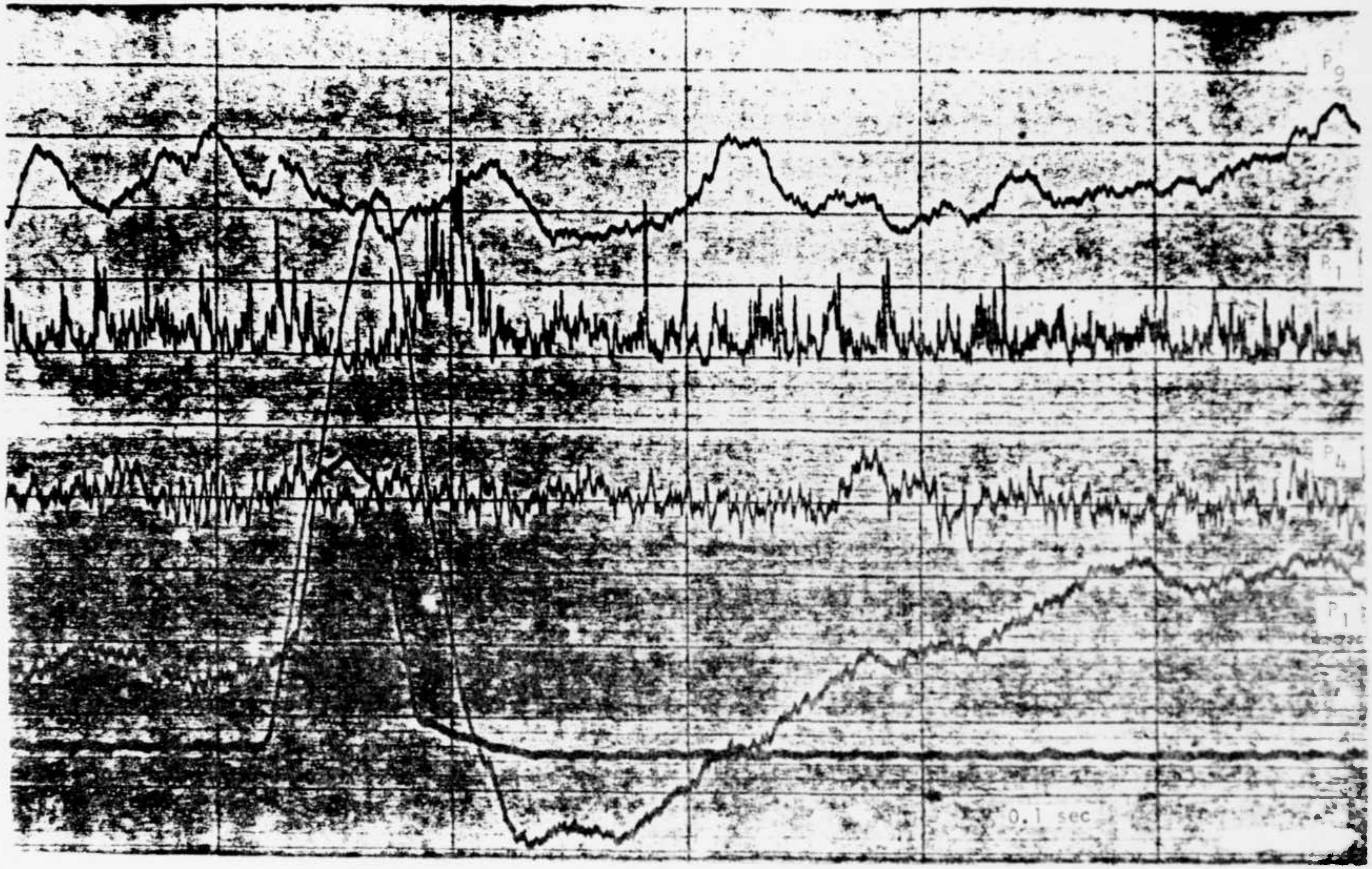

Figure 59. Unsteady Pressure and Radiation Characteristics
Series 8, Test 77-Short Small Amplitude Pulse

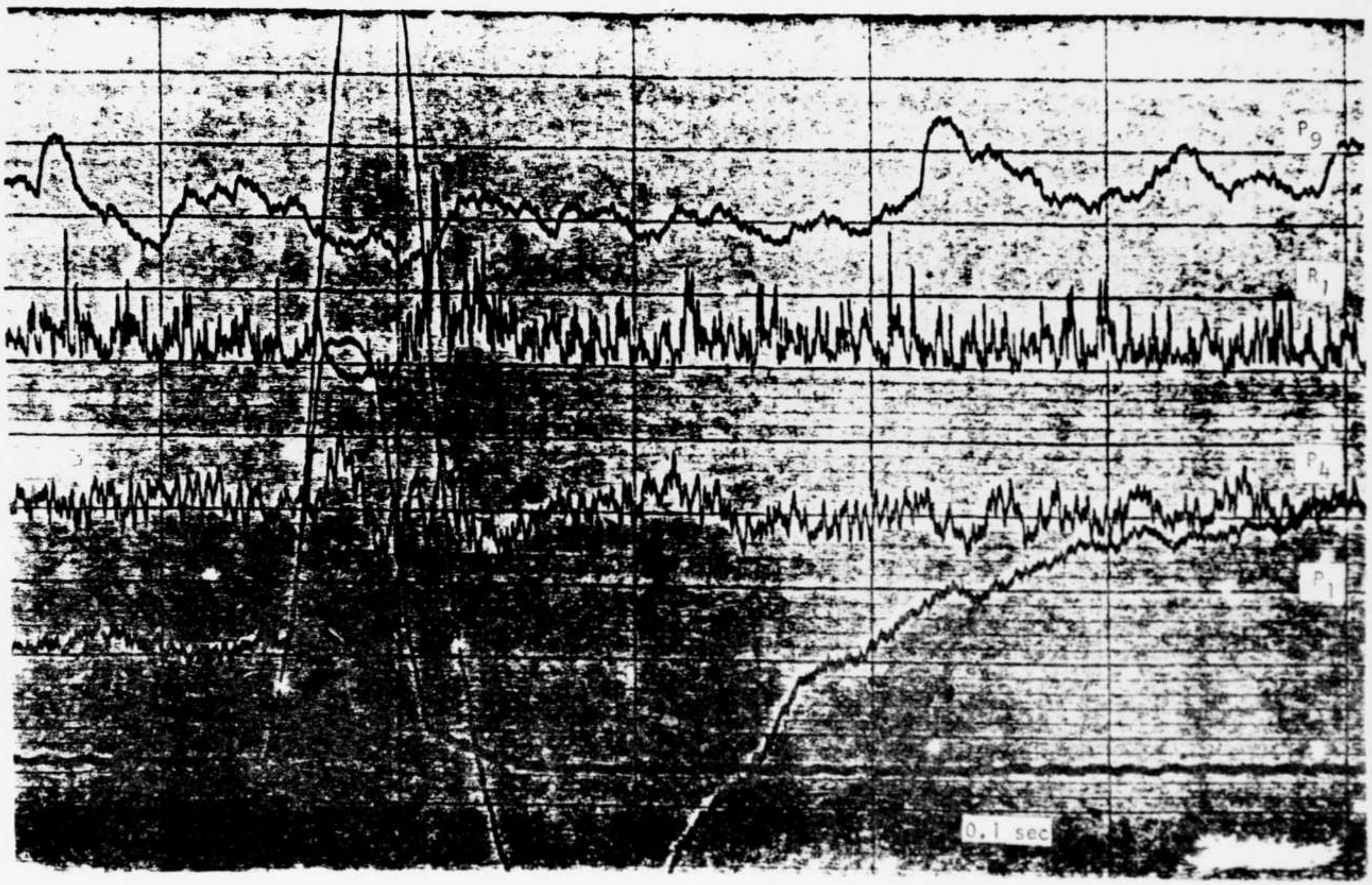

Figure 60. Unsteady Pressure and Radiation Characteristics Series 8, Test 77-Larger Amplitude Pulse in Fan Stream

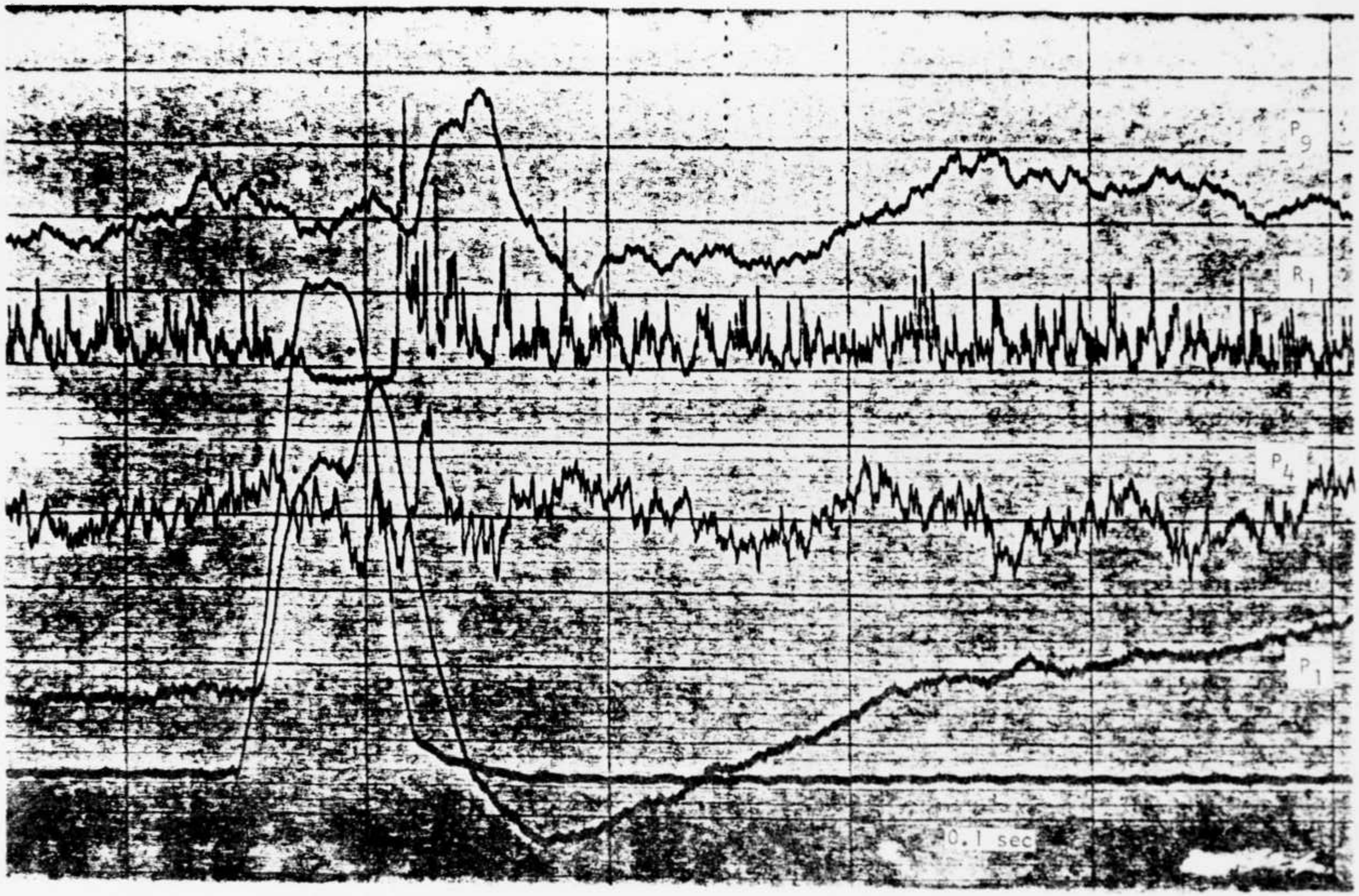

Figure 61. Unsteady Pressure and Radiation Characteristics
Series 8, Test 77-Simultaneous Fan and Core Stream Pulses

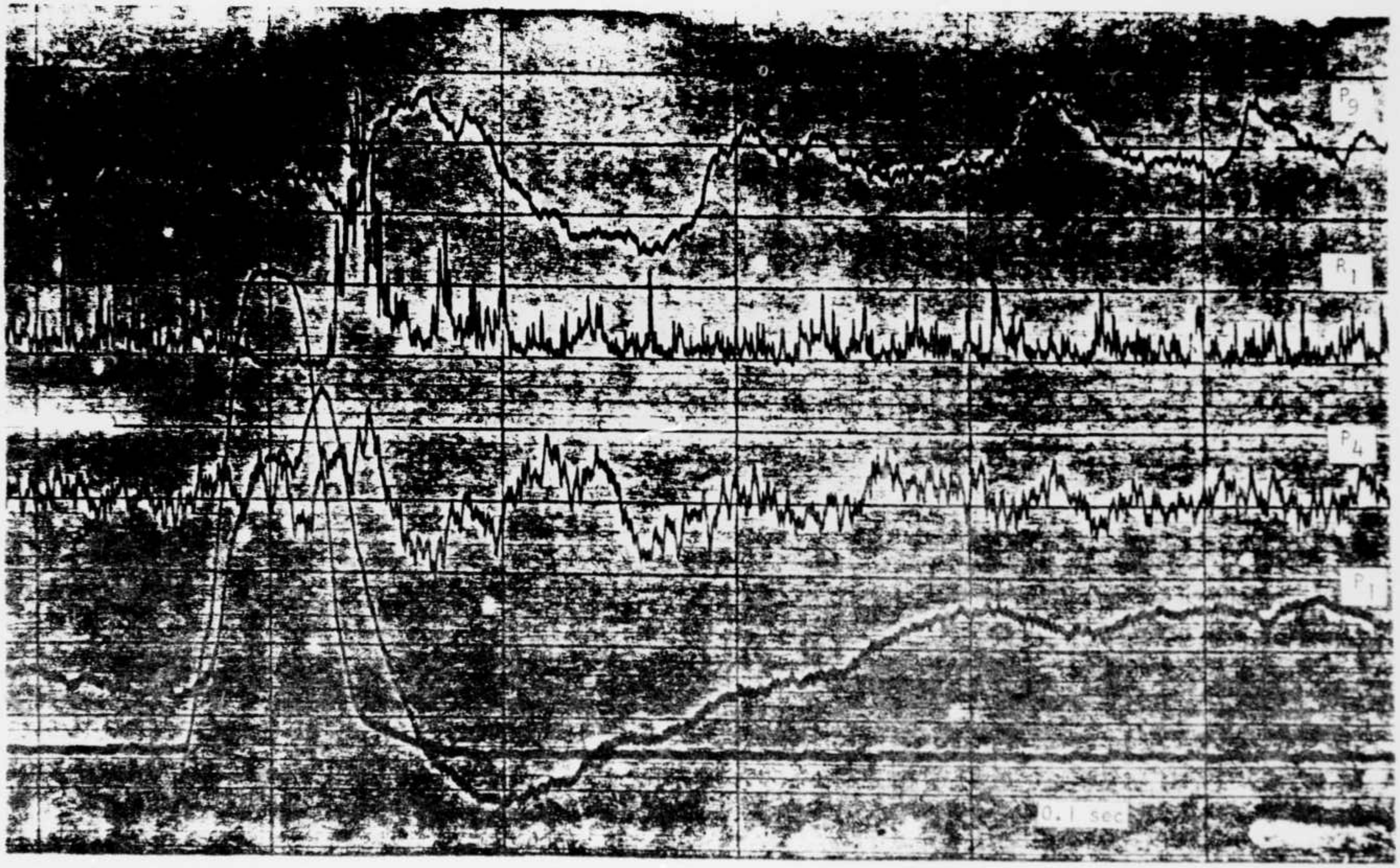

Figure 62. Unsteady Pressure and Radiation Characteristics
Series 8, Test 77-Simultaneous Fan and Core Stream Pulses

REFERENCES

1. Lefebvre, A. H. and Reid, R., "The Influence of Turbulence on the Structure and Propagation of Enclosed Flames", Journal of Combustion and Flame, vol. 10, no. 4, December, 1966, pp. 355-366.

2. Combustion in Advanced Gas Turbine Systems, Proceedings of an International Propulsion Symposium held at the College of Aeronautics, Cranfield, England, Edited by I. E. Smith, April, 1967.

3. Clark, Thomas P. and Bittker, David A., A Study of the Radiation From Laminar and Turbulent Open Propane-Air Flames as a Function of Flame Area, Equivalence Ratio and Fuel Flow Rate (NACA-RM-E54F29), National Advisory Committee for Aeronautics, Washington, August 24, 1954.

4. John, Richard R. and Summerfield, Martin, "Effect of Turbulence on Radiation Intensity from Propane-Air Flames", Jet Propulsion, February, 1957, pp. 169-178.